



HAL
open science

Large-time asymptotics of anomalous fluctuations in heavy-tailed renewal-reward processes

Hiroshi Horii

► **To cite this version:**

Hiroshi Horii. Large-time asymptotics of anomalous fluctuations in heavy-tailed renewal-reward processes. Probability [math.PR]. Université Paris Cité, 2022. English. NNT : 2022UNIP7192 . tel-04382005

HAL Id: tel-04382005

<https://theses.hal.science/tel-04382005v1>

Submitted on 9 Jan 2024

HAL is a multi-disciplinary open access archive for the deposit and dissemination of scientific research documents, whether they are published or not. The documents may come from teaching and research institutions in France or abroad, or from public or private research centers.

L'archive ouverte pluridisciplinaire **HAL**, est destinée au dépôt et à la diffusion de documents scientifiques de niveau recherche, publiés ou non, émanant des établissements d'enseignement et de recherche français ou étrangers, des laboratoires publics ou privés.



UNIVERSITÉ PARIS CITÉ École Doctorale de Sciences
Mathématiques de Paris Centre
Laboratoire de Probabilités, Statistique et Modélisation

Thèse de doctorat
Discipline : Mathématiques

présentée par
Hiroshi Horii

**Large-time asymptotics of anomalous fluctuations in
heavy-tailed renewal-reward processes**

sous la direction de **Raphaël Lefevre** et **Takahiro Nemoto**

Présentée et Soutenue à Paris le 7 Juillet 2022 devant le jury composé de

Mauro Mariani	Associate professor, HSE University	Rapporteur
Raphaël Chetrite	CR, Université de Nice Sophia-Antipolis	Rapporteur
Cédric Bernardin	PR, Université de Nice Sophia-Antipolis	Examineur
Sandrine Péché	PR, Université Paris Cité	Examineur
Raphaël Lefevre	MCF, Université Paris Cité	Directeur de thèse
Takahiro Nemoto	Assistant professor, Kyoto University	co-Directeur de thèse

裾の重い再生報酬過程における
異常ゆらぎの長時間漸近挙動の解析

Acknowledgment

To complete my Ph.D. thesis, I would like to mention that a lot of kind people have supported me. If not for their support, I would not have been able to write my Ph.D. thesis. I am very grateful to them. My research life in Paris was an even more wonderful thing than I had imagined when I arrive because of the people around me. It was hard to handle sometimes, but it was a beautiful period of my life.

First of all, I would like to thank my thesis director, Raphaël Lefevre, who carefully guided me, and taught me a lot of mathematical things and behavior as a researcher. Before coming to Paris, actually, I gave up to continue my research life and I was working in a company. But he has given me this wonderful opportunity to do research finally and I can complete my Ph.D. thesis. It really changed my life. Second, I would like to thank my thesis co-director, Takahiro Nemoto, who also carefully guided me, and spent a lot of time teaching me about physics and how to conduct research among others. He has always supported me step by step inside and outside of research. I learned a lot of things from both of them and it is the basis as a researcher for me. I also would like to thank to Robert Jack, who work in Cambridge university, and Hisashi Inaba, who work in university of Tokyo, for supporting my visiting research. Moreover, I am grateful to Masato Itami, who work together for analysis of anomalous fluctuations in the non-equilibrium physical model with stochastic boundary condition. I look forward to working with again.

I would like to thank all the friends of LPSM for sharing great moments together!: Aaraona, Abdel, Antoine, Assaf, Barbara, Benjamin, Bohdan, Clément, Clément, Côme, Cyril, Enzo, Fabio, Guillaume C., Guillaume S., Houzhi, Ibrahim, Junchao, Laure, Luca, Lucas, Marc, Maximilien, Mohan, Simon, Sothea, Sylvain, William, Xuanye, Yann, Yiyang and Ziad. I spent a great time with you all like grabbing a beer at a bar, having lunch, sometimes going to rock climbing, and having coffee around 4 pm together. Also, I would like to thank Valerie and Nathalie who are the secretaries of LPSM at Sophie Germain. I look forward to seeing you all again.

Also, I am grateful to the MathInParis program and the coordinator of the program, Ariela Briani who supports me every time. This program gave me wonderful experiences and the opportunity to work abroad.

Finally, I would like to thank my friends and my family. Sometimes, I telephoned them and they took me outside of work. They always cheer me and it keeps me motivated to research. In particular, my parents always supported me in whatever I did since the old days. It always makes me happy.

Abstract

In this thesis, we mainly study the finite-time behavior of anomalous fluctuations in heavy-tailed renewal-reward processes. A heavy-tailed distribution produce more extream events (rare events) than an exponential distribution in a system. In general, the tail of probability distributions is related to a rare event and has a small impact on the entire system. However, when probability distributions are heavy-tailed, this insight does not work. For instance, in the financial market, the melt-up or shock of the market is a rare event following a heavy-tailed distribution. In infectious disease spreading, a super spreader is a rare event in the system, whose occurrence is also distributed by a heavy-tailed distribution. This random phenomenon can be explained using a heavy-tailed renewal-reward process and by constructing the model, we can estimate the fluctuations of the interested stochastic process. In addition, the behavior of the stochastic process contains anomalous fluctuations because of memory effects. In this thesis, we study the anomalous behavior of heavy-tailed renewal reward processes using the large deviation principle (LDP), variational principle, and a renewal equation.

In this thesis, we first introduce the background of our research in chapter 2. Our main results are described in chapter 3, chapter 4, and chapter 5.

In chapter 3, we give proof for the large-time asymptotics of a moment generating function (or cumulant generating function) in a heavy-tailed renewal-reward process. The moment generating function has the singularity within the specific range of biasing field. We have clarified the behavior of the singularity part in a finite-time range. In addition, we have analyzed a finite time rate function using numerical simulation. For the results, The finite time behavior of probability is no longer an exponential function within a flat part. This is because a heavy-tailed waiting time distribution produce a lot of moving slow particles and convergence law is different from using exponential distribution. Occurring a lot of rare events affects the convergence law of LDF and the finite-time moment generating function behaves as a power-law within a flat part.

In chapter 4, we re-derive an affine part in cumulant generating functions (CGFs) by using a variational principle developed in large deviation theory. This variational principle has been applied to study a singularity appearing in the LDF in, among others, kinetically constrained models (KCM) and active matters. These models are defined using Markov processes, because of which the LDF of time-averaged quantities does not have any singularity whenever the system size (not the averaging time) is finite. Our focus is on how the same methodology can be extended to our non-Markovian problem to derive the affine part.

In chapter 5, first, we studied a counting process with two heavy-tailed waiting time distributions: the Pareto distribution and the inverse Rayleigh distribution. These two

waiting time distributions have an asymptotic form exponent of the power-law is -3 when the waiting time is large, implying that the variance of the waiting time diverges. Because of this divergence, we discussed that the scaled variance of the counting process also diverges in the large time limit. We indeed derived that the scaled variance is asymptotically proportional with $\log(t)$, diverging as time goes to infinity. Second, as with the conclusion of a counting process, we have clarified the asymptotic behavior of the variance of the time-averaged current. That inter-arrival time follows the inverse Rayleigh distribution, so we can obtain the scaled variance is asymptotically proportional with $\log(t)$, diverging as time goes to infinity. The memory effect of a stochastic process is related to the anomalous divergence of moments.

Keywords Large deviation theory, Renewal-reward process (continuous-time random walk), Heavy-tailed waiting time distribution, Dynamical phase transition, Knudsen gas model, Variational principle for LDF, Anomalous scaling of cumulants

Résumé

Dans cette thèse, nous étudions principalement le comportement en temps fini des fluctuations anormales dans les processus de renouvellement-récompense à queue lourde. Une distribution à queue lourde produit plus d'événements extrêmes (événements rares) qu'une distribution exponentielle dans un système. En général, la queue des distributions de probabilité est liée à un événement rare et a un faible impact sur l'ensemble du système. Cependant, lorsque les distributions de probabilité ont une queue lourde, cette idée ne fonctionne pas. Par exemple, sur le marché financier, l'effondrement ou le choc du marché est un événement rare suivant une distribution à queue lourde. Dans la propagation des maladies infectieuses, un super propagateur est un événement rare dans le système, dont l'occurrence est également distribuée selon distribution à queue lourde. Ce phénomène aléatoire peut être expliqué à l'aide d'un processus de renouvellement-récompense à queue lourde. En construisant le modèle, nous pouvons estimer les fluctuations du processus stochastique concerné. De plus, le comportement du processus stochastique contient des fluctuations anormales à cause des effets de mémoire. Dans cette thèse, nous étudions le comportement anormal des processus de récompense de renouvellement à queue lourde en utilisant le principe des grandes déviations (LDP), le principe variationnel et une équation de renouvellement.

Dans cette thèse, nous introduisons d'abord le contexte de notre recherche dans le chapitre 2. Nos principaux résultats sont décrits dans le chapitre 3, le chapitre 4 et le chapitre 5.

Dans le chapitre 3, nous donnons la preuve de l'asymptotique en grand temps d'une fonction génératrice de moment (ou fonction génératrice des cumulants) dans un processus de renouvellement-récompense à queue lourde. La fonction génératrice des moments présente une singularité dans une plage spécifique du champ de biais. Nous avons clarifié le comportement de la partie singulière dans une plage de temps finie. De plus, nous avons analysé une fonction de taux en temps fini en utilisant la simulation numérique. Le comportement en temps fini de la probabilité n'est plus une fonction exponentielle dans une partie plate. Cela est dû au fait qu'une distribution du temps d'attente à queue lourde produit un grand nombre de particules lentes en mouvement et que la loi de convergence est différente de celle de la distribution exponentielle. L'apparition d'un grand nombre d'événements rares affecte la loi de convergence de la LDF et la fonction génératrice de moments en temps fini se comporte comme une loi de puissance dans une partie plate.

Dans le chapitre 4, nous redérivons une partie affine dans les fonctions génératrices cumulantes (CGF) en utilisant un principe variationnel développé dans la théorie des grandes déviations. Ce principe variationnel a été appliqué pour étudier une singularité apparaissant dans la CGF dans, entre autres, les modèles à contrainte cinétique (KCM) et les matières actives. Ces modèles sont définis à l'aide de processus de Markov, ce qui fait que la LDF

des quantités moyennées dans le temps ne présente aucune singularité lorsque la taille du système (et non le temps de moyennage) est finie. Nous nous concentrons sur la façon dont la même méthodologie peut être étendue à notre problème non-markovien pour dériver la partie affine.

Dans le chapitre 5, nous avons d'abord étudié un processus de comptage avec deux distributions de temps d'attente à queue lourde : la distribution de Pareto et la distribution inverse de Rayleigh. Ces deux distributions de temps d'attente ont une forme asymptotique : l'exposant de la loi de puissance est -3 lorsque le temps d'attente est grand, ce qui implique que la variance du temps d'attente diverge. En raison de cette divergence, nous avons discuté que la variance échelonnée du processus de comptage diverge également dans la grande limite de temps. Nous avons en effet dérivé que la variance échelonnée est asymptotiquement proportionnelle à $\log(t)$, divergeant lorsque le temps va vers l'infini. Deuxièmement, comme pour la conclusion d'un processus de comptage, nous avons clarifié le comportement asymptotique de la variance du courant moyenné dans le temps. Ce temps inter-arrivée suit la distribution inverse de Rayleigh, nous pouvons donc obtenir que la variance échelonnée est asymptotiquement proportionnelle à $\log(t)$, divergeant lorsque le temps passe à l'infini. L'effet mémoire d'un processus stochastique est lié à la divergence anormale des moments.

Mots-clés Théorie des grandes déviations, Processus de renouvellement-récompense (marche aléatoire à temps continu), Distribution du temps d'attente à queue lourde, Transition de phase dynamique, Modèle de gaz de Knudsen, Principe variationnel pour la LDF, Échelonnement anormal des cumulants.

Contents

1	Introduction	21
2	Background	33
2.1	Renewal Theory	33
2.1.1	Definition	33
2.1.2	Basic Theory	35
2.1.3	Renewal Equation	39
2.1.4	Renewal Equation for a Moment Generating Function	41
2.1.5	Inverse Laplace Transform Method for a MGF	42
2.2	Large Deviation Theory	44
2.2.1	Large Deviation Principle	44
2.2.2	Gärtner-Ellis Theorem	45
2.2.3	Varadhan’s Lemma	47
2.2.4	Strong Large Deviation Theorem	48
2.3	Large Deviations Approach in Statistical Mechanics	51
2.3.1	Macroscopic Fluctuation Theory	52
2.A	Saddle-point Approximation for Gärtner-Ellis Theorem	55
2.B	Edgeworth Expansion	56
2.C	Physical Approach of MFT	58
3	Analysis of Finite Time LDF	61
3.1	Background	61
3.1.1	The Affine Part of LDF	61
3.1.2	Tsirelson’s Work	62
3.2	Set-up	65
3.3	Results	66
3.4	Uniform Bounds	69
3.5	Numerical Study	71
3.5.1	Generality of Theorem 3.3.1	71
3.5.2	Study of the Rate Function	74
3.6	Conclusion	77
3.A	Perturbative Construction of MGF	77

4	Variational Principle for SCGF	79
4.1	Background	79
4.1.1	Model	79
4.1.2	Properties of a Path Probability	80
4.1.3	A Bound Function of CGF	81
4.1.4	Population Dynamics Algorithm to Compute $\lim_{t \rightarrow \infty} \phi(h, t)/t$	82
4.2	Bound Functions for the Heat-conduction System	83
4.2.1	A Control System with Modifying Wall Temperatures	83
4.2.2	A Control System with $N_t = 0$	84
4.2.3	Taking Hydrodynamic Limit	86
4.3	Numerical Study	87
4.A	Optimal Control System in a Stochastic Differential Equation	88
4.B	Analytical Expressions for the Lower Bound of $\phi(h, t)$	89
5	Analysis of Anomalous Fluctuations	91
5.1	Background	92
5.1.1	Model	92
5.1.2	Renewal Equations for q th-moments	93
5.2	Convergence Law of a Counting Process	93
5.2.1	Convergence of the First Moment	93
5.2.2	Convergence of the Variance	95
5.2.3	Numerical Study	96
5.3	A Particle Confined between Two Hot Walls	96
5.3.1	Knudsen Gas Model	96
5.3.2	Convergence of the Current: First Moment	98
5.3.3	Variance of the Current of Energy between Heat Baths	100
5.3.4	Convergence of the Thermal Energy	102
5.3.5	Numerical Simulations	103
5.4	Discussion	103
5.4.1	A Counting Process with Smaller Power-law Exponents	103
5.4.2	Many Particles Confined in the Two Hot Walls	104
5.4.3	Related Studies	105
5.A	k -th moment of a heavy-tailed counting process	105
5.B	Tauberian Theorem	109
5.C	Simulation Detail	110

Résumé détaillé en français

Résumé du chapitre 3

Nous considérons un processus de comptage N_t défini comme suit

$$N_t = \sup\{k : S_k \leq t\},$$

où $S_k = \tau_1 + \dots + \tau_k$ et $(\tau_j)_{j=1}^k$ est une séquence des temps de renouvellement, distribués indépendamment selon des distributions à queue lourde $p(t)$. Pour les distributions à queue lourde, nous considérons d'abord la distribution de Pareto $p(t)$ avec un paramètre $m > 2$:

$$p(t) : = \begin{cases} 0 & t \leq 0 \\ \frac{(m-1)}{(1+t)^m} & t > 0 \end{cases} \quad (0.0.1)$$

Le processus de comptage correspond au nombre d'événements qui se sont produits jusqu'au temps $t > 0$. Nous définissons la fonction génératrice de moments d'un processus de comptage comme $M(t, h) = \mathbb{E}[e^{hN_t}]$. Le résultat principal de ce chapitre est alors donné par le théorème suivant.

Theorem 3.3.1 Soit $(N_t)_{t \geq 0}$ le processus de comptage avec des temps d'attente distribués selon une loi de Pareto avec un paramètre entier $m \geq 3$, alors pour tout $h < 0$:

$$\lim_{t \rightarrow \infty} t^{m-1} M(t, h) = \frac{1}{1 - e^h}. \quad (0.0.2)$$

Nous étudions numériquement les fonctions génératrices de moments du processus de comptage $M(t, h)$ pour plusieurs distributions de temps d'attente : la distribution de Pareto, la distribution inverse de Rayleigh

$$p_{Ray}(t) : = \begin{cases} 0 & t \leq 0 \\ \frac{\beta}{t^3} e^{-\frac{\beta}{2t^2}} & t > 0 \end{cases} \quad (0.0.3)$$

avec un paramètre β et une distribution log-normale

$$p_{log}(t) : = \begin{cases} 0 & t \leq 0 \\ \frac{1}{\sqrt{2\pi}\sigma t} e^{-\frac{(\log(t)-\mu)^2}{2\sigma^2}} & t > 0 \end{cases} \quad (0.0.4)$$

avec les paramètres μ et σ . Nous traçons ensuite $M(t, h)/M_0(t)$ (où $M_0(t) = 1 - F(t)$ avec la fonction de répartition $F(t)$) dans la Fig.1.2 ainsi que $1/(1 - e^h)$, démontrant la validité du théorème 3.3.1 au-delà de son hypothèse.

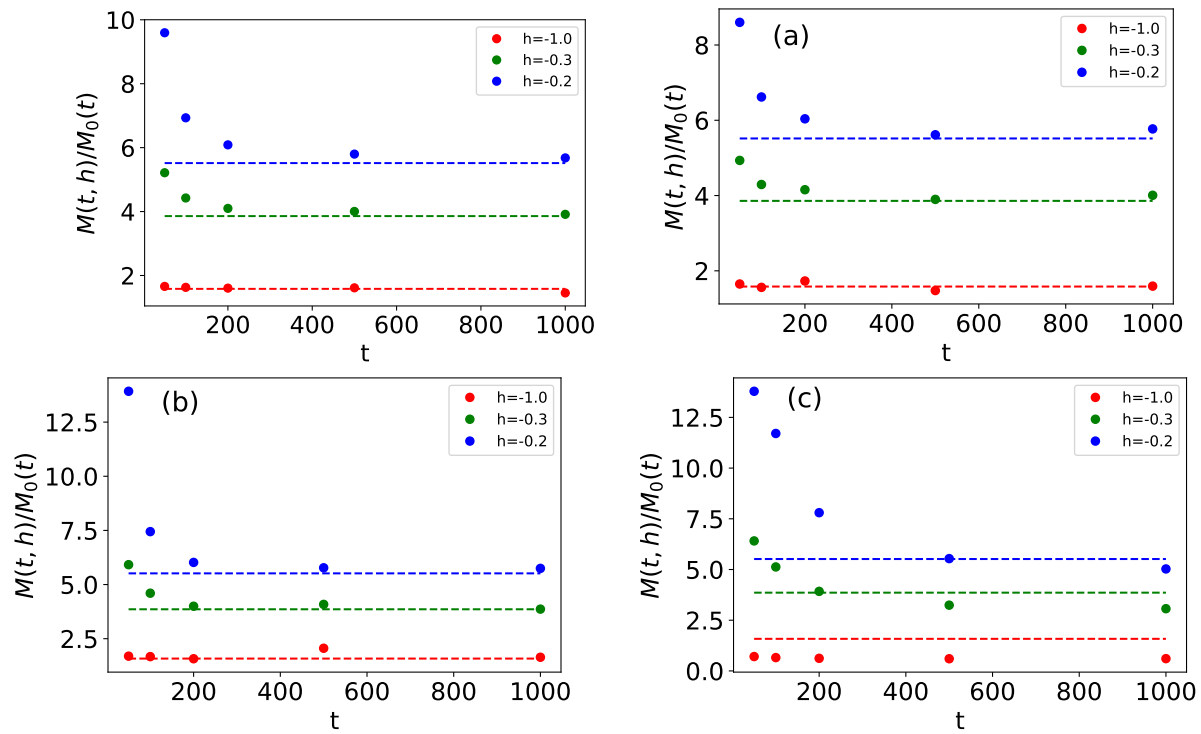


Fig. 1: Résultats numériques de $M(t, h)/M_0(t)$ (cercles remplis) et de $1/(1 - e^h)$ (lignes pointillées) pour la distribution de Pareto avec $m = 3, 0$ (a), la distribution de Pareto avec $m = 3, 5$ (b), la distribution de Rayleigh inverse avec $\beta = 1$ (c) et la distribution log-normale du temps d'attente avec $\mu = 0$ et $\sigma = 1, 5$ (d). Ici, $M_0(t) = 1 - F(t)$ et $F(t)$ est une fonction de répartition.

Nous étudions également le comportement asymptotique de $\log \mathbb{P}[N_t < xt]$ dans nos simulations numériques et observons la forme asymptotique générale suivante

$$\log \mathbb{P}[N_t < xt] \sim a \log M_0(t) + \log(t) + b \quad (0.0.5)$$

avec les constantes a, b (qui peuvent potentiellement dépendre de x) dans la Fig.1.3. Pour les distributions de temps d'attente de Pareto et de Rayleigh inverse, a semble être égal à 1, tandis que a est différent de 1 pour la distribution log-normale du temps d'attente.

Résumé du chapitre 4

Dans ce chapitre, nous redérivons une partie affine dans les fonctions génératrices des cumulants (CGF) [1] en utilisant un principe variationnel développé dans la théorie des grandes déviations. Ce principe variationnel a été appliqué pour étudier une singularité apparaissant dans les CGF dans, entre autres, les modèles à contrainte cinétique (KCM) [2] et les matières actives [3]. Ces modèles sont définis à l'aide de processus de Markov, grâce auxquels la LDF des quantités moyennées dans le temps ne présente aucune singularité lorsque la taille du système (et non le temps de moyennage) est finie. Nous nous concentrons sur la façon dont la même méthodologie peut être étendue à notre problème non-markovien pour dériver la partie affine.

Rappelant le contexte de l'article [1], nous considérons le processus de renouvellement-récompense avec la distribution inverse du temps d'attente de Rayleigh. Nous confignons une particule dans une boîte unidimensionnelle qui a deux températures différentes aux deux extrémités. La particule confiné a une vitesse aléatoire v distribuée selon la distribution suivante :

$$q_{\beta_{-1,1}}(v) = \beta_{-1,1} v e^{-\beta_{-1,1} \frac{v^2}{2}} \mathbb{1}_{(v>0)} \quad (0.0.6)$$

où $\beta_{-1,1} = 1/T_{-1,1}$ est la température inverse de la paroi gauche ou droite où la collision a lieu. Nous introduisons une variable de signe σ_k qui prend une valeur soit 1 soit -1 selon la direction vers laquelle la particule se déplace entre la k -ième et la $(k+1)$ -ième collision. Nous désignons l'espace d'état de cette variable par $E \equiv \{-1, +1\}$. La position et la vitesse initiales de la particule sont notées (x_0, v_0) , dont on déduit $\sigma_0 = v_0/|v_0|$, $\sigma_k = (-1)^k \sigma_0$. Nous définissons également la vitesse v_k de la particule entre la k -ième et la $(k+1)$ -ième collision. Elle est tirées, aléatoirement d'une des distributions de Rayleigh (1.0.6) en fonction de la paroi chaude précédente avec laquelle la particule entre en collision. Nous désignons par S_k l'instant où se produit la $(k+1)$ ième collision. En introduisant $\hat{\sigma}_k = \frac{1}{2}(\sigma_k + 1)$, le temps de la première collision avec une paroi s'écrit comme suit

$$S_0 = S_0(x_0, v_0) := \frac{\hat{\sigma}_0 - x_0}{v_0} > 0. \quad (0.0.7)$$

Notez que le k -ième temps inter-arrivée est donné par

$$\tau_k := \frac{\sigma_k}{v_k}, \quad (0.0.8)$$

qui est distribué comme

$$p(\tau_k | \sigma_{k-1}) = \frac{\beta_{\sigma_{k-1}}}{\tau^3} \exp\left(-\frac{\beta_{\sigma_{k-1}}}{2\tau^2}\right) \mathbb{1}_{(\tau)>0}. \quad (0.0.9)$$

Le temps d'arrivée S_k s'écrit alors comme suit

$$S_k := S_0 + \tau_1 + \tau_2 + \cdots + \tau_k, \quad k \geq 1. \quad (0.0.10)$$

L'énergie échangée entre les deux parois pendant un intervalle de temps $[0, t]$ est donnée par

$$J[0, t] := \frac{1}{2} \sum_{k \geq 1: S_k \leq t} v_k^2 \sigma_k. \quad (0.0.11)$$

Nous introduisons ensuite la borne inférieure pour le CGF. Pour cela, nous désignons d'abord par \mathcal{C} un chemin (ou une trajectoire) de l'état du système et par $\mathbb{P}(\mathcal{C})$ la probabilité de \mathcal{C} (la probabilité du chemin). Voir le chapitre 4 pour l'expression détaillée de la probabilité du chemin. Nous introduisons ensuite un système de contrôle défini comme, par exemple, le modèle de particules confinées avec des températures différentes de celles d'origine. La probabilité du chemin du système de contrôle est notée \mathbb{P}^{con} . Ensuite, nous avons la limite suivante pour la fonction génératrice des cumulants $\phi(h, t) (= \log \mathbb{E}[e^{-hJ}])$.

$$\phi(h, t) \geq -h\mathbb{E}_{\text{con}}[A] - D(\mathbb{P}^{\text{con}}|\mathbb{P}), \quad (0.0.12)$$

où

$$D(\mathbb{P}^{\text{con}}|\mathbb{P}) = \mathbb{E}_{\text{con}} \left[\log \frac{\mathbb{P}^{\text{con}}(t, \mathcal{C})}{\mathbb{P}(t, \mathcal{C})} d\mathcal{C} \right], \quad (0.0.13)$$

est une divergence de Kullback-Leibler (KL).

La partie affine peut être dérivée en utilisant cette limite avec un système de contrôle où l'état du système est limité à la condition initiale :

$$\mathbb{P}^{\text{con}} = \delta_{N_t, 0}, \quad (0.0.14)$$

i.e.,

$$\lim_{t \rightarrow \infty} \frac{\phi(h, t)}{t} \geq 0 \quad (0.0.15)$$

De plus, en considérant comme système de contrôle le modèle de particules confinées avec des températures $\beta_{\pm 1}^{\text{con}}$ différentes de celles d'origine, on obtient

$$\lim_{t \rightarrow \infty} \frac{\phi(h, t)}{t} \geq -\kappa^{\text{con}} \left[\frac{-h - \beta_1^{\text{con}} + \beta_1}{\beta_1^{\text{con}}} + \frac{h - \beta_{-1}^{\text{con}} + \beta_{-1}}{\beta_{-1}^{\text{con}}} + \log \frac{\beta_1^{\text{con}} \beta_{-1}^{\text{con}}}{\beta_1 \beta_{-1}} \right]. \quad (0.0.16)$$

Une limite hydrodynamique (voir le chapitre 4 en détail) nous permet de calculer une expression analytique de la limite optimale sous ce système de contrôle. Il est important de noter que le côté droit de cette limite optimale et (1.0.15) ne sont rien d'autre que l'expression analytique du CGF obtenue dans [4], ce qui indique que ces limites sont saturées.

Résumé du chapitre 5

Dans ce chapitre, nous nous concentrons sur les fluctuations anormales des quantités moyennées en temps dans les processus de renouvellement à queue lourde. En particulier, nous analysons la variance des distributions des temps d'attente à queue lourde. La variance peut nous indiquer directement à quel point les quantités moyennées fluctuent. Nous nous concentrons d'abord sur la fluctuation d'un processus de comptage, qui est le modèle le plus simple d'un processus de renouvellement-récompense, avec des distributions de temps d'attente à queue lourde. En rappelant la définition d'un processus de comptage, il est donné par

$$N_t = \sup\{k : S_k \leq t\}, \quad (0.0.17)$$

where $S_k = \tau_1 + \dots + \tau_k$. Nous désignons son moment d'ordre q par $m_q(t)$:

$$m_q(t) := \mathbb{E}[N_t^q]. \quad (0.0.18)$$

Pour analyser l'asymptotique de $m_q(t)$, nous nous appuyons sur les équations de renouvellement : un outil puissant pour analyser les processus de renouvellement-récompense. À partir d'un calcul simple, on peut établir l'équation de renouvellement suivante pour $m_1(t)$ [5]:

$$m_1(t) = F(t) + \int_0^t ds m_1(t-s)p(s), \quad (0.0.19)$$

où F est la fonction de distribution cumulative du temps d'attente. De cette équation, on déduit une expression simple pour la transformée de Laplace de $m(t)$. On définit de la transformée de Laplace d'une fonction f par

$$\tilde{f}(s) := \int_0^\infty e^{-st} f(t) dt, \quad (0.0.20)$$

on déduit alors, à partir de l'équation (1.0.19),

$$\tilde{m}_1(s) = \frac{\tilde{F}(s)}{1 - s\tilde{F}(s)}, \quad (0.0.21)$$

où nous avons utilisé $\tilde{p}(s) = s\tilde{F}(s)$.

De même, on peut aussi dériver une équation de renouvellement pour $m_2(t)$,

$$\begin{aligned} m_2(t) &= \int_0^t \mathbb{E}[N_{t-s}^2] p(s) ds \\ &+ 2 \int_0^t m_1(t-s) p(s) ds + F(t), \end{aligned} \quad (0.0.22)$$

à partir de laquelle la transformée de Laplace de $m_2(t)$ est obtenue comme suit

$$\tilde{m}_2(s) = \tilde{m}_1(s)(1 + 2s\tilde{m}_1(s)). \quad (0.0.23)$$

Ici, nous utilisons la distribution de Rayleigh inverse

$$p_\beta(\tau) = \frac{\beta}{\tau^3} \exp\left(-\frac{\beta}{2\tau^2}\right) \mathbb{1}(\tau > 0), \quad (0.0.24)$$

et la distribution de Pareto

$$p_\alpha(\tau) = \frac{\alpha - 1}{(1 + \tau)^\alpha} \mathbb{1}(\tau > 0) \quad (0.0.25)$$

avec $\alpha = 3$, les deux n'ayant pas de second moment fini, *i.e.*, $\mathbb{E}[\tau^2] = \infty$ pour considérer la variance des distributions de temps d'attente à queue lourde. Pour la distribution inverse de Rayleigh, nous obtenons

$$\frac{m_1(t)}{t} - \sqrt{\frac{2}{\beta\pi}} = \frac{\ln(t)}{t\pi} + o\left(\frac{\ln(t)}{t}\right) \quad (0.0.26)$$

et la variance $c_2(t)$ est de

$$c_2(t) = \frac{2\sqrt{2}}{\sqrt{\beta}\pi^{3/2}} \frac{\ln(t)}{t} + o\left(\frac{\ln(t)}{t}\right) \quad (0.0.27)$$

pour une grande valeur de t , où nous définissons la variance comme suit

$$c_2(t) = \frac{m_2(t) - m_1(t)^2}{t^2}. \quad (0.0.28)$$

Comme pour le calcul de ce cas, pour la distribution de Pareto, on obtient

$$\frac{m_1(t)}{t} - 1 = \frac{\ln(t)}{t} + o\left(\frac{\ln(t)}{t}\right). \quad (0.0.29)$$

et

$$c_2(t) = 2\frac{\ln t}{t} + o\left(\frac{\ln(t)}{t}\right). \quad (0.0.30)$$

Nous étudions également le comportement des fluctuations du courant d'énergie transporté par une particule, qui est introduit dans (1.0.11). En particulier, nous réécrivons le courant comme suit

$$J_\theta(t) := \frac{1}{2} \sum_{k=1}^{N_t} v_k^2 \sigma_k \quad (0.0.31)$$

avec une condition initiale $\theta = (x_0, v_0)$. De plus, nous désignons par $m_{\theta,q}(t)$ le q ième moment de $J_\theta(t)$:

$$m_{\theta,q}(t) = \mathbb{E}[J_\theta^q(t)]. \quad (0.0.32)$$

Ainsi, nous pouvons calculer les fluctuations du courant à l'aide de cette formule.

Ensuite, pour simplifier, nous ne considérons que les deux types de conditions initiales suivantes :

$$\theta_+ = (0, v_0) \quad (0.0.33)$$

avec $v_0 < 0$ et

$$\theta_- = (1, v_0) \quad (0.0.34)$$

avec $v_0 > 0$, *i.e.*, les cas d'une particule juste avant de frapper la paroi gauche (température β_+) et d'une particule juste avant de frapper la paroi droite (température inverse β_-). Soit

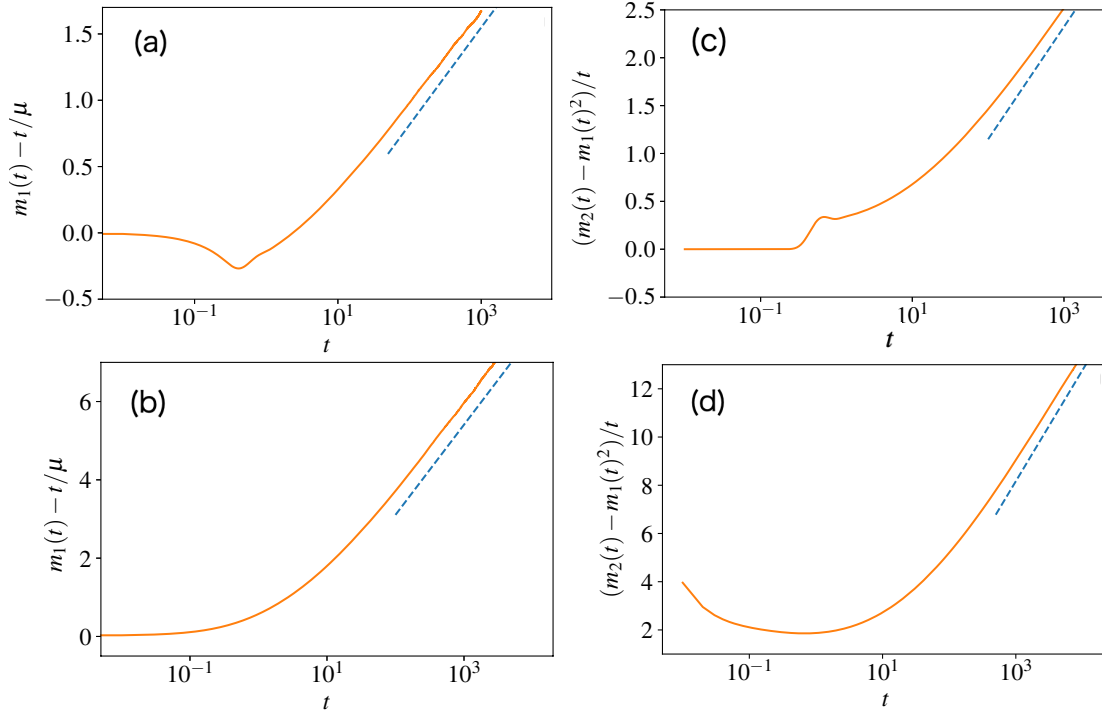


Fig. 2: **(a,b)** $m_1(t) - t/\mu$ obtenus à partir de simulations numériques du processus de comptage N_t (avec 10^8 échantillons) sont tracés en fonction du temps en échelle logarithmique sous forme de lignes orange. Pour la distribution inverse du temps d'attente de Rayleigh (a), $\beta = 1$ et $\mu = 1/\sqrt{2/(\beta\pi)}$, tandis que pour la distribution du temps d'attente de Pareto (b), $m = 3$ et $\mu = 1$. Les valeurs de $\ln(t)/\pi + \text{const.}$ et $\ln(t) + \text{const.}$ sont également tracées sous forme de lignes pointillées bleues pour (a) et (b). **(c,d)** Les $(m_2(t) - m_1(t)^2)/t$ obtenus à partir des mêmes simulations numériques sont tracés en fonction du temps sous forme de lignes orange pour la distribution inverse du temps d'attente de Rayleigh (c) et pour la distribution du temps d'attente de Pareto (d). $\frac{2\sqrt{2}}{\sqrt{\beta\pi^{3/2}}}\ln(t) + \text{const.}$ pour (c) et $2\ln(t) + \text{const.}$ pour (d) sont également tracés sous forme de lignes pointillées bleues dans les mêmes figures. Les accords entre les pentes des lignes orange et celles des lignes bleues dans ces graphiques semi-logarithmiques démontrent la validité de (5.2.10), (5.2.13), (5.2.20) et (5.2.21), comme détaillé dans le texte principal.

une particule de position initiale $q \in [0, 1]$ et de vitesse $v > 0$, la direction de la vitesse initiale est notée $\sigma = v/|v|$. Comme la particule frappe immédiatement chaque paroi au début du processus, la valeur de la vitesse initiale v_0 est sans importance. Nous désignons donc par $+$ la condition initiale θ_+ et par $-$ la condition initiale θ_- . Nous pouvons alors obtenir la forme asymptotique de la moyenne et de la variance du courant moyenné dans le temps comme pour la dérivation des fluctuations du processus de comptage. Celles-ci sont données par

$$\frac{m_{\pm,1}(t)}{t} = \kappa \left(\frac{1}{\beta_+} - \frac{1}{\beta_-} \right) + \kappa^2 \frac{(\beta_+ + \beta_-)}{2} \left(\frac{1}{\beta_+} - \frac{1}{\beta_-} \right) \frac{\ln t}{t} + o\left(\frac{\ln(t)}{t}\right) \quad (0.0.35)$$

$$\text{Var} \left(\frac{J_{\pm}(t)}{t} \right) = \kappa^3 (\beta_+ + \beta_-) \left(\frac{1}{\beta_+} - \frac{1}{\beta_-} \right)^2 \frac{\ln(t)}{t} + o\left(\frac{\ln(t)}{t}\right). \quad (0.0.36)$$

pour grand temps. En résumé, nous avons d'abord étudié un processus de comptage N_t

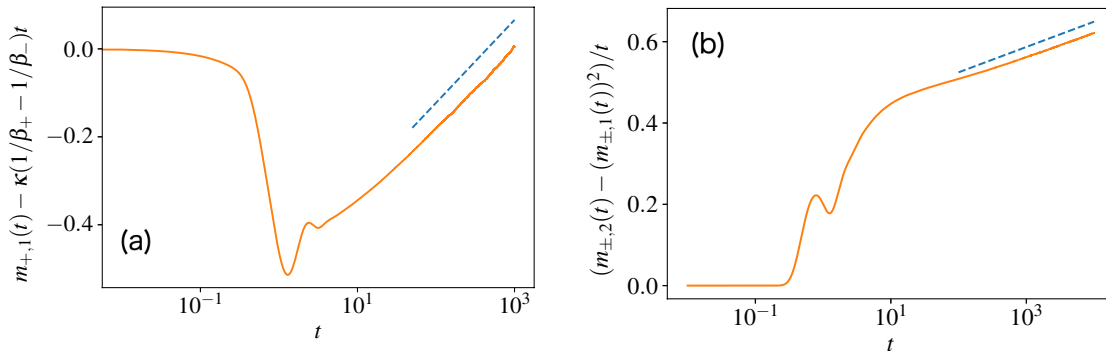


Fig. 3: Les lignes orange représentent $m_{+,1}(t) - \kappa(1/\beta_+ - 1/\beta_-)$ (a) et $m_{\pm,2}(t)/t^2 - (m_{\pm,1}(t))^2/t^2$ (b) obtenues à partir de simulations numériques (avec 10^8 échantillons). $\beta_+ = 1$, $\beta_- = 2$. Les lignes pointillées bleues représentent $(\kappa^2/2)(\beta_+ + \beta_-) (1/\beta_+ - 1/\beta_-) (\ln t)/t + \text{const.}$ et $\kappa^3(\beta_+ + \beta_-) (1/\beta_+ - 1/\beta_-)^2 + \text{const.}$ Les pentes des résultats de la simulation numérique en échelle semi-logarithmique convergent vers celles des lignes de référence en pointillés, ce qui montre la validité de (5.3.17) et de (5.3.29).

avec deux distributions de temps d'attente à queue lourde : la distribution de Pareto avec $\alpha = 3$ et la distribution inverse de Rayleigh. Ces deux distributions du temps d'attente ont une forme asymptotique $1/\tau^3$ lorsque le temps d'attente τ est grand, ce qui implique que la variance du temps d'attente $\mathbb{E}[\tau^2]$ diverge. En raison de cette divergence, nous avons discuté que la variance échelonnée du processus de comptage N_t diverge également dans la limite des grands t . Nous avons en effet dérivé que la variance échelonnée est asymptotiquement proportionnelle à $\log(t)$, divergeant comme $t \rightarrow \infty$. Deuxièmement, nous avons clarifié le comportement asymptotique de la variance du courant moyenné dans le temps $J_\theta(t)$. Ce temps inter-arrivée suit la distribution inverse de Rayleigh, de sorte que nous pouvons obtenir que la variance échelonnée est asymptotiquement proportionnelle à $\log(t)$, divergeant comme $t \rightarrow \infty$. L'effet mémoire d'un processus stochastique est lié à la divergence anormale des moments.

Chapter 1

Introduction

“The most important questions of life are indeed, for the most part, really only problems of probability.” As written by Pierre-Simon Laplace(1749-1827) in his celebrated book “Théorie analytique des probabilités” [6], probabilistic phenomena are everywhere and understanding them in terms of mathematics is important. For example, how many times do we have to change the light bulb in a room in 10 years? Each light bulb has different lifetimes and they are distributed randomly according to, for example, the gamma distribution. Knowing this distribution, one can estimate not only how many light bulbs are needed on average during 10 years, but also the range of the number of required light bulbs in 95% probability. Following the same approach, probability theory has been applied to the managements of factory and of company’s office to evaluate the maintenance cost. Probability theory has been used as a tool to understand physical and social phenomena for many centuries, and has had a great impact on the advance of technology. In theoretical physics, Ludwig Eduard Boltzmann(1844-1906) and Josiah Willard Gibbs(1839-1903) constructed statistical mechanics in the 19th century. In recent years, the probability theory has been applied to phenomena that attract a lot of public attention, such as financial markets, climate change and epidemiology.

Let us look back on the history of probability theory. A mainstream opinion is that it started from the exchange of letters between Blaise Pascal(1623-1662) and Pierre de Fermat(1607-1665) for discussing dice games [7]. Chevalier de Méré (1607-1684) was a French nobility and he loved gambling. At some point he lost a lot of money and he asked Pascal why he lost in the game. Pascal then asked Fermat, who had been already famous at that moment as a great mathematician, for advice to solve the question. They started exchanging letters and the research of probability theory has begun. Pierre-Simon Laplace eventually wrote “Théorie analytique des probabilités”, completing the classical probability theory. Later, french mathematicians Émile Borel(1871-1956) and Henri Lebesgue(1875-1941) introduced the measure theory. Andrei Kolmogorov(1903-1987) has finally founded the modern probability theory by using an axiomatic approach.

Many random phenomena around us appear as a sequence. Examples are countless, such as a share price, temperature in a room, the number of new covid-19 cases, and so on. The theory of stochastic processes was introduced around 1950 to describe sequences of random variables [8]. One of the most well-studied stochastic process is a memoryless Markov process, which assumes that the future in the sequence is independent of the past, given the present. The majority of random sequences around us however are not Markovian and

contain memory effects. A renewal-reward process is one of the simplest stochastic processes that can describe these effects. The process is defined by two i.i.d. sequences, where the first one is the sequence of the state of the system, while the second one is the sequence of waiting times, after each of which the system changes its state from one to the other. When the waiting time is distributed exponentially, the corresponding renewal-reward process is Markovian, known to be equivalent to a continuous-time Markov process, whereas when it is distributed otherwise, it becomes non-Markovian. More prominent differences from Markov processes appear when the waiting time is distributed according to a heavy-tailed power law distribution.

In general, the tail of probability distributions is related to a rare event and has a small impact for the entire system. However, when probability distributions are heavy-tailed, this insight does not work. For instance, in the financial market, the melt up or shock of the market is a rare event following a heavy-tailed distribution [9, 10]. In infectious disease spreading, a super spreader is a rare event in the system, whose occurrence is also distributed by a heavy-tailed distribution [11, 12]. A mathematical theory that illustrates the importance of a rare event of a single power-law distributed variable is the *single big jump principle* [13]. It proves that the sum of independent and identically distributed random variables extracted from a heavy-tailed distribution is dominated by their maximum.

To study rare events in a probabilistic set-up, one uses the large deviation principle (LDP), which studies fluctuations of the arithmetic mean of independent or shortly-correlated random variables. For uncorrelated variables, the variance of the empirical mean decreases proportionally with the inverse of the number of the variables. The LDP focuses on rare events whose empirical mean largely deviates from its expectation when the number of the variables is large. Concretely, the principle introduces the large deviation function (LDF) using the logarithm of the probability distribution of the arithmetic mean. This logarithm divided by the averaging number (the number of the variables) converges to a certain function in the large averaging number limit. This limit function, called LDF, provides asymptotic information about the probability of rare events. The single big jump principle mentioned above can be stated as follows: the LDF can be calculated from the probability of a single variable, when each variable follows a heavy-tailed distribution.

In renewal-reward processes with heavy-tailed waiting time distribution, similar phenomena, where an extreme event plays an important role, could be expected. In the article [14], the authors studied this problem and proved that the LDF of the target variable (the time average of the state) was indeed dominated by an event with a single waiting time, i.e., by an event where the state of the system does not change at all. When this happens, the LDF vanishes in a certain range of the target variable. LDF is not analytic at the two ends of this zero region. The logarithm of the probability distribution is subproportional to the averaging time in this range, and is proportional otherwise. These singularities and the zero region are called an *affine part* throughout this thesis (See Fig.1.1). Studying how the affine part develops as the averaging time increases is interesting, but hampered by a lack of general theory that can be used to study the asymptotics of LDP. For example, strong large deviation principle [15] was proposed to study the asymptotics, but this theory seems not helpful in our context. Another related work has been done by Tsirelson [16], giving rigorous proofs for the large time asymptotics of the Legendre transform of LDF (scaled cumulant generating function) in renewal reward processes for general waiting time distributions. However,

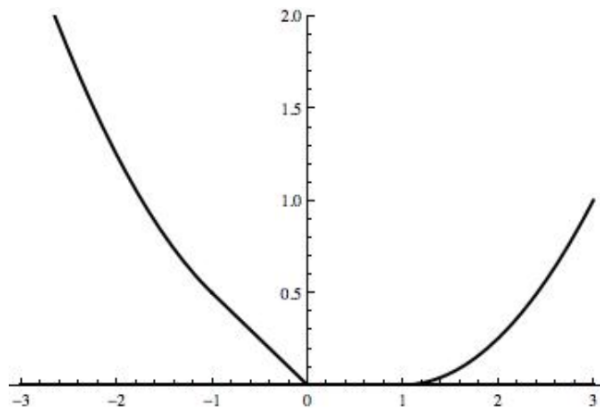


Fig. 1.1: The rate function with the affine part. In heavy-tailed renewal-reward processes, the rate function shows an affine part (the flat bottom of the rate function). This figure is taken from [1].

unfortunately, he used a condition in which the LDF did not have any singularity.

The goal of this thesis is to tackle this problem by focusing on specific examples. We summarize our results below. In this thesis, we first introduce the background of our research in chapter 2. Our main results are described in chapter 3, chapter 4 and chapter 5.

Summary of Chapter 3

We consider a counting process N_t defined as

$$N_t = \sup\{k : S_k \leq t\},$$

where $S_k = \tau_1 + \dots + \tau_k$ and $(\tau_j)_{j=1}^k$ is a sequence of the renewal times, independently distributed according to heavy-tailed distributions $p(t)$. For the heavy-tailed distributions, we first consider the Pareto distribution $p(t)$ with a parameter $m > 2$:

$$p(t) : = \begin{cases} 0 & t \leq 0 \\ \frac{(m-1)}{(1+t)^m} & t > 0 \end{cases} \quad (1.0.1)$$

The counting process is the number of events that have occurred up to time $t > 0$. We define the moment generating function of a counting process as $M(t, h) = \mathbb{E}[e^{hN_t}]$. The main result of this chapter is then given by the following theorem.

Theorem 3.3.1 Let $(N_t)_{t \geq 0}$ the counting process with waiting times distributed according to a Pareto's law with an integer parameter $m \geq 3$, then for any $h < 0$:

$$\lim_{t \rightarrow \infty} t^{m-1} M(t, h) = \frac{1}{1 - e^h}. \quad (1.0.2)$$

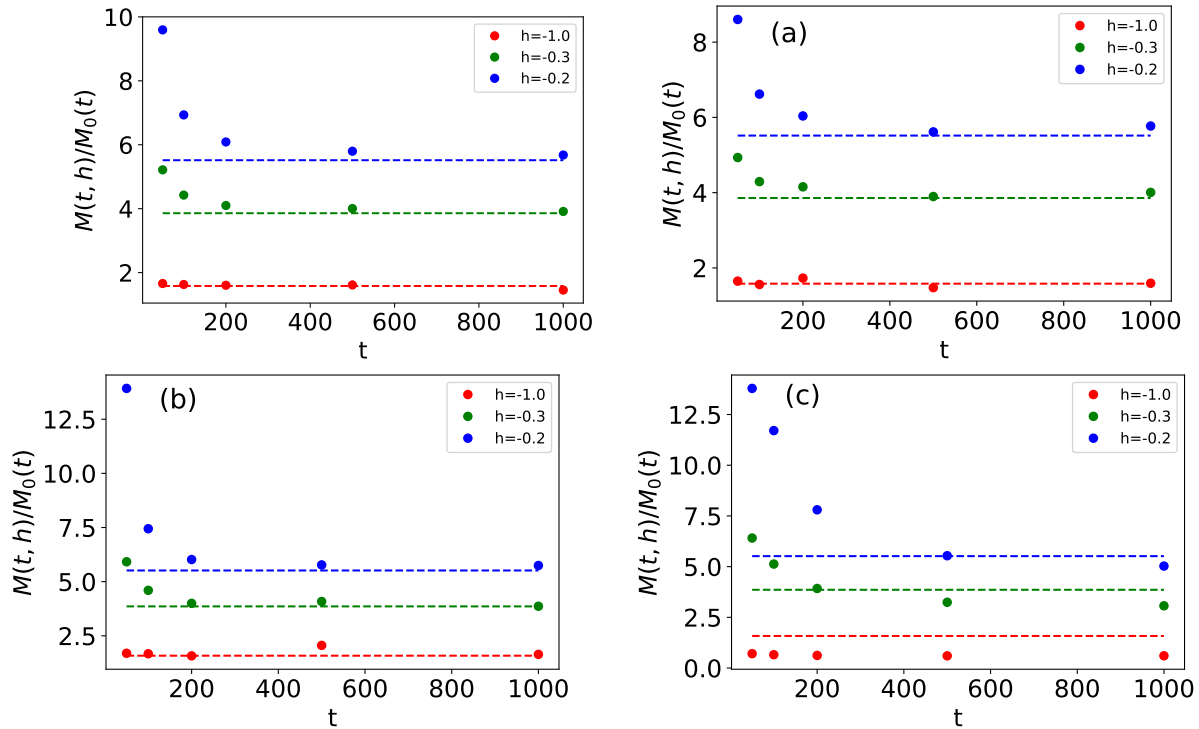


Fig. 1.2: The numerical results of $M(t, h)/M_0(t)$ (filled circles) together with $1/(1 - e^h)$ (dashed lines) for Pareto distribution with $m = 3.0$ (a), Pareto distribution with $m = 3.5$ (b), inverse Rayleigh distribution with $\beta = 1$ (c) and log-normal waiting-time distribution with $\mu = 0$ and $\sigma = 1.5$ (d). Here, $M_0(t) = 1 - F(t)$ and $F(t)$ is a cumulative distribution function.

We numerically study the moment generating functions of the counting process $M(t, h)$ for several waiting time distributions: the Pareto distribution, the inverse Rayleigh distribution

$$p_{Ray}(t) : = \begin{cases} 0 & t \leq 0 \\ \frac{\beta}{t^3} e^{-\frac{\beta}{2t^2}} & t > 0 \end{cases} \quad (1.0.3)$$

with a parameter β and log-normal distribution

$$p_{log}(t) : = \begin{cases} 0 & t \leq 0 \\ \frac{1}{\sqrt{2\pi}\sigma t} e^{-\frac{(\log(t)-\mu)^2}{2\sigma^2}} & t > 0 \end{cases} \quad (1.0.4)$$

with parameters μ and σ . We then plot $M(t, h)/M_0(t)$ (where $M_0(t) = 1 - F(t)$ with the cumulative distribution $F(t)$) in Fig.1.2 together with $1/(1 - e^h)$, demonstrating the validity of Theorem 3.3.1 beyond its assumption.

We also study the asymptotic behavior of $\log \mathbb{P}[N_t < xt]$ in our numerical simulations and observe the following general asymptotic form

$$\log \mathbb{P}[N_t < xt] \sim a \log M_0(t) + \log(t) + b \quad (1.0.5)$$

with constants a, b (that can potentially depend on x) in Fig.1.3. For the Pareto and the inverse Rayleigh waiting time distributions, a seems to be 1, while a is different from 1 for the log-normal waiting-time distribution.

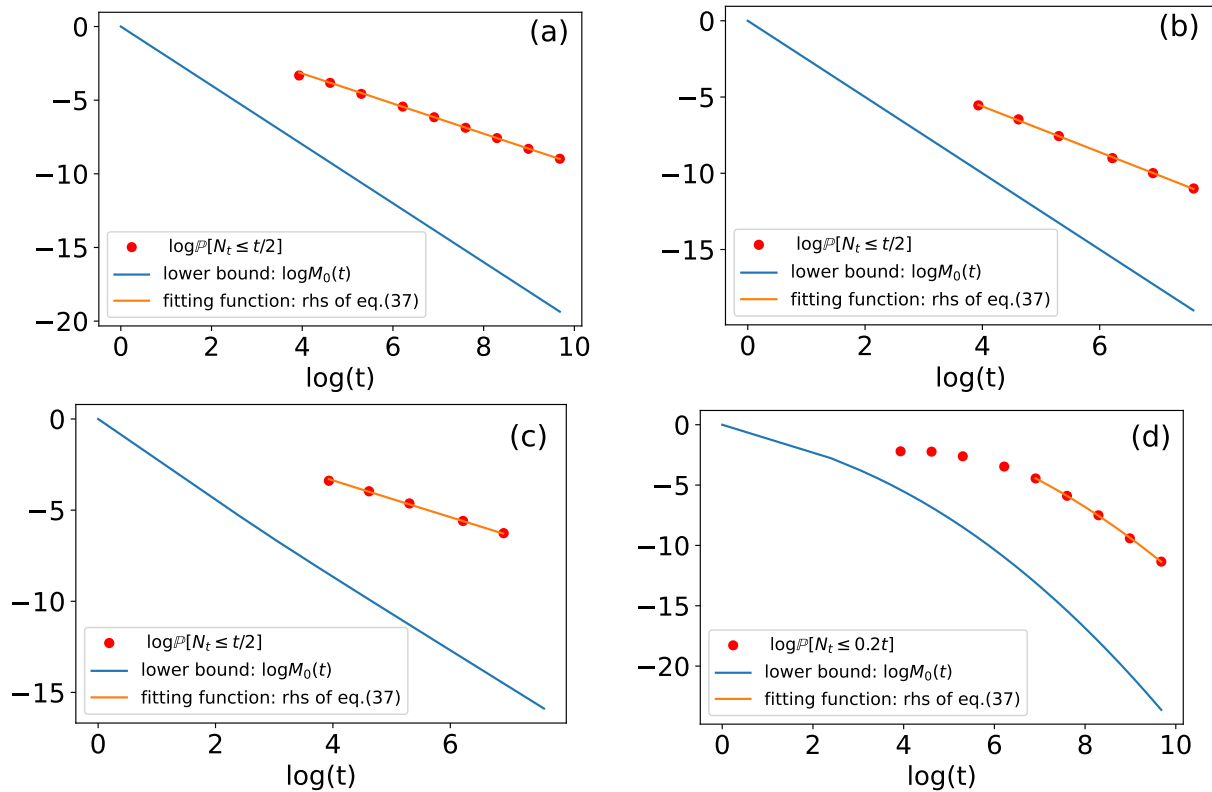


Fig. 1.3: $\log \mathbb{P}[N_t < xt]$ for several waiting time distributions: (a) Pareto distribution with $m = 3$, (b) Pareto distribution with $m = 3.5$, (c), inverse Rayleigh distribution with $\beta = 1$ and (d) the log-normal waiting-time distribution with $\mu = 0$ and $\sigma = 1.5$. The blue line (lower bound) is $\log M_0(t)$ and a fitting function is $a \log M_0(t) + \log(t) + b$ (with fitting parameters a, b). These fitting parameters are determined as $a = 1.01, b = 0.92$ for (a), $a = 1.00, b = 0.43$ for (b), $a = 1.00, b = 2.00$ for (c) and $a = 0.89, b = 2.51$ for (d).

Summary of Chapter 4

In this chapter, we re-derive an affine part in cumulant generating functions (CGFs) [1] by using a variational principle developed in large deviation theory. This variational principle has been applied to study a singularity appearing in the LDF in, among others, kinetically constrained models (KCM) [2] and active matters [3]. These models are defined using Markov processes, because of which the LDF of time-averaged quantities does not have any singularity whenever the system size (not the averaging time) is finite. Our focus is on how the same methodology can be extended to our non-Markovian problem to derive the affine part.

Recalling the set-up of the article [1], we consider the renewal-reward process with the inverse Rayleigh waiting time distribution. We confine a tracer particle in a one-dimensional box that has two different temperatures at both ends. The confined tracer has a random speed v distributed according to the following distribution:

$$q_{\beta_{-1,1}}(v) = \beta_{-1,1} v e^{-\beta_{-1,1} \frac{v^2}{2}} \mathbb{1}_{(v)>0} \quad (1.0.6)$$

where $\beta_{-1,1} = 1/T_{-1,1}$ is the inverse temperature of the left- or right-wall where the collision takes place. We introduce a sign variable σ_k that takes a value either 1 or -1 depending on the direction to which the particle moves between k -th and $(k+1)$ -th collisions. We denote the state space of this variable by $E \equiv \{-1, +1\}$. The initial position and velocity of the particle are denoted by (x_0, v_0) , from which we can derive $\sigma_0 = v_0/|v_0|$, $\sigma_k = (-1)^k \sigma_0$. We also define the velocity v_k of the particle between k -th and $(k+1)$ -th collisions. These are drawn randomly from one of the Rayleigh distributions (1.0.6) depending on the previous hot wall with which the particle collides. We denote by S_k the time at which $(k+1)$ -th collision occurs. Introducing $\hat{\sigma}_k = \frac{1}{2}(\sigma_k + 1)$, the time of the first collision with a wall is written as

$$S_0 = S_0(x_0, v_0) := \frac{\hat{\sigma}_0 - x_0}{v_0} > 0. \quad (1.0.7)$$

Note that k -th inter-arrival time is given as

$$\tau_k := \frac{\sigma_k}{v_k}, \quad (1.0.8)$$

which is distributed as

$$p(\tau_k | \sigma_{k-1}) = \frac{\beta_{\sigma_{k-1}}}{\tau^3} \exp\left(-\frac{\beta_{\sigma_{k-1}}}{2\tau^2}\right) \mathbb{1}_{(\tau)>0}. \quad (1.0.9)$$

The arrival time S_k is then written as

$$S_k := S_0 + \tau_1 + \tau_2 + \cdots + \tau_k, \quad k \geq 1. \quad (1.0.10)$$

The energy exchanged between the two walls during a time interval $[0, t]$ is given by

$$J[0, t] := \frac{1}{2} \sum_{k \geq 1: S_k \leq t} v_k^2 \sigma_k. \quad (1.0.11)$$

We next introduce the lower bound for the CGF. For this, we first denote by \mathcal{C} a path (or a trajectory) of the state of the system and by $\mathbb{P}(\mathcal{C})$ the probability of \mathcal{C} (the path probability). See Chapter 4 for the detailed expression of the path probability. We then introduce a control system defined as, for example, the tracer particle model with temperatures different from the original ones. The path probability of the control system is denoted \mathbb{P}^{con} . Then, we have the following bound for the cumulant generating function $\phi(h, t) (= \log \mathbb{E}[e^{-hJ}])$

$$\phi(h, t) \geq -h\mathbb{E}_{\text{con}}[A] - D(\mathbb{P}^{\text{con}}||\mathbb{P}), \quad (1.0.12)$$

where

$$D(\mathbb{P}^{\text{con}}||\mathbb{P}) = \mathbb{E}_{\text{con}} \left[\log \frac{\mathbb{P}^{\text{con}}(t, \mathcal{C})}{\mathbb{P}(t, \mathcal{C})} d\mathcal{C} \right], \quad (1.0.13)$$

is a Kullback-Leibler (KL) divergence.

The affine part can be derived using this bound with a control system where the state of the system is confined to the initial condition:

$$\mathbb{P}^{\text{con}} = \delta_{N_t, 0}, \quad (1.0.14)$$

i. e.,

$$\lim_{t \rightarrow \infty} \frac{\phi(h, t)}{t} \geq 0 \quad (1.0.15)$$

Furthermore, considering as a control system the tracer particle model with temperatures $\beta_{\pm 1}^{\text{con}}$ different from the original ones, we obtain

$$\lim_{t \rightarrow \infty} \frac{\phi(h, t)}{t} \geq -\kappa^{\text{con}} \left[\frac{-h - \beta_1^{\text{con}} + \beta_1}{\beta_1^{\text{con}}} + \frac{h - \beta_{-1}^{\text{con}} + \beta_{-1}}{\beta_{-1}^{\text{con}}} + \log \frac{\beta_1^{\text{con}} \beta_{-1}^{\text{con}}}{\beta_1 \beta_{-1}} \right]. \quad (1.0.16)$$

A hydrodynamic limit (see Chapter 4 in detail) allows us to compute an analytical expression of the optimal bound under this control system. Interestingly, the right-hand side of this optimal bound and (1.0.15) are nothing but the analytical expression of CGF obtained in [4], indicating that these bounds are saturated.

Summary of Chapter 5

In this chapter, we focus on the anomalous fluctuations of the time-averaged quantities in heavy tailed renewal processes. In particular, we analyze the variance of heavy waiting time distributions. The variance can tell us directly how much the averaged quantities fluctuate. We first focus on the fluctuation of a counting process, which is the simplest model of a renewal-reward process, with heavy-tailed waiting time distributions. Recalling the definition of a counting process, it is given by

$$N_t = \sup\{k : S_k \leq t\}, \quad (1.0.17)$$

where $S_k = \tau_1 + \dots + \tau_k$. We denote its q -th order moment by $m_q(t)$:

$$m_q(t) := \mathbb{E}[N_t^q]. \quad (1.0.18)$$

To analyse the asymptotics of $m_q(t)$, we rely on renewal equations: a powerful tool to analyse renewal-reward processes. From a straightforward computation, one can establish the following renewal equation for $m_1(t)$ [5]:

$$m_1(t) = F(t) + \int_0^t ds m_1(t-s)p(s), \quad (1.0.19)$$

where F is the cumulative waiting time distribution function. From this equation, a simple expression for the Laplace transform of $m(t)$ is derived. Defining the Laplace transform of a function f by

$$\tilde{f}(s) := \int_0^\infty e^{-st} f(t) dt, \quad (1.0.20)$$

we then derive, from the equation (1.0.19),

$$\tilde{m}_1(s) = \frac{\tilde{F}(s)}{1 - s\tilde{F}(s)}, \quad (1.0.21)$$

where we have used $\tilde{p}(s) = s\tilde{F}(s)$.

Similarly, one can also derive a renewal equation for $m_2(t)$,

$$\begin{aligned} m_2(t) &= \int_0^t \mathbb{E}[N_{t-s}^2] p(s) ds \\ &+ 2 \int_0^t m_1(t-s) p(s) ds + F(t), \end{aligned} \quad (1.0.22)$$

from which the Laplace transform of $m_2(t)$ is obtained as

$$\tilde{m}_2(s) = \tilde{m}_1(s)(1 + 2s\tilde{m}_1(s)). \quad (1.0.23)$$

Here, we use the inverse Rayleigh distribution

$$p_\beta(\tau) = \frac{\beta}{\tau^3} \exp\left(-\frac{\beta}{2\tau^2}\right) \mathbb{1}(\tau > 0), \quad (1.0.24)$$

and the Pareto distribution

$$p_\alpha(\tau) = \frac{\alpha - 1}{(1 + \tau)^\alpha} \mathbb{1}(\tau > 0) \quad (1.0.25)$$

with $\alpha = 3$, both of which do not have a finite second moment, *i.e.*, $\mathbb{E}[\tau^2] = \infty$ to consider the variance of heavy-tailed waiting time distributions. For the inverse Rayleigh distribution, we obtain

$$\frac{m_1(t)}{t} - \sqrt{\frac{2}{\beta\pi}} = \frac{\ln(t)}{t\pi} + o\left(\frac{\ln(t)}{t}\right) \quad (1.0.26)$$

and the variance $c_2(t)$

$$c_2(t) = \frac{2\sqrt{2}}{\sqrt{\beta}\pi^{3/2}} \frac{\ln(t)}{t} + o\left(\frac{\ln(t)}{t}\right) \quad (1.0.27)$$

for large t , where we define the variance as

$$c_2(t) = \frac{m_2(t) - m_1(t)^2}{t^2}. \quad (1.0.28)$$

As with the calculation of this case, for the Pareto distribution, we obtain

$$\frac{m_1(t)}{t} - 1 = \frac{\ln(t)}{t} + o\left(\frac{\ln(t)}{t}\right). \quad (1.0.29)$$

and

$$c_2(t) = 2\frac{\ln t}{t} + o\left(\frac{\ln(t)}{t}\right). \quad (1.0.30)$$

We also study the behavior of the fluctuations of the current of energy carried by a particle, which is introduced in (1.0.11). In particular, we rewrite the current as

$$J_\theta(t) := \frac{1}{2} \sum_{k=1}^{N_t} v_k^2 \sigma_k \quad (1.0.31)$$

with an initial condition $\theta = (x_0, v_0)$. In addition, we denote by $m_{\theta,q}(t)$ the q -th moment of $J_\theta(t)$:

$$m_{\theta,q}(t) = \mathbb{E}[J_\theta^q(t)]. \quad (1.0.32)$$

Thus, we can calculate the fluctuations of the current using this formula.

Next, for simplicity, we consider only the following two types of initial conditions:

$$\theta_+ = (0, v_0) \quad (1.0.33)$$

with $v_0 < 0$ and

$$\theta_- = (1, v_0) \quad (1.0.34)$$

with $v_0 > 0$, *i.e.*, the cases of a particle just before hitting the left wall (temperature β_+) and of a particle just before hitting the right wall (inverse temperature β_-). As the particle immediately hits each wall when the process starts, the value of the initial velocity v_0 is unimportant. We thus denote by $+$ the initial condition θ_+ and by $-$ the initial condition θ_- . Then, we can obtain the asymptotic form of the expected value and the variance of the time averaged current as with the derivation of the fluctuations of the counting process. Those are given by

$$\frac{m_{\pm,1}(t)}{t} = \kappa \left(\frac{1}{\beta_+} - \frac{1}{\beta_-} \right) + \kappa^2 \frac{(\beta_+ + \beta_-)}{2} \left(\frac{1}{\beta_+} - \frac{1}{\beta_-} \right) \frac{\ln t}{t} + o\left(\frac{\ln(t)}{t}\right) \quad (1.0.35)$$

$$\text{Var}\left(\frac{J_\pm(t)}{t}\right) = \kappa^3 (\beta_+ + \beta_-) \left(\frac{1}{\beta_+} - \frac{1}{\beta_-} \right)^2 \frac{\ln(t)}{t} + o\left(\frac{\ln(t)}{t}\right). \quad (1.0.36)$$

for large time.

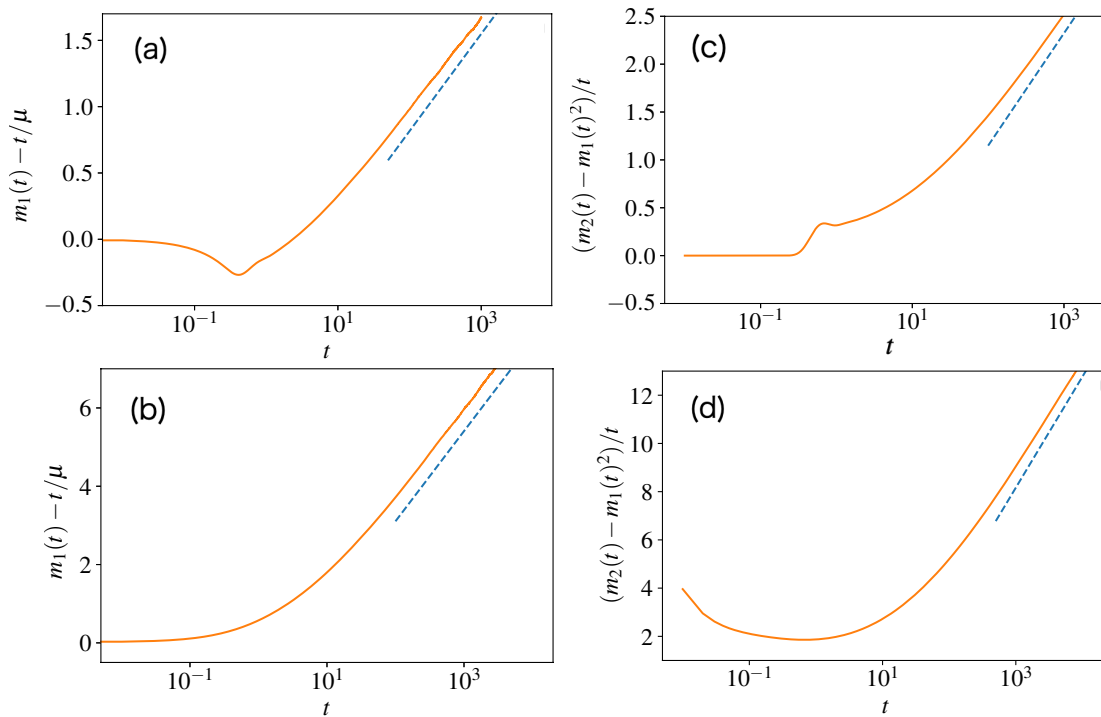


Fig. 1.4: **(a,b)** $m_1(t) - t/\mu$ obtained from numerical simulations of the counting process N_t (with 10^8 samples) are plotted as a function of time in log-scale as orange lines. For the inverse Rayleigh waiting time distribution (a), $\beta = 1$ and $\mu = 1/\sqrt{2/(\beta\pi)}$, while for the Pareto waiting time distribution (b), $m = 3$ and $\mu = 1$. $\ln(t)/\pi + \text{const.}$ and $\ln(t) + \text{const.}$ are also plotted as blue dashed lines for (a) and (b). **(c,d)** $(m_2(t) - m_1(t)^2)/t$ obtained from the same numerical simulations are plotted as a function of time as orange lines for the inverse Rayleigh waiting time distribution (c) and for the Pareto waiting time distribution (d). $\frac{2\sqrt{2}}{\sqrt{\beta\pi^{3/2}}} \ln(t) + \text{const.}$ for (c) and $2 \ln(t) + \text{const.}$ for (d) are also plotted as blue dashed lines in the same figures. The agreements between the slopes of orange lines and those of blue lines in these semi-log graphs demonstrate the validity of (5.2.10), (5.2.13), (5.2.20) and (5.2.21), as detailed in the main text.

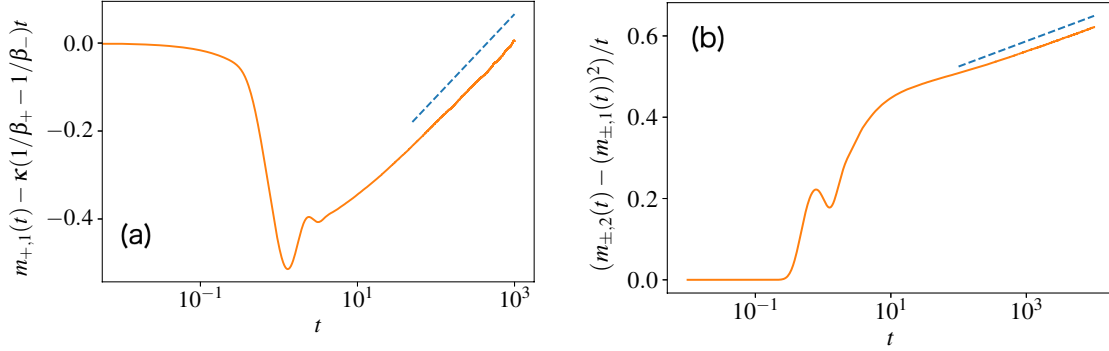


Fig. 1.5: $m_{+,1}(t) - \kappa(1/\beta_+ - 1/\beta_-)$ (a) and $m_{\pm,2}(t)/t^2 - (m_{\pm,1}(t))^2/t^2$ (b) obtained from numerical simulations (with 10^8 samples) are plotted as orange lines. $\beta_+ = 1$, $\beta_- = 2$. Blue dashed lines are $(\kappa^2/2)(\beta_+ + \beta_-)(1/\beta_+ - 1/\beta_-)(\ln t)/t + \text{const.}$ and $\kappa^3(\beta_+ + \beta_-)(1/\beta_+ - 1/\beta_-)^2 + \text{const.}$ The slopes of the numerical-simulation results in semi-log scale converge to those of the dashed reference lines, showing the validity of (5.3.17) and (5.3.29).

In summary, first, we have studied a counting process N_t with two heavy-tailed waiting time distributions: the Pareto distribution with $\alpha = 3$ and the inverse Rayleigh distribution. These two waiting time distributions have an asymptotic form $1/\tau^3$ when the waiting time τ is large, implying that the variance of the waiting time $\mathbb{E}[\tau^2]$ diverges. Because of this divergence, we discussed that the scaled variance of the counting process N_t also diverges in the large t limit. We indeed derived that the scaled variance is asymptotically proportional with $\log(t)$, diverging as $t \rightarrow \infty$. Second, as with the conclusion of N_t , we have clarified the asymptotic behavior of the variance of the time-averaged current $J_\theta(t)$. That inter-arrival time follows the inverse Rayleigh distribution, so that we can obtain the scaled variance is asymptotically proportional with $\log(t)$, diverging as $t \rightarrow \infty$. The memory effect of a stochastic process is related to anomalous divergence of moments.

Chapter 2

Background

In this chapter, I introduce some methods and theories, which are related to my research. In particular, the large deviations theory is the center of my research and it is a powerful way to analyse the probability of rare events. Our results are based on the large deviations theory and the theory of renewal-reward processes. Thus, before showing the main results, we start by considering both theories and introducing the basic tools of our research.

2.1 Renewal Theory

Up to the present, *renewal-reward processes* have been extensively studied in mathematics, physics and biology among other fields. In particular, the renewal equation is a useful approach to various phenomena involving the study of sum of independent random variables. For instance, in physics, a continuous time random walk (CTRW) can be formulated as a renewal-reward process and is observed in some physical experiments [17]. A renewal-reward process can be seen as a stochastic model that is defined as a sequence of pairs made of a waiting time and a random variable representing a “reward”. In addition, when using stochastic models with waiting times having a heavy-tailed distribution, it is possible to take into the account the memory effect in the system. In this context, we will try to consider the influence of the rare events of phenomena modelled by renewal-reward processes. In the following subsection, we introduce the definition of a renewal-reward process and the basic theorems in renewal theory.

2.1.1 Definition

First of all, let us consider a continuous time 1D random walk with arbitrary distributions of jump lengths and waiting times. Both waiting times (τ_i) , $i = 1, 2, \dots$ and jump lengths $(X_i \in \mathbb{R})$, $i = 1, 2, \dots$ are *i.i.d.* whose probability densities are denoted by respectively p (such that $\tau > 0$ a.s. and $\mathbb{E}\tau = \mu < \infty$) and q . The *renewal-reward process* $R(t)$ is then defined as

$$R(t) = X_1 + \dots + X_n, \tag{2.1.1}$$

where the number of jumps n satisfies

$$\tau_1 + \dots + \tau_n \leq t < \tau_1 + \dots + \tau_{n+1}. \tag{2.1.2}$$

A simple example of the renewal-reward process is a counting process N_t defined by $q(x) = \delta(x - 1)$, (so that X_i only takes the value 1), *i.e.* N_t corresponds to the number of jumps until time t . The mathematical definition of a counting process is given by

$$N_t = \sum_{n=1}^{\infty} \mathbf{1}(S_n \leq t), \quad t \in [0, \infty). \quad (2.1.3)$$

Here, S_n is a sum of arrival times :

$$S_n = \sum_{i=1}^n \tau_i. \quad (2.1.4)$$

Formally, a renewal-reward process is defined as a sequence of pairs of $(X_i, \tau_i)_{i \in \mathbb{N}}$ and a counting process is of course a simple example of a renewal-reward process. In addition, we can consider the n -th arrival time that is defined as

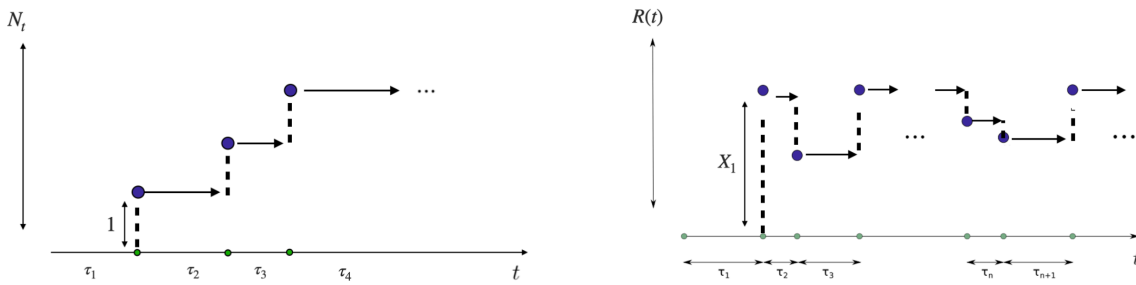


Fig. 2.1: The figures of a counting process and renewal-reward process.

Next, let F_n denote the distribution function of S_n , namely,

$$F_n(t) = \mathbb{P}(S_n \leq t). \quad (2.1.5)$$

Obviously, we have

$$\begin{aligned} \mathbb{E}[S_n] &= n\mu \\ \text{Var}(S_n) &= n\sigma^2. \end{aligned}$$

Here, σ^2 is the variance of τ_1 . The expected value of a counting process N_t is called as the *renewal function* and the expected value of sum of the rewards $R(t)$ is called the *reward function*. Those are given by

$$m(t) = \mathbb{E}[N_t] \quad (2.1.6)$$

$$g(t) = \mathbb{E}[R(t)]. \quad (2.1.7)$$

In renewal theory, the renewal function and reward function follows a universal convergence law called the *elementary renewal theorem*. If we consider a physical phenomenon modelled by a renewal-reward process, we can therefore give the asymptotic value of related random physical quantities. We next list some mathematical models of real-life phenomena described by a renewal-reward process.

Example 1 Consider an electric bulb that fails at times τ_1, τ_2, \dots and is replaced at the time of failure by a new electric bulb of the same sort. The number of bulbs replaced by time t is N_t . Knowing the behavior of $\mathbb{E}[N_t]$ (renewal function), we can roughly understand how many the bulbs have to be replaced to replace by time t , when t is large.

Example 2 Consider driven vehicles with the same constant velocity starting their journey at successive random times. The vehicles are driving in one direction only. Then we can count the number of passing cars. The number of cars is a counting process N_t and they have each inter-arrival times as τ_i . This renewal-process is applied to the mathematical model of traffic flow.

Example 3 Let's consider now an insurance company. Assume that the claims incurred by an insurance company arrive according to a counting process N_t and the sizes of the claims are i.i.d. non-negative random variables X_1, X_2, \dots , with common distribution F , and that the inflow of premium up to time t is ct . Thus the risk reserve at time t is

$$U_t = u + ct - \sum_{i=1}^{N_t} X_i, \quad (2.1.8)$$

where u is the initial value. If $U_t = 0$, we can consider as the insurance company is bankrupt. Therefore, we can estimate the probability of bankruptcy of the insurance company.

The above examples are part of many mathematical models using renewal-reward processes. We can consider that studying expected value of the sum of the random variables derive some unique properties of the systems. Therefore, the renewal function or the reward function are important physical quantities in a renewal-reward process model.

2.1.2 Basic Theory

Here, we study some limit theorems for renewal-reward processes. First of all, we start by considering the strong law of large numbers in probability theory. This will help us to construct basic theory of a renewal-reward process.

Theorem 2.1.1. (Strong Law of Large Numbers (Kolmogorov's law))

Let $(X_i)_{i \in \mathbb{N}}$ be a sequence of mutually independent and identically distributed random variables such that $\mathbb{E}[|X_1|] < \infty$. Then, almost surely

$$\lim_{n \rightarrow \infty} Y_n = \mathbb{E}[X_1]. \quad (2.1.9)$$

where $Y_n = \frac{1}{n} \sum_{i=1}^n X_i$, for $n \geq 1$.

Here, we recall the classical proof under the assumption

$$\sum_{n=1}^{\infty} \frac{1}{n^2} \text{Var}(X_n) < \infty. \quad (2.1.10)$$

Proof. Let X_1, X_2, X_3, \dots be a sequence of *i.i.d.* random variables with finite mean μ and $Y_n = \frac{1}{n} \sum_{i=1}^n X_i$. Without loss of generality, we assume $\mathbb{E}[X_n] = 0$ ($n = 1, 2, \dots$). For $\epsilon > 0$, we define

$$A(\epsilon) = \bigcup_{N=1}^{\infty} \bigcap_{n=N}^{\infty} \{|Y_n| < \epsilon\}$$

Our goal is to prove for any $\epsilon > 0$, $P(A(\epsilon)) = 1$.

For deriving the above statement, we introduce, for $m \geq 1$

$$B_m(\epsilon) \equiv \bigcup_{n=2^{m-1}}^{2^m-1} \{|Y_n| \geq \epsilon\} = \{\max_{2^{m-1} \leq n < 2^m} |Y_n| \geq \epsilon\}. \quad (2.1.11)$$

And for any $l = 1, 2, \dots$, we have

$$A(\epsilon)^c = \bigcap_{N=1}^{\infty} \bigcup_{n=N}^{\infty} \{|Y_n| \geq \epsilon\} \subset \bigcup_{m=l}^{\infty} B_m(\epsilon). \quad (2.1.12)$$

Next, we evaluate the probability $P(B_m(\epsilon))$. Let, $Z_n = \sum_{k=1}^n X_k (= nY_n)$ be a sum of the random variables.

$$\begin{aligned} P(B_m(\epsilon)) &= P\left(\max_{2^{m-1} \leq n < 2^m} \frac{1}{n} |Z_n| \geq \epsilon\right) \\ &\leq P\left(\max_{2^{m-1} \leq n < 2^m} |Z_n| \geq \epsilon 2^{m-1}\right) \\ &\leq P\left(\max_{1 \leq n < 2^m} |Z_n| \geq \epsilon 2^{m-1}\right) \\ &\leq \frac{1}{\epsilon^2 2^{2m-2}} \sum_{k=1}^{2^m} \text{Var}(X_k), \end{aligned} \quad (2.1.13)$$

where we used Kolmogorov's inequality for last line. Therefore, the evaluation of $P(B_m(\epsilon))$ is given by

$$\begin{aligned} P(B_m(\epsilon)) &\leq \frac{4}{\epsilon^2} \sum_{m=1}^{\infty} \frac{1}{2^{2m}} \sum_{k=1}^{2^m} \text{Var}(X_k) \\ &= \frac{4}{\epsilon^2} \sum_{m=1}^{\infty} \sum_{k=1}^{\infty} \frac{1}{2^{2m}} \text{Var}(X_k) \\ &= \frac{4}{\epsilon^2} \sum_{k=1}^{\infty} \text{Var}(X_k) \sum_{m'=m_k}^{\infty} \frac{1}{2^{2m'}} \\ &\leq \frac{16}{3\epsilon^2} \sum_{k=1}^{\infty} \text{Var}(X_k) \frac{1}{k^2} < \infty, \end{aligned} \quad (2.1.14)$$

where the integer m_k satisfies $2^{m_k-1} < k \leq 2^{m_k}$. Under the assumption (2.1.10), the last line converges. Finally, according to (2.1.14) and *Borel-Cantelli lemma*, we can prove

$$P(A(\epsilon)^c) = 0 \Leftrightarrow P(A(\epsilon)) = 1. \quad (2.1.15)$$

□

When we consider the case of $\mathbb{E}[X_n] = \mu_n$, we replace $|Y_n| < \epsilon$ with $|Y_n - \mu_n| < \epsilon$ in the above proof. It gives the same result.

The law of large numbers has a very central role in probability theory. Moreover, the strong law of large numbers is useful for proving the law of large numbers in a renewal-reward process.

Theorem 2.1.2. (Law of Large Numbers in a Renewal Process)

When $0 < \mu < \infty$, the counting process N_t satisfies

$$\lim_{t \rightarrow \infty} \frac{N_t}{t} = \frac{1}{\mu} \quad (2.1.16)$$

with probability 1.

Proof. From the definition of a renewal-reward process, $S_{N_t} \leq t < S_{N_t+1}$ for $t > 0$, which gives

$$\frac{S_{N_t}}{N_t} \leq \frac{t}{N_t} < \frac{S_{N_t+1}}{N_t}. \quad (2.1.17)$$

From the strong law of large numbers, we know $S_n/n \rightarrow \mu$ as $n \rightarrow \infty$ with probability 1. It follows that $S_{N_t}/N_t \rightarrow \mu$ as $t \rightarrow \infty$ since $N_t \rightarrow +\infty$ as $t \rightarrow +\infty$ *a.s.*. Moreover, we can see $(N_t + 1)/N_t \rightarrow 1$ as $t \rightarrow \infty$ with probability 1. Thus,

$$\lim_{t \rightarrow \infty} \frac{t}{N_t} = \mu. \quad (2.1.18)$$

□

In the study of a stochastic process, we often calculate random sums and expected values of it. Wald's identity is an important identity for calculating expected value of random sums of random variables.

Lemma 2.1.3. (Wald's Identity)

Let X_1, X_2, X_3, \dots be a sequence of *i.i.d.* random variables with finite mean. Let N be an integer-valued stopping time with $\mathbb{E}[N] < \infty$. Then, we have,

$$\mathbb{E}[X_1 + X_2 + \dots + X_N] = \mathbb{E}[X_1]\mathbb{E}[N]. \quad (2.1.19)$$

Proof. A random sum of random variables is calculated as

$$\begin{aligned} \mathbb{E}[X_1 + X_2 + \dots + X_N] &= \mathbb{E} \left[\sum_{n=1}^{\infty} X_n \mathbf{1}\{N \geq n\} \right] = \sum_{n=1}^{\infty} \mathbb{E} [X_n \mathbf{1}\{N \geq n\}] \\ &= \sum_{n=1}^{\infty} \mathbb{E} [\mathbb{E}[X_n \mathbf{1}\{N \geq n\} | X_1, \dots, X_{n-1}]]. \end{aligned} \quad (2.1.20)$$

where n is a positive integer. Note that since N is a stopping time, $\mathbb{1}\{N \geq n\} = 1 - \mathbb{1}\{N \leq n - 1\}$ is a function of X_1, \dots, X_{n-1} because the event $\{N \leq n - 1\}$ is determined by X_1, \dots, X_{n-1} . Therefore, we can divide indicator function and random variables.

$$\begin{aligned} \sum_{n=1}^{\infty} \mathbb{E} [\mathbb{E}(X_n \mathbb{1}\{N \geq n\} | X_1, \dots, X_{n-1})] &= \sum_{n=1}^{\infty} \mathbb{E} [\mathbb{1}\{N \geq n\} \mathbb{E}(X_n | X_1, \dots, X_{n-1})] \\ &= \sum_{n=1}^{\infty} \mathbb{E} [\mathbb{1}\{N \geq n\} \mathbb{E}[X_n]] \\ &= \mathbb{E}[X_1] \sum_{n=1}^{\infty} \mathbb{P}(N \geq n) = \mathbb{E}[X_1] \mathbb{E}[N] \quad (2.1.21) \end{aligned}$$

□

Theorem 2.1.4. (Elementary Renewal Theorem)

Let, N_t be a counting process such that $\mu = \mathbb{E}[\tau_1]$ satisfies $0 < \mu < \infty$. Then the renewal function $\mathbb{E}[N_t] = m(t)$ satisfies

$$\lim_{t \rightarrow \infty} \frac{m(t)}{t} = \frac{1}{\mu}. \quad (2.1.22)$$

Proof. First of all, we show a lower bound on $m(t)/t$ by using S_{N_t+1} , which is the epoch of the first arrival after time t . From Wald's identity and $t < S_{N_t+1}$

$$\begin{aligned} t < \mathbb{E}[S_{N_t+1}] &= (m(t) + 1)\mu \\ \Leftrightarrow \frac{m(t)}{t} &> \frac{1}{\mu} - \frac{1}{t} \end{aligned} \quad (2.1.23)$$

Clearly this lower bound approaches $1/\mu$ as $t \rightarrow \infty$. For the upper bound, we introduce truncated arrival times. For an arbitrary constant $a > 0$, let $\tau_{a,i} = \min(a, \tau_i)$ and consider the renewal process with the sequence of inter-arrival times $\boldsymbol{\tau}_a = (\tau_{a,1}, \tau_{a,2}, \dots)$. Since these truncated random variables are *i.i.d.*, they form a related renewal counting process $N_{a,t}$ with $m_a(t) = \mathbb{E}[N_{a,t}]$. Moreover, we have $m_a(t) \leq m(t)$. As with deriving the lower bound, Wald's identity gives $(m_a(t) + 1)\mu_a \leq t + a$. Therefore,

$$\frac{m(t)}{t} \leq \frac{m_a(t)}{t} \leq \left(\frac{1}{\mu_a} + \frac{a}{t\mu_a} \right) - \frac{1}{t}. \quad (2.1.24)$$

Finally, $\lim_{t \rightarrow \infty} m(t)/t \rightarrow 1/\mu_a$ and $\mu_a \rightarrow \mu$ as $a \rightarrow \infty$. Thus, the upper bound approaches $1/\mu$ as $t \rightarrow \infty$. □

For the reward function $g(t)$, we can derive the elementary renewal theorem for reward function by using the elementary renewal theorem for the renewal function. Wald's identity shows $\mathbb{E}[R(t) + X_{n+1}] = \mathbb{E}[X_1](m(t) + 1)$. Then, we can derive

$$\frac{\mathbb{E}[X_1]m(t) + \mathbb{E}[X_1]}{t} = \frac{\mathbb{E}[X_1]}{\mu} + \frac{\mathbb{E}[X_1]}{t} \rightarrow \frac{\mathbb{E}[X_1]}{\mu} \quad (2.1.25)$$

as $t \rightarrow \infty$.

The elementary renewal theorem for a reward function implies that the expected value of the sum of random reward increases in proportion to time with the density of the average of rewards.

Theorem 2.1.5. (Blackwell's theorem (Renewal Theorem))

Let, N_t be a counting process such that $\mu = \mathbb{E}[\tau_1]$ satisfies $0 < \mu < \infty$. Asymptotically, the expected number of renewals in an interval is proportional to the length of the interval. Namely,

$$\lim_{t \rightarrow \infty} [m(t+a) - m(t)] = \frac{a}{\mu} \quad (2.1.26)$$

for all $a \geq 0$.

By using the elementary renewal theorem, we can prove Blackwell's theorem.

Proof. First, we define

$$g(x) := \lim_{t \rightarrow \infty} [m(t+x) - m(t)] \quad (x \geq 0). \quad (2.1.27)$$

Note that

$$m(t+x+y) - m(t) = m(t+x+y) - m(t+x) + m(t+x) - m(t). \quad (2.1.28)$$

Let $t \rightarrow \infty$, we conclude that

$$g(x+y) = g(x) + g(y) \quad (x, y \geq 0). \quad (2.1.29)$$

Namely, the function $g(x)$ is a linear function. Therefore, for any $x \geq 0$, $g(x)$ is given by

$$g(x) = cx, \quad (2.1.30)$$

where c is a constant. For deriving the value of c , we define a sequence

$$x_n = m(n) - m(n-1) \quad (n \in \mathbb{N}). \quad (2.1.31)$$

Note that, $\sum_{i=1}^n x_i = m(n)$ and $\lim_{n \rightarrow \infty} x_n = g(1) = c$. Therefore, we have

$$\lim_{n \rightarrow \infty} \frac{\sum_{i=1}^n x_i}{n} = \lim_{n \rightarrow \infty} \frac{m(n)}{n} = \frac{1}{\mu}. \quad (2.1.32)$$

Here, by noting that $\sum_{i=1}^n x_i/n = c$ for any $n \geq 1$ we obtain $c = 1/\mu$. □

2.1.3 Renewal Equation

In this subsection, we discuss the renewal equation. It will be the base of our discussion of the finite time correction to the renewal theorem. We start by introducing the conditional expectation of a counting process with first arrival time for deriving the renewal equation. The renewal function is:

$$m(t) = \mathbb{E}[N_t] = \mathbb{E}[\mathbb{E}(N_t | \tau_1)], \quad (2.1.33)$$

where t is time and the probability distribution function is $p(t)$. In addition, splitting the domain of integration $[0, \infty)$ into two parts $[0, t]$ and (t, ∞) :

$$m(t) = \int_0^{\infty} \mathbb{E}[N_t | \tau_1 = s] p(s) ds = \int_0^t \mathbb{E}[N_t | \tau_1 = s] p(s) ds + \int_t^{\infty} \mathbb{E}[N_t | \tau_1 = s] p(s) ds. \quad (2.1.34)$$

If $s > t$ then $\mathbb{E}[N_t | \tau_1 = s] = 0$. If $0 \leq s \leq t$, the *renewal property* says that $\mathbb{E}[N_t | \tau_1 = s] = 1 + m(t - s)$. Thus we have

$$m(t) = \int_0^t [1 + m(t - s)]p(s)ds = F(t) + (m * p)(t), \quad (2.1.35)$$

where $F(t)$ is a cumulative distribution function (CDF). This equation includes the information of how to renew the events and the memory of the process. Let's consider the renewal equation for a Poisson process. In that case we have $F(t) = 1 - e^{-rt}$ for the cumulative distribution function. This cumulative distribution function satisfies $F(\infty) = 1$ and $F(0) = 0$. The renewal equation is given by

$$m(t) = 1 - e^{-rt} + \int_0^t m(t - s)re^{-rs}ds. \quad (2.1.36)$$

Substituting $x = t - s$ in the integral gives

$$m(t) = 1 - e^{-rt} + re^{-rt} \int_0^t m(x)e^{-rx}dx. \quad (2.1.37)$$

multiplying through by e^{rt} , differentiating with respect to t the equation is

$$\begin{aligned} (m(t)e^{rt})' &= re^{rt} + r\left(\int_0^t m(x)e^{-rx}dx\right)' \\ m'(t) &= r \\ \Rightarrow m(t) &= rt \end{aligned} \quad (2.1.38)$$

because $m(0) = 0$. the result follows. Of course, we recover the result of the renewal theorem

$$\lim_{t \rightarrow \infty} \frac{m(t)}{t} = \frac{1}{\mu} \quad (2.1.39)$$

where μ is the mean value of an inter-arrival times. We will extensively use the Laplace transform of the renewal equation in the next chapter. The Laplace transform of a renewal equation is one of the way to analyse this convolution equation. Laplace transform is defined as

$$\mathcal{L}[f](s) = \tilde{f}(s) = \int_0^\infty e^{-st}f(t)dt. \quad (2.1.40)$$

By using the Laplace transform, the convolution term of a renewal equation is divided in a product. Therefore, the Laplace transform of a renewal equation is calculated as

$$\begin{aligned} \int_0^\infty e^{-st}m(t)dt &= \int_0^\infty e^{-st}F(t)dt + \int_0^\infty dt \int_0^t e^{-st}m(t - x)p(x) \\ \tilde{m}(s) &= \tilde{F}(s) + \int_0^\infty dt \int_0^t e^{-s(t-x)}e^{-sx}m(t - x)p(x) \\ &= \tilde{F}(s) + \int_0^\infty dy e^{-sy}m(y) \int_0^\infty e^{-sx}p(x) \\ &= \tilde{F}(s) + \tilde{m}(s)\tilde{p}(s), \end{aligned} \quad (2.1.41)$$

where we performed change of variables as $t - x = y$. The cumulative distribution function F and the renewal function m have the relation as follows:

$$\begin{aligned}\tilde{m}(s) &= \frac{\tilde{F}(s)}{1 - \tilde{p}(s)} \\ &= \frac{\tilde{F}(s)}{1 - s\tilde{F}(s)}.\end{aligned}\tag{2.1.42}$$

As with (5.1.5), we consider exponential distribution for solving (2.1.42). Laplace transform of $F(t) = 1 - e^{-rt}$ is given by

$$\tilde{F}(s) = \int_0^\infty e^{-st}(1 - e^{-rt})dt = \frac{1}{s} - \frac{1}{s+r}.\tag{2.1.43}$$

We substitute the result of the $\tilde{F}(s)$ into (2.1.42).

$$\begin{aligned}\tilde{m}(s) &= \frac{\tilde{F}(s)}{1 - \tilde{p}(s)} \\ &= \frac{\frac{1}{s} - \frac{1}{s+r}}{1 - s\left(\frac{1}{s} - \frac{1}{s+r}\right)} \\ &= \frac{r}{s^2}.\end{aligned}\tag{2.1.44}$$

Thus taking the inverse Laplace transform, we recover $m(t) = rt$.

2.1.4 Renewal Equation for a Moment Generating Function

It is also possible to obtain a renewal equation for the moment generating function (MGF). For constructing the renewal equation of MGF of N_t , we calculate the expected value of e^{hN_t} as in the previous subsection ($h \in \mathbb{R}$ is a biasing field). The expected value of the MGF of N_t is given by

$$M(t) = \mathbb{E}[e^{hN_t}] = \mathbb{E}[\mathbb{E}[e^{hN_t} \mid \tau_1]]\tag{2.1.45}$$

and breaks the domain of integration $[0, \infty)$ into two parts $[0, t]$ and (t, ∞) :

$$\begin{aligned}M(t) &= \int_0^\infty \mathbb{E}[e^{hN_t} \mid \tau_1 = s]p(s)ds = \int_0^t \mathbb{E}[e^{hN_t} \mid \tau_1 = s]p(s)ds + \int_t^\infty \mathbb{E}[e^{hN_t} \mid \tau_1 = s]p(s)ds \\ &= e^h \int_0^t \mathbb{E}[e^{hN_{t-s}}]p(s)ds + \int_t^\infty p(s)ds \\ &= [1 - F(t)] + e^h \int_0^t M(t-s)p(s)ds\end{aligned}\tag{2.1.46}$$

When $h < 0$, the Laplace transformation of (2.1.46) is

$$\tilde{M}(s) = \frac{\frac{1}{s} - \tilde{F}(s)}{1 - e^h s \tilde{F}(s)}.\tag{2.1.47}$$

Again, we apply this relation to the simple case of a Poisson process. Namely, we consider the case of $F(t) = 1 - e^{-rt}$ and calculate the renewal equation.

$$\begin{aligned}
M(t) &= [1 - F(t)] + e^h \int_0^t M(t-s)p(s)ds = e^{-rt} + e^h \int_0^t M(t-s)re^{-rs}ds \\
&= e^{-rt} + re^h e^{-rt} \int_0^t M(y)e^{ry}dy \quad (y = t-s) \\
\rightarrow \frac{dM(t)}{dt} &= -re^{-rt} - r^2 e^h e^{-rt} \int_0^t M(y)e^{ry}dy + re^h M(t) \\
&= -re^{-rt} - r^2 e^h \frac{M(t) - e^{-rt}}{re^h} + re^h M(t) \\
&= rM(t)(e^h - 1). \tag{2.1.48}
\end{aligned}$$

Accordingly we derived differential equation of $M(t) = \mathbb{E}[e^{hN_t}]$. Therefore $M(t)$ is given by

$$M(t) = e^{-rt(1-e^h)} \tag{2.1.49}$$

because $M(0) = 1$. When we consider the renewal equation of the MGF with heavy-tailed distribution, the calculation is more complex than the case of exponential distribution because of the singularity of the power law function. We will explain the calculation in main part of this thesis.

2.1.5 Inverse Laplace Transform Method for a MGF

Here, we study the derivation of the asymptotic form of MGF by using inverse Laplace transform. From the previous subsection, we derived the MGF in Laplace space:

$$\tilde{M}(s) = \frac{\frac{1}{s} - \tilde{F}(s)}{1 - e^h s \tilde{F}(s)}. \tag{2.1.50}$$

By using the relation $s\tilde{F} = \tilde{p}$, we can rewrite the above equation as

$$\tilde{M}(s) = \frac{\frac{1}{s} - \tilde{F}(s)}{1 - e^h \tilde{p}(s)}. \tag{2.1.51}$$

To describe the large time asymptotic form of MGF, we expand $\tilde{p}(s)$. It is given by

$$\tilde{p}(s) = \sum_{i=0} c_i s^i, \tag{2.1.52}$$

where c_i is an expansion coefficient. Then, $\tilde{M}(s)$ is calculated as

$$\begin{aligned}
\tilde{M}(s) &= \frac{\frac{1}{s} - \tilde{F}(s)}{1 - e^h \tilde{p}(s)} \\
&= \frac{\frac{1}{s} - \tilde{F}(s)}{1 - e^h \sum_{i=0} c_i s^i} \\
&= \frac{1}{1 - e^h} \frac{\frac{1}{s} - \tilde{F}(s)}{1 - \frac{e^h}{1 - e^h} \sum_{i=1} c_i s^i} \\
&= \frac{\frac{1}{s} - \tilde{F}(s)}{(1 - e^h)} \left(1 + \frac{e^h}{1 - e^h} \sum_{i=1} c_i s^i + \left(\frac{e^h}{1 - e^h} \sum_{i=1} c_i s^i \right)^2 + \dots \right). \quad (2.1.53)
\end{aligned}$$

In addition, $1/s - \tilde{F}(s)$ can be described as $1 - F(t)$ in normal space. Finally, for large time asymptotic form, we can get $M(t)$ by using inverse Laplace transform. It is given by

$$M(t) \sim \frac{1 - F(t)}{1 - e^h} \quad (2.1.54)$$

as $t \rightarrow \infty$.

2.2 Large Deviation Theory

The theory of large deviations is the mathematical framework for analyzing the asymptotic behavior of the probabilities of rare events (or fluctuations) in probability theory. In particular, it focuses on the exponential decay of probability distributions of such events. In addition, in statistical mechanics, the large deviations theory corresponds to some physical statements. Large deviations theory is one of the methods to analyze non-equilibrium and equilibrium fluctuations in systems made of a large number of components. It provides a rigorous formulation of statistical mechanics, and a generalization of Einstein's fluctuation theory. Roughly speaking, the large deviation principle (LDP) states

$$\mathbb{P}(S_n \simeq s) \sim e^{-nI(s)}, \quad \text{as } n \rightarrow \infty, \quad (2.2.1)$$

where the some positive function I is called the rate function and S_n is a stochastic process taking value in \mathbb{R} . Note that, the rate function I need to satisfy some mathematical conditions for large deviations principle. In good cases, the rate function I is equal to the Legendre transform of the scaled cumulant generating function (CGF) $\varphi : \mathbb{R} \rightarrow \mathbb{R}$

$$\varphi(h) = \lim_{n \rightarrow \infty} \frac{1}{n} \log \mathbb{E}[e^{hS_n}], \quad (2.2.2)$$

i.e., $I(s) = \sup_{h \in \mathbb{R}} \{hs - \varphi(h)\}$. Here $h \in \mathbb{R}$ is called a biasing field. In the following subsection, we introduce the formulation of the large deviation theory by using some mathematical theorems.

2.2.1 Large Deviation Principle

Here, we refer to the condition of the rate function I for LDP. The rigorous definition of the large deviation principle is constructed by the following elements. This subsection follows Hollander's book [18]. Let E be a Polish space with distance $d : E \times E \rightarrow [0, \infty)$.

Definition 2.2.1. $f : E \rightarrow [-\infty, \infty]$ is lower semi-continuous if it satisfies any of the following equivalent properties:

- (i) $\liminf_{n \rightarrow \infty} f(x_n) \geq f(x)$ for all (x_n) , x such that $x_n \rightarrow x$ in E .
- (ii) $\lim_{\epsilon \downarrow 0} \inf_{y \in B_\epsilon(x)} f(y) = f(x)$ with $B_\epsilon(x) = \{y \in E : d(x, y) < \epsilon\}$.
- (iii) f has closed level sets, *i.e.*, $f^{-1}([-\infty, c]) = \{x \in E : f(x) \leq c\}$ is closed for all $c \in \mathbb{R}$.

Next, we introduce the key definitions of large deviation theory.

Definition 2.2.2. The function $I : E \rightarrow [0, \infty]$ is called a rate function if

- (i) $I \not\equiv \infty$.
- (ii) I is lower semi-continuous
- (iii) I has compact level sets.

Definition 2.2.3. A sequence of probability measures (P_n) on E is said to satisfy the LDP with rate n and with rate function I if

- (i) I is a rate function in the sense of Definition 2.2.2.
- (ii) $\limsup_{n \rightarrow \infty} \frac{1}{n} \log \mathbb{P}_n(C) \leq -I(C) \quad \forall C \subset E \text{ closed.}$
- (iii) $\liminf_{n \rightarrow \infty} \frac{1}{n} \log \mathbb{P}_n(O) \geq -I(O) \quad \forall O \subset E \text{ open.}$

Here, the bounds are in terms of the set function defined by

$$I(S) = \inf_{x \in S} I(x), \quad S \subset E. \quad (2.2.3)$$

The goal of large deviation theory is to build up an arsenal of theorems based on these two definitions. When I has compact level sets, I is called as a "good rate function". LDP holds under some mathematical conditions of probability measures. Roughly, LDP states that the probability measures have a similar expression as $\mathbb{P}_n(dy) \sim e^{-nI(y)} dy$ under the above conditions. In order to apply them to concrete situations, one must verify that the triple $(E, (\mathbb{P}_n), I)$ one is working with satisfies the LDP. We note that one could define a large deviations principle with rate a_n where (a_n) is an increasing sequence going to infinity. Finally, the definition of the large deviation for a sequence of random variables directly follows the one of probability measures.

Definition 2.2.4. A sequence of random variables (X_n) with values in E and law P_n satisfies a large deviation principle if and only if the sequence (P_n) satisfies a large deviation principle.

2.2.2 Gärtner-Ellis Theorem

We now consider the case of a sequence of random variables (Z_n) taking values in \mathbb{R} . We assume that the scaled CGF satisfies the following conditions

1. $\lim_{n \rightarrow \infty} \frac{1}{n} \log \mathbb{E}[e^{hZ_n}] = \varphi(h) \in [-\infty, \infty]$
2. There exists an open neighbourhood O of 0 such that $\varphi(h) < \infty$ for every $h \in O$.

Gärtner-Ellis theorem links a probability of rare events (rate function) with a sCGF by using the Legendre-Fenchel transform of a SCGF.

Theorem 2.2.1. (Gärtner-Ellis Theorem) *If the SCGF φ is differentiable and such that $\varphi(h) < \infty$ for every $h \in \mathbb{R}$, then the sequence of random variables (Z_n) satisfies a LDP with the rate function I given by the Legendre-Fenchel transform of $\varphi(h)$:*

$$I(x) = \sup_{h \in \mathbb{R}} \{hx - \varphi(h)\}. \quad (2.2.4)$$

The idea of the Gärtner-Ellis Theorem is the following. First, we assume

$$\mathbb{P}(A_n \in da) \asymp e^{-nI(a)} da. \quad (2.2.5)$$

Here, A_n is a real random variable and it is parameterized by the positive integer n . Then, a MGF is calculated as

$$\langle e^{nhA_n} \rangle \asymp \int_{\mathbb{R}} e^{n[ha - I(a)]} da. \quad (2.2.6)$$

Next, by using saddle-point approximation or Laplace's approximation for this integral, we can extract only the largest value of this integrand. Therefore, assuming that the maximum of $ha - I(a)$ exists and is unique, we obtain

$$\langle e^{nhA_n} \rangle \asymp \exp \left(n \sup_{a \in \mathbb{R}} \{ha - I(a)\} \right). \quad (2.2.7)$$

and so

$$\varphi(h) = \lim_{n \rightarrow \infty} \frac{1}{n} \log \langle e^{nhA_n} \rangle = \sup_{a \in \mathbb{R}} \{ha - I(a)\}. \quad (2.2.8)$$

For deriving $I(a)$ in terms of $\varphi(h)$, we then use the fact that Legendre-Fenchel transforms can be inverted when $\varphi(h)$ is everywhere differentiable. In this case, we can write

$$I(a) = \sup_{h \in \mathbb{R}} \{ha - \varphi(h)\}. \quad (2.2.9)$$

In more detail, we give an heuristic proof using the saddle-point approximation in appendix. The object of our research will concern situations where the Gartner-Ellis can *not* be applied because of the lack of differentiability of the SCGF. A special case of the Gartner-Ellis is the well-known Cramer's theorem which consider the case of Z_n given by a sum independent random variables.

Theorem 2.2.2. (Cramer's Theorem) *Let an i.i.d sequence of random variables (X_i) and their a sample mean defined as*

$$Y_n = \frac{1}{n} \sum_{i=1}^n X_i. \quad (2.2.10)$$

We assume that X_i satisfies

$$\mathbb{E}[e^{hX_1}] < \infty. \quad (2.2.11)$$

Then, for all $a > \mathbb{E}[X_1]$, we have

$$\lim_{n \rightarrow \infty} \frac{1}{n} \log \mathbb{P}(Y_n \geq a) = -I(a), \quad (2.2.12)$$

where

$$I(a) = \sup_{h \in \mathbb{R}} [ah - \log \mathbb{E}[e^{hX_1}]]. \quad (2.2.13)$$

In this case the SCGF has the simple form

$$\varphi(h) = \lim_{n \rightarrow \infty} \frac{1}{n} \log \mathbb{E} \left[e^{\frac{1}{n} \sum_{i=1}^n X_i} \right] = \lim_{n \rightarrow \infty} \frac{1}{n} \log \prod_{i=1}^n \mathbb{E} [e^{hX_i}] = \log \mathbb{E} [e^{hX}], \quad (2.2.14)$$

where X is any of the summands X_i . When we calculate the large deviation function by using the Legendre-Fenchel transform of CGF $\varphi(h)$, we need to take into the account the differentiability of $\varphi(h)$. However, $\mathbb{E} [e^{hX}]$ is always real analytic when it exists for all $h \in \mathbb{R}$.

2.2.3 Varadhan's Lemma

Varadhan's lemma is known as a version of Laplace's method for infinite-dimensional spaces. The Laplace principle is known as

$$\int_a^b e^{nf(x)} g(x) dx \asymp \exp \left[n \sup_{[a,b]} f(x) \right], \quad n \rightarrow \infty \quad (2.2.15)$$

where f, g are the continuous functions $f, g > 0$ on the bounded closed interval $[a, b]$. Moreover, from a view point of Gärtner-Ellis theorem, if A_n satisfies a LDP with rate function $I(a)$, then a CGF $\phi(k)$ is the Legendre-Fenchel transform of $I(a)$:

$$\varphi(k) = \lim_{n \rightarrow \infty} \frac{1}{n} \mathbb{E} [e^{nkA_n}] = \sup_a \{ka - I(a)\}. \quad (2.2.16)$$

Replacing the product kA_n by an arbitrary continuous function f of A_n yields the more general result

$$\varphi(f) = \lim_{n \rightarrow \infty} \frac{1}{n} \log \mathbb{E} [e^{nf(A_n)}] = \sup_a \{f(a) - I(a)\}. \quad (2.2.17)$$

The above relation is known as *Varadhan's lemma*.

Lemma 2.2.3. *For any $\epsilon > 0$, if A_ϵ are random variables in a metric space M , obeying an LDP with rate $1/\epsilon$ and the rate function I , and $f : M \rightarrow \mathbb{R}$ is continuous and bounded from above, then*

$$\varphi(f) \equiv \lim_{\epsilon \rightarrow 0} \epsilon \log \mathbb{E} [e^{f(A_\epsilon)/\epsilon}] = \sup_{a \in M} \{f(a) - I(a)\}. \quad (2.2.18)$$

Here, we take continuous parameter ϵ instead of $1/n$.

Proof. For the proof, we consider the lower bound and upper bound of RHS of (2.2.18).

Lower bound

To consider the \liminf , we take $a \in A_\epsilon$ and arbitrary ball of radius δ around it, $B_{\delta,a}$. Then, we have

$$\begin{aligned} \liminf_{\epsilon \rightarrow 0} \epsilon \log \mathbb{E} [e^{f(A_\epsilon)/\epsilon}] &\geq \liminf_{\epsilon \rightarrow 0} \epsilon \log \mathbb{E} [e^{f(A_\epsilon)/\epsilon} \mathbb{1}_{B_{\delta,a}}(A_\epsilon)] \\ &= \liminf_{\epsilon \rightarrow 0} \epsilon \log \int_{B_{\delta,a}} [e^{f(a)/\epsilon} \mu_\epsilon(A_\epsilon \in da)] \\ &\geq \inf_{y \in B_{\delta,a}} f(y) - \inf_{y \in B_{\delta,a}} I(y) \\ &\geq \inf_{y \in B_{\delta,a}} f(y) - I(a), \end{aligned} \quad (2.2.19)$$

where we use the Laplace's principle (without sup for lower bound) and LDP with sufficient small ϵ for denoting third line. Since δ was arbitrary, we can let it go to zero. Hence, $\inf_{y \in B_{\delta,a}} f(y) \rightarrow f(a)$. Therefore, we have

$$\lim_{\epsilon \rightarrow 0} \epsilon \log \mathbb{E} [e^{f(A_\epsilon)/\epsilon}] \geq f(a) - I(a) \rightarrow \sup_a \{f(a) - I(a)\} \quad (2.2.20)$$

since this relation holds for arbitrary a .

Upper bound

Since f is bounded, there exists $C \in (0, \infty)$ such that $-C \leq f(a) \leq C$ for all $a \in M$. For N positive integer, and $j \in \{1, \dots, N\}$, we consider the closed subset of M

$$F_{N,j} = \left\{ a \in M : -C + \frac{2(j-1)C}{N} \leq f(a) \leq -C + \frac{2jC}{N} \right\}, \quad (2.2.21)$$

so that $\bigcup_{j=1}^N F_{N,j} = M$. Then, we have from the large deviation upper bound on (A_ϵ) .

$$\begin{aligned} \limsup_{\epsilon \rightarrow 0} \epsilon \log \mathbb{E} \left[e^{f(A_\epsilon)/\epsilon} \right] &= \limsup_{\epsilon \rightarrow 0} \epsilon \log \int_M e^{f(A_\epsilon)/\epsilon} \mu_\epsilon(A_\epsilon \in da) \\ &\leq \limsup_{\epsilon \rightarrow 0} \epsilon \log \left(\sum_{j=1}^N \int_{F_{N,j}} e^{f(A_\epsilon)/\epsilon} \mu_\epsilon(A_\epsilon \in da) \right) \\ &\leq \limsup_{\epsilon \rightarrow 0} \epsilon \log \left(\sum_{j=1}^N e^{(-C + \frac{2jC}{N})/\epsilon} \mu_\epsilon(A_\epsilon \in F_{N,j}) \right) \\ &\leq \limsup_{\epsilon \rightarrow 0} \epsilon \log \left(N \max_{j=1, \dots, N} e^{(-C + \frac{2jC}{N})/\epsilon} \mu_\epsilon(A_\epsilon \in F_{N,j}) \right) \\ &\leq \max_{j=1, \dots, N} \left(-C + \frac{2jC}{N} + \limsup_{\epsilon \rightarrow 0} \epsilon \log \mu_\epsilon(A_\epsilon \in F_{N,j}) \right) \\ &\leq \max_{j=1, \dots, N} \left(-C + \frac{2jC}{N} + \sup_{a \in F_{N,j}} [-I(a)] \right) \\ &\leq \max_{j=1, \dots, N} \left(-C + \frac{2jC}{N} + \sup_{a \in F_{N,j}} [f(a) - I(a)] - \inf_{a \in F_{N,j}} [f(a)] \right) \\ &\leq \sup_{a \in M} [f(a) - I(a)] + \frac{2M}{N} \end{aligned} \quad (2.2.22)$$

Letting $N \rightarrow \infty$, we obtain the upper bound for satisfying *Varadhan's lemma*. □

2.2.4 Strong Large Deviation Theorem

The large deviation theory describes the connection between SCGF and the probability (rate function). Here, we describe the so-called strong large deviation theory. A strong large deviation theory is an extension of the large deviation theory for describing finite time asymptotic form of CGF and the probability of rare events. This subsection is based on [15]. In 1960, Bahadur and Rao established an asymptotic expansion for the large deviations of the sample mean in [19]. Let (X_n) be a sequence of *iid* random variables with zero mean and finite variance σ^2 . As usual, the sample mean is defined as $\bar{X}_n = n^{-1} \sum_{k=1}^n X_k$. An asymptotic expansion of the large deviation type for the tail probabilities of the sample mean is of the form

$$\mathbb{P}(\bar{X}_n \geq c) = \frac{e^{-nI(c)}}{\sqrt{2\pi n\sigma_c\tau_c}} [1 + O(1)], \quad c > 0. \quad (2.2.23)$$

when n is sufficient large. Moreover, for any $p > 0$, the refinement of (2.2.23) is:

$$\mathbb{P}(\bar{X}_n \geq c) = \frac{e^{-nI(c)}}{\sqrt{2\pi n\sigma_c\tau_c}} \left[1 + \sum_{j=1}^p \frac{d_j}{n^j} + O\left(\frac{1}{n^p}\right) \right] \quad (2.2.24)$$

where $d_j \in \mathbb{R}$, and $\tau_c > 0$, $\sigma_c > 0$ are parameters depending on c . The function I is the rate function.

Here, we consider the case of $p = 1$ (it can be extended to any $p \geq 1$ by using stronger assumption). We start by describing some assumptions on the random variables.

Set-up

Let Z_n be a sequence of random variables and b_n be a sequence of real positive numbers such that $\lim_{n \rightarrow \infty} b_n = \infty$. Let ϕ_n be the MGF of $b_n Z_n$,

$$\varphi_n(t) = \mathbb{E}[e^{tb_n Z_n}], \quad t \in \mathbb{R}, \quad (2.2.25)$$

and we consider the normalized CGF $\phi(t)$, which is given by

$$\phi_n(t) = \frac{1}{b_n} \log \mathbb{E}[e^{tb_n Z_n}]. \quad (2.2.26)$$

We assume ϕ is a differentiable function in $(0, \alpha)$, $\alpha > 0$, such that $\lim_{n \rightarrow \infty} \phi_n(t) = \phi(t)$ for any $t \in (0, \alpha)$. Let a be a real number such that $a > \phi'(0)$ and assume that there exists $\tau_a \in (0, \alpha)$ satisfying $\phi'(\tau_a) = a$. Moreover, we have $I(a) := \sup_{t \in \mathbb{R}} \{ta - \phi(t)\} = \tau_a a - \phi(\tau_a)$. Let K_n be the distribution function of $b_n Z_n$ and let Z_n^* be a new variable such that $b_n Z_n^*$ is distributed with K_n^* given by

$$K_n^*(u) = \int_{-\infty < y < u} e^{y\tau_a - b_n \phi(\tau_a)} dK_n(y). \quad (2.2.27)$$

Let us define the standardized random variable V_n as follows:

$$V_n = \frac{Z_n^* - \mu_n}{\sqrt{\text{Var}(Z_n^*)}}, \quad (2.2.28)$$

where $\mu_n = \mathbb{E}[Z_n^*]$. Note that, $\text{Var}(Z_n^*) = b_n^{-1} \phi''(\tau_a)$. Then, V_n may be expressed

$$V_n = \sqrt{b_n} \frac{Z_n^* - \mu_n}{\sigma_n}, \quad (2.2.29)$$

where $\sigma_n = \phi''(\tau_a)$. We just prepare above the definitions of the system and we can describe the assumptions for discussing a strong large deviation theory. In this context, a strong large deviation theory is the expansion for the upper tail probability of Z_n , which is $\mathbb{P}(Z_n \geq a)$, where $a > \phi'(0)$.

Assumption for a Strong Large Deviation Theory

By using the Edgeworth expansion, we can observe the correction terms for the rate function. We will discuss the details of Edgeworth expansion in appendix A. Those correction terms have the different type of decay from the original rate function. Therefore, a strong large deviation theory is one of the way to analyze the finite time rate function (probability) and sometimes it is a very useful approach. We assume that there exist functions J and L such that for all n large enough.

$$\begin{aligned}\phi(\tau_a) &= \phi(\tau_a) + b_n^{-1}J(\tau_a) + b_n^{-2}L(\tau_a) + O(b_n^{-2}) \\ \phi^{(k)}(\tau_a) &= \phi^{(k)}(\tau_a) + b_n^{-1}J^{(k)}(\tau_a) + O(b_n^{-1}) \quad k = 1, 2 \\ \phi^{(k)}(\tau_a) &= \phi^{(k)}(\tau_a) + O(1) \quad k = 3, 4 \\ \phi^{(5)}(\tau_a) &= O(1)\end{aligned}\tag{2.2.30}$$

Here $\phi_n^{(k)}$ is the k -th derivative of ϕ_n , the functions ϕ and J are, respectively, four times and twice differentiable at τ_a , and $\phi''(\tau_a) > 0$. The number of derivative is given by the order of Edgeworth expansion. In this Edgeworth expansion, we expand it with terms up to order $b_n^{-3/2}$. By using the Hermite polynomials H_k , the Edgeworth expansion of F_n , which is the distribution function of V_n is given by

$$F_n(y) = \Phi(y) - \frac{\Lambda_{3,n}H_2(y)\varphi(y)}{6b_n^{1/2}} - \frac{\Lambda_{4,n}H_3(y)\varphi(y)}{24b_n} - \frac{\Lambda_{3,n}^2H_5(y)\varphi(y)}{72b_n} - \frac{P_{4,n}\varphi(y)}{b_n^{3/2}} + O(b_n^{-3/2}),\tag{2.2.31}$$

where $\Phi(y)$ is a cumulative distribution function and the remainder term $O(b_n^{-3/2})$ is uniform in y . Also, the Hermite polynomials are given by

$$\begin{aligned}H_2(y) &= y^2 - 1 \\ H_3(y) &= y^3 - 3y \\ H_5(y) &= y^5 - 10y^3 + 15y.\end{aligned}$$

In addition, $P_{4,n}$ is a linear combination of Hermite polynomials H_4, H_6 and H_8 and also depends on $\Lambda_{k,n}$, $k = 3, 4, 5$, where

$$\Lambda_{k,n} = \frac{\phi_n^{(k)}(\tau_a)}{\sigma_n^k} \quad \text{with} \quad \sigma_n = \sqrt{\phi_n''(\tau_a)}\tag{2.2.32}$$

Theorem 2.2.4. *Let a be a real number such that $a > \phi'(0)$ and let assumptions (2.2.30)-(2.2.31) hold. Then, the probability is given by*

$$\mathbb{P}(Z_n \geq a) = \frac{e^{-b_n I(a) + J(\tau_a)}}{\tau_a \sqrt{2\pi b_n \phi''(\tau_a)}} [1 + b_n^{-1}d_1 + O(b_n^{-1})]\tag{2.2.33}$$

for sufficient large n . Here, $\tau_a > 0$ is such that $\phi'(\tau_a) = a$ and $I(a) = \tau_a a - \phi(\tau_a)$ and

$$\begin{aligned}d_1 = L(\tau_a) + \frac{1}{\phi''(\tau_a)} \left(-\frac{J''(\tau_a)}{2} - \frac{(J'(\tau_a))^2}{2} + \frac{\phi^{(3)}(\tau_a)J'(\tau_a)}{2\phi''(\tau_a)} - \frac{5}{24} \frac{(\phi^{(3)}(\tau_a))^2}{(\phi''(\tau_a))^2} \right. \\ \left. + \frac{\phi^{(4)}(\tau_a)}{8\phi''(\tau_a)} + \frac{J'(\tau_a)}{\tau_a} - \frac{\phi^{(3)}(\tau_a)}{2\tau_a\phi''(\tau_a)} - \frac{1}{\tau_a^2} \right).\end{aligned}\tag{2.2.34}$$

Proof. The proof is explained in section 2. in [15] □

2.3 Large Deviations Approach in Statistical Mechanics

At present, the large deviation theory is applied to study the properties of physical systems, which are consisting of many particles. Actually, the rate functions are related to thermodynamic functions, for instance, entropy. To clarify the relation between the large deviation theory and statistical mechanics, we start by considering a probability measure $\mathbb{P}(d\omega)$ on Λ_n , which is the set or space of all microstates ω . Here, microstates ω are defined as a sequence $\omega = (\omega_1, \omega_2, \dots, \omega_n)$ in n -particles system. Moreover, the physical interactions or dependencies between the n particles are determined by a Hamiltonian or energy function $H_n(\omega)$. Also, $h_n(\omega) = H_n(\omega)/n$ is the mean energy or energy per particle. The probability distribution of h_n within the range of du , which is an infinitesimal interval in the neighborhood the mean energy, is given by

$$\mathbb{P}(h_n \in du) = \int_{\{\omega \in \Lambda_n: h_n(\omega) \in du\}} \mathbb{P}(d\omega). \quad (2.3.1)$$

In the so-called microcanonical formalism, the probability measure is given by $\mathbb{P}(d\omega) = d\omega/|\Lambda_n|$. Let Ω

$$\Omega(h_n \in du) = \int_{\{\omega \in \Lambda_n: h_n(\omega) \in du\}} d\omega, \quad (2.3.2)$$

be the number of microstates such that $h(\omega) \in du$. When the probability measure satisfies LDP, the rate function is calculated as

$$I(u) = \lim_{n \rightarrow \infty} -\frac{1}{n} \log \mathbb{P}(h_n \in du). \quad (2.3.3)$$

Then, recalling that the probability is defined by the volume, we have

$$I(u) = \log|\Lambda| - s(u), \quad (2.3.4)$$

where

$$s(u) = \lim_{n \rightarrow \infty} \frac{1}{n} \log \Omega(h_n \in du). \quad (2.3.5)$$

is the microcanonical entropy or entropy density. In the following, we shall absorb the constant $\log|\Lambda|$ by re-defining the entropy using the limit

$$s(u) = \lim_{n \rightarrow \infty} \frac{1}{n} \log \mathbb{P}(h_n \in du). \quad (2.3.6)$$

for the probability measure. For this re-definition, we can see $I(u) = -s(u)$. Note that, we use $k_b = 1$, which is the Boltzmann constant.

On the other hand, once we observe the relation between entropy and a rate function, then we expect that the CGF of the energy has a relation with some thermodynamic functions. The CGF is given by

$$\varphi(k) = \lim_{n \rightarrow \infty} \frac{1}{n} \log \mathbb{E}[e^{nkh_n}]. \quad (2.3.7)$$

This satisfies

$$\varphi(k) = -\psi(\beta)|_{\beta=-k} - \log|\Lambda|, \quad (2.3.8)$$

where

$$\psi(\beta) = \lim_{n \rightarrow \infty} -\frac{1}{n} \log \Xi_n(\beta), \quad (2.3.9)$$

and

$$\Xi_n(\beta) = \int_{\Lambda_n} e^{-n\beta h_n(\omega)} \mathbb{P}(d\omega) = \int_{\Lambda_n} e^{-\beta H_n(\omega)} \mathbb{P}(d\omega). \quad (2.3.10)$$

β is the inverse temperature and $\Xi_n(\beta)$ is the well-known n -particles partition function associated with H_n , which is Hamiltonian or energy function. As we did with the entropy, we shall absorb the constant $\log|\Lambda|$ in $\psi(\beta)$ by re-defining this function as

$$\psi(\beta) = \lim_{n \rightarrow \infty} -\frac{1}{n} \log \int_{\Lambda_n} e^{-n\beta h_n(\omega)} \mathbb{P}(d\omega) = \lim_{n \rightarrow \infty} -\frac{1}{n} \log \mathbb{E} [e^{-n\beta h_n(\omega)}]. \quad (2.3.11)$$

Actually, in statistical mechanics, the thermodynamic function $f(\beta)$ is $\psi(\beta)/\beta$ and $\psi(\beta)$ is sometimes called the *Massieu potential*. Therefore, by using Gärtner-Ellis Theorem or Varadhan's lemma, we can construct an entropy function as Legendre-Fenchel transform of a Massieu potential (free energy function), and vice versa. Those are given by

$$s(u) = \inf_{\beta} \{\beta u - \psi(\beta)\} \quad (2.3.12)$$

$$\psi(\beta) = \inf_u \{\beta u - s(u)\}. \quad (2.3.13)$$

Therefore, we see that classical thermodynamic relations maybe interpreted as usual relations in the context of large deviations theory.

2.3.1 Macroscopic Fluctuation Theory

Macroscopic fluctuation theory (MFT) is a general approach to study non-equilibrium diffusive systems in modern statistical physics. Moreover, the MFT is useful to calculate large deviation functions of diffusive systems [20–22]. In this subsection, we follow the approach of macroscopic fluctuation theory in diffusive system. In large deviation theory, we can estimate the logarithm of the probability distribution of the arithmetic mean of microscopic stochastic processes. However, in MFT, by using path integral, we can describe of the distribution of the physical quantities by deriving the rate function in the large deviation theory method.

Let us consider of a conservative system. The evolution of a field $\rho = \rho(\tau, x)$, which is local density of thermodynamic variable, where τ and x are the macroscopic time and space coordinates, is given by the continuity equation

$$\partial_\tau \rho = \nabla \cdot [D(\rho) \nabla \rho - \chi(\rho) E] = -\nabla \cdot J(\rho), \quad (2.3.14)$$

where $D(\rho)$ is the diffusion constant matrix, $\chi(\rho)$ is the mobilityn E is the external field and

$$J(\rho) := -D(\rho) \nabla \rho + \chi(\rho) E, \quad (2.3.15)$$

where $\rho = \rho(\tau, x)$. For diffusive systems, one uses fluctuating hydrodynamics to describe such a system in the large system size L limit; in such a diffusion system, one defines hydrodynamics coordinates $x = u/L$ and $\tau = t/L^2$ where u and t are position and time, respectively. The hydrodynamic equation represents a law of large numbers with respect to the probability measure \mathbb{P}_s conditioned on an initial state X_0 . The path probability, which depends on X_0 , is denoted by \mathbb{P}_{X_0} . We define the free energy $F(\rho)$ as a functional of the density profile $\rho = \rho(x)$. It gives the asymptotic probability of density fluctuations for the invariant measure μ . It is given by

$$\mu(\pi_L(X) \approx \rho) \asymp e^{-L^d F(\rho)}, \quad (2.3.16)$$

where d is the dimension of the system and π_L is the local density. In general, $\rho = \rho(\tau, x)$ is the limit of the local density $\pi_L(X_t)$. The meaning of $\pi_L(X) \approx \rho$ is closeness with respect to some metric and \asymp is logarithmic equivalence as $L \rightarrow \infty$. By using the local density and the free energy, the probability is given by

$$\mathbb{P}_s(\pi_L(X_{L^2\tau}) \approx \rho_1(\tau), \tau \in [\tau_1, \tau_2]) \asymp \exp\{-L^d[F(\rho_1(\tau_1)) + \mathcal{F}_{[\tau_1, \tau_2]}(\rho_1)]\}, \quad (2.3.17)$$

where \mathcal{F} is a functional which vanishes if $\rho_1(\tau)$ is a solution of (2.3.14) and $F(\rho_1(\tau_1))$ is the free energy cost to produce the initial density profile $\rho_1(\tau_1)$.

For discussing the current fluctuations, we introduce a vector-valued observable $\mathcal{J}^L(\{X_\sigma, 0 \leq \sigma \leq \tau\})$ of the trajectory X which measures the local net flow of particles. By taking into account the path probability of initial state X_0 in the diffusive system, we have

$$\mathbb{P}_{X_0}(\mathcal{J}^L(X) \approx j(\tau, x)) \asymp e^{-L^d \mathcal{I}_{[0, \tau]}(j)} \quad (2.3.18)$$

where the rate functional is

$$\mathcal{I}_{[0, T]}(j) = \frac{1}{4} \int_0^T d\tau \langle [j - J(\rho)], \chi^{-1}(\rho)[j - J(\rho)] \rangle. \quad (2.3.19)$$

and

$$\langle f, g \rangle = \int_{\Lambda} dx f(x)g(x).$$

$J(\rho)$ is obtained by solving the continuity equation with the initial condition $\rho(0) = \rho_0$ which is associated to X_0 . The fact that when we take $j = J(\rho)$, the rate functional takes the 0 value reflects the law of large numbers for the observable \mathcal{J}^L . The functional formula is given by (2.3.19) because the probability is calculated as the Gaussian integral, which is given by the random variables in the system. Moreover, we can be interpreted the functional (2.3.19) as an action on the set of density paths. The corresponding Lagrangian is calculated as

$$\mathcal{L}(\rho, \partial_\tau \rho) = \frac{1}{4} \int_{\Lambda} dx [\partial_\tau \rho + \nabla \cdot J(\rho)] K^{-1}(\rho) [\partial_\tau \rho + \nabla \cdot J(\rho)], \quad (2.3.20)$$

where the positive operator $K(\rho)$ is defined on functions $\hat{\rho} : \Lambda \rightarrow \mathbb{R}$ vanishing at the boundary $\partial\Lambda$ by

$$K(\rho)\hat{\rho} = -\nabla \cdot (\chi(\rho)\nabla\hat{\rho}). \quad (2.3.21)$$

The Hamiltonian $\mathcal{H}(\hat{\rho}, \rho)$, $\hat{\rho}$ is another field, is obtained by the Legendre transform of $\mathcal{L}(\rho, \partial_\tau \rho)$:

$$\begin{aligned} \mathcal{H}(\hat{\rho}, \rho) &= \sup_k \left\{ \int_\Lambda dx \hat{\rho} k - \mathcal{L}(\rho, k) \right\} \\ &= \int_\Lambda dx \{ \nabla \hat{\rho} \cdot \chi(\rho) \nabla \hat{\rho} - \hat{\rho} \nabla \cdot J(\rho) \}. \end{aligned} \quad (2.3.22)$$

Thus, the equation of motions are given by

$$\partial_\tau \rho = \nabla \cdot (D(\rho) \nabla \rho) - \nabla \cdot \chi(\rho) (E + 2 \nabla \hat{\rho}) \quad (2.3.23)$$

$$\partial_\tau \hat{\rho} = -\nabla \hat{\rho} \cdot \chi'(\rho) (E + \nabla \hat{\rho}) - \text{Tr}\{D(\rho) \text{Hess}(\hat{\rho})\}. \quad (2.3.24)$$

Here, $\hat{\rho}$ vanishes at the boundary of Λ . $\text{Hess}(\hat{\rho})$ is Hessian of $\hat{\rho}$. In addition, we introduce the functional Φ , which is given by

$$\Phi(J) = \lim_{T \rightarrow \infty} \inf_{j \in \mathcal{A}_{T,J}} \frac{1}{T} \mathcal{I}_{[0,T]}(j), \quad (2.3.25)$$

where the infimum is carried over all paths $j = j(\tau, x)$ having time average J and $\mathcal{A}_{T,J}$ is defined as

$$\mathcal{A}_{T,J} = \left\{ j = j(\tau, x) : \frac{1}{T} \int_0^T d\tau j(\tau, x) = J(x) \right\}. \quad (2.3.26)$$

By using LDP (2.3.18), for T and L large, we have

$$\mathbb{P}_{\rho_0}^L \left(\frac{1}{T} \int_0^T d\tau \mathcal{J}^L(\tau) \approx J \right) \asymp e^{-L^d T \Phi(J)}, \quad (2.3.27)$$

where ρ_0 is the initial state and the logarithmic equivalence is understood by taking first $L \rightarrow \infty$ and then $T \rightarrow \infty$. This asymptotic form can be formulated in terms of the MGF of the empirical current. Then we have

$$\lim_{T \rightarrow \infty} \lim_{L \rightarrow \infty} \frac{1}{T L^d} \log \mathbb{E}_{\rho_0}^L \left(e^{L^d \int_0^T d\tau \langle \mathcal{J}^L(\tau), h(\cdot, \tau) \rangle} \right) = \Phi^*(h), \quad (2.3.28)$$

where h is a smooth function playing the role of a biasing field. Here, $\Phi^*(h)$ is the Legendre transform of $\Phi(J)$, which has the following relation

$$\Phi^*(h) = \sup_J \{ \langle h, J \rangle - \Phi(J) \}. \quad (2.3.29)$$

In addition, we introduce the functional \mathcal{U} on the set of time independent profiles $\rho = \rho(x)$, $j = j(x)$ and $\nabla \cdot j = 0$.

$$\mathcal{U}(\rho, j) = \frac{1}{4} \langle [j - J(\rho)] \cdot \chi^{-1}(\rho) [j - J(\rho)] \rangle \quad (2.3.30)$$

$$U(j) = \inf_\rho \mathcal{U}(\rho, j). \quad (2.3.31)$$

Here, the minimum in the definition of $U(j)$ is carried over all profiles ρ satisfying the boundary condition of the diffusion equation. This functional is constructed by the point of view of rate functional formulation. Finally, we substitute the functional \mathcal{U} into the Legendre transform. Then we have

$$\begin{aligned} U^*(h) &= \sup_{J, \rho} \left\{ \langle h, J \rangle - \frac{1}{4} \langle [J - J(\rho)], \chi^{-1}(\rho)[J - J(\rho)] \rangle \right\} \\ &= \sup_{J, \rho} \left\{ -\frac{1}{4} \langle [J - J(\rho) - \chi(\rho)h], \chi^{-1}(\rho)[J - J(\rho) - \chi(\rho)h] \rangle + \frac{1}{4} \langle h, \chi(\rho)h \rangle + \langle h, J(\rho) \rangle \right\}. \end{aligned}$$

For computing the supremum over J , we decompose the vector field $J(\rho) + \chi(\rho)h$ as follows

$$J(\rho) + \chi(\rho)h = \chi(\rho)\nabla\psi + [J(\rho) + \chi(\rho)(h - \nabla\psi)], \quad (2.3.32)$$

where ψ has the constraints

$$\nabla \cdot (\chi(\rho)\nabla\psi) = \nabla \cdot (J(\rho) + \chi(\rho)h) \quad x \in \Lambda \quad (2.3.33)$$

$$\psi(x) = 0 \quad x \in \partial\Lambda \quad (2.3.34)$$

By using the decomposition form, finally we get

$$U^*(h) = \sup_{\rho} \left\{ -\frac{1}{4} \langle \nabla\psi, \chi(\rho)\nabla\psi \rangle + \frac{1}{4} \langle h, \chi(\rho)\nabla\psi \rangle + \langle h, J(\rho) \rangle \right\}, \quad (2.3.35)$$

where the supremum is over all density profiles ρ , which is satisfies $F'_0(\rho(x)) = h_0(x), x \in \partial\Lambda$. This derivation is based on the LDP for the rate functional, which is roughly (2.3.18). Once the probability measure satisfies LDP, we can describe the probability by using the rate function (functional). In such the (diffusive) systems, we can construct the path probability through the external random field. The MFT can denote the path probability by using the macroscopic equation and it is related to the fluctuations (cumulant) of the distribution function deeply. In appendix, we introduce the physical approach of MFT.

2.A Saddle-point Approximation for Gärtner-Ellis Theorem

Let $S_n(\omega)$ be a stochastic process and $\omega = (\omega_1, \omega_2, \dots, \omega_n)$ be the n random variables. Without loss of generality, assume that the ω_i 's are also real random variables, so that $\omega \in \mathbb{R}^n$. Then the probability density $p_{S_n}(s)$ is given by

$$p_{S_n}(s) = \int_{\{\omega \in \mathbb{R}^n: S_n(\omega)=s\}} p(\omega) d\omega = \int_{\mathbb{R}^n} \delta(S_n(\omega) - s) p(\omega) d\omega = \mathbb{E}[\delta(S_n - s)]. \quad (2.A.1)$$

Here, $\delta(x)$ is a delta function. In addition, by using inverse Laplace transform the integral representation of Dirac's delta function is expressed as

$$\delta(s) = \frac{1}{2\pi i} \int_{a-i\infty}^{a+i\infty} e^{\theta s} d\theta \quad a \in \mathbb{R}, \quad (2.A.2)$$

where we use the fact that Laplace transform of a delta function is 1. Therefore, $p_{S_n}(s)$ is calculated as

$$p_{S_n}(s) = \frac{1}{2\pi i} \int_{a-i\infty}^{a+i\infty} d\theta \int_{\mathbb{R}^n} e^{\theta|S_n(\omega)-s|} p(\omega) d\omega = \frac{1}{2\pi i} \int_{a-i\infty}^{a+i\infty} d\theta e^{-\theta s} \int_{\mathbb{R}^n} e^{\theta S_n(\omega)} p(\omega) d\omega. \quad (2.A.3)$$

At this point, we anticipate the scaling of the large deviation principle by performing the change of variable $\theta \rightarrow n\theta$, and note that if

$$\varphi(\theta) = \lim_{n \rightarrow \infty} \frac{1}{n} \mathbb{E}[e^{n\theta S_n}] \quad (2.A.4)$$

exists, then

$$p_{S_n}(s) \asymp \int_{a-i\infty}^{a+i\infty} d\theta e^{-n[\theta s - \varphi(\theta)]} \quad (2.A.5)$$

with sub-exponential corrections in n . Here, \asymp can be interpreted as expressing an equality relationship on a logarithmic scale. In large deviation theory, the sign \asymp is often commonly used. The mathematical meaning of $c_n \asymp d_n$ is given by

$$\lim_{n \rightarrow \infty} \frac{1}{n} \log c_n = \lim_{n \rightarrow \infty} \frac{1}{n} \log d_n. \quad (2.A.6)$$

In addition, by deforming the contour so that it goes through the saddle-point θ^* of $\theta s - \varphi(\theta)$, and by considering only the exponential contribution to the integral coming from the saddle-point, we then describe

$$p_{S_n}(s) \asymp \int_{\theta^*-i\infty}^{\theta^*+i\infty} d(-i\theta) e^{-n[\theta s - \varphi(\theta)]} \asymp e^{-n[\theta^* s - \varphi(\theta^*)]} \quad (2.A.7)$$

The last approximation is the saddle-point approximation. For using the approximation method, the integrand satisfies that it has extremum and the value of integrand decreases sharply out of range of extremum. Moreover, if we assume that $\varphi(\theta)$ is analytic, then θ^* is the unique minimum of $\theta s - \varphi(\theta)$ satisfying $\varphi'(\theta^*) = s$ along the contour. Finally, we can denote

$$\lim_{n \rightarrow \infty} -\frac{1}{n} \log p_{S_n}(s) = \sup_{k \in \mathbb{R}} \{ks - \varphi(k)\}. \quad (2.A.8)$$

The Gärtner-Ellis theorem shows the connection between SCGF and the probability. For instance, when we consider the random variables of physical quantities for SCGF, we can describe the rate function by using the form of Legendre-Fenchel transform.

2.B Edgeworth Expansion

For a strong large deviation theory, we have applied the Edgeworth expansion to derive the higher order asymptotic form of the probability distribution function. Here, we introduce the way of the Edgeworth expansion. Without loss of generality, let $\{Z_i\}_{i \in \mathbb{N}}$ be a sequence of *i.i.d.* random variables with the conditions $\mathbb{E}[Z_i] = 0$ and $\text{Var}[Z_i] = 1$. Also, Z_n is

$V_n = n^{-1/2} \sum_{i=1}^n Z_i$ (standardizing random variables in statistics). For the asymptotic form of the probability distribution function, we consider the expansion of the characteristic function, which is calculated as

$$\begin{aligned} \log \mathbb{E}[e^{iuV_n}] &= n \log \mathbb{E}[e^{iuZ_1/\sqrt{n}}] \\ &= n \log \left(1 - \frac{u^2}{2n} + \frac{(iu)^3 \kappa_3}{6n^{3/2}} + \frac{(iu)^4 \kappa_4}{24n^2} + \frac{(iu)^6 \kappa_3^2}{72n^2} + O\left(\frac{1}{n^{5/2}}\right) \right) \\ &= -\frac{u^2}{2} + \frac{(iu)^3 \kappa_3}{6n^{1/2}} + \frac{(iu)^4 \kappa_4}{24n} + \frac{(iu)^6 \kappa_3^2}{72n} + O\left(\frac{1}{n^{3/2}}\right). \end{aligned} \quad (2.B.1)$$

Here, $\kappa_i (i = 1, 2, \dots)$ is the cumulant. Then, the MGF is

$$\begin{aligned} \mathbb{E}[e^{iuV_n}] &= \exp \left(-\frac{u^2}{2} + \frac{(iu)^3 \kappa_3}{6n^{1/2}} + \frac{(iu)^4 \kappa_4}{24n} + \frac{(iu)^6 \kappa_3^2}{72n} + O\left(\frac{1}{n^{3/2}}\right) \right) \\ &= e^{-\frac{u^2}{2}} \left(1 + \frac{(iu)^3 \kappa_3}{6n^{1/2}} + \frac{(iu)^4 \kappa_4}{24n} + \frac{(iu)^6 \kappa_3^2}{72n} + O\left(\frac{1}{n^{3/2}}\right) \right). \end{aligned} \quad (2.B.2)$$

Therefore, by using an inverse Fourier transform \mathcal{F}^{-1} , the probability density function $p_n(y)$ of V_n is given by

$$\begin{aligned} p_n(y) &= \mathcal{F}^{-1}[\mathbb{E}[e^{iuV_n}]](y) \\ &= \frac{1}{2\pi} \int_{\mathbb{R}} e^{-iuy} e^{-\frac{u^2}{2}} \left(1 + \frac{(iu)^3 \kappa_3}{6n^{1/2}} + \frac{(iu)^4 \kappa_4}{24n} + \frac{(iu)^6 \kappa_3^2}{72n} + O\left(\frac{1}{n^{3/2}}\right) \right) dy \\ &= \frac{1}{2\pi} \int_{\mathbb{R}} \left(1 + \frac{(-\partial_y)^3 \kappa_3}{6n^{1/2}} + \frac{(-\partial_y)^4 \kappa_4}{24n} + \frac{(-\partial_y)^6 \kappa_3^2}{72n} + O\left(\frac{1}{n^{3/2}}\right) \right) e^{-iuy} e^{-\frac{u^2}{2}} dy \\ &= \left(1 + \frac{(-\partial_y)^3 \kappa_3}{6n^{1/2}} + \frac{(-\partial_y)^4 \kappa_4}{24n} + \frac{(-\partial_y)^6 \kappa_3^2}{72n} + O\left(\frac{1}{n^{3/2}}\right) \right) \varphi(y). \end{aligned} \quad (2.B.3)$$

Here, $\varphi(y)$ is the characteristic function of $e^{-u^2/2}$. Note that, if $\varphi(y)$ denotes standard normal density function. then we define the Hermite polynomials $H_i(y)$ by the equation

$$(-1)^i \frac{d^i}{dy^i} \varphi(y) = H_i(y) \varphi(y). \quad (2.B.4)$$

Thus, we obtain

$$p_n(y) = \varphi(y) + \frac{\kappa_3}{6n^{1/2}} H_3(y) \varphi(y) + \frac{\kappa_4}{24n} H_4(y) \varphi(y) + \frac{\kappa_3^2}{72n} H_4(y) \varphi(y) + O\left(\frac{1}{n^{3/2}}\right). \quad (2.B.5)$$

Moreover, the asymptotic form of the probability distribution function $P(V_n \leq z)$ is given by $P(V_n \leq z) = \int_{-\infty}^z p_n(y) dy$. The Edgeworth expansion is one of the ways to denote the asymptotic behavior of the probability with small finite n . Conversely, when we consider sufficient large n , the standardizing random variables V_n converges to $N(0, 1)$ as $n \rightarrow \infty$ (central limit theorem). Therefore, when we consider the case of small n , we may need to use approximate method for the probability distribution function in limit theorem because the probability distribution function is out of the normal distribution. In the context of a strong large deviation theory, by using the Edgeworth expansion, we can discuss the finite time asymptotic behavior of the rate function (probability).

2.C Physical Approach of MFT

We start by considering the non-equilibrium steady state of a one-dimensional system coupled with two hot walls (heat baths), which have different temperatures. One uses fluctuating hydrodynamics to describe such a system in the large system size L limit; in systems where diffusion is the transport mechanism, one defines hydrodynamics coordinates $x = X/L$ and $\tau = t/L^2$ where X and t are position and time, respectively. Let $\rho(x, \tau)$ be a hydrodynamic density and $J(x, \tau)$ be a hydrodynamic current, then the conservation law and Fick's law with fluctuating hydrodynamics are given by

$$\partial_\tau \rho(x, \tau) = \partial_x J(x, \tau) \quad (2.C.1)$$

$$J(x, \tau) + D(\rho(x, \tau))\partial_x \rho(x, \tau) = \xi(x, \tau), \quad (2.C.2)$$

where $D(\rho)$ is the diffusivity and $\xi(x, \tau)$ is a Gaussian random noise. The random noise satisfies

$$\langle \xi(x, \tau)\xi(y, \tau') \rangle = \frac{1}{L}\sigma(\rho(x, \tau))\delta(x - y)\delta(\tau - \tau'), \quad (2.C.3)$$

where $\sigma(\rho)$ is the mobility. Also, $\langle \mathcal{O} \rangle$ is an expected value of observable \mathcal{O} .

By using the equations (2.C.1), the generating function is given by

$$\begin{aligned} \left\langle e^{L \int_0^T d\tau \int_0^1 dx h(x, \tau) J(x, \tau)} \right\rangle &= \int d\xi \delta(\partial_\tau \rho + \partial_x J) e^{L \int_0^T d\tau \int_0^1 dx h(x, \tau) J(x, \tau)} e^{-\frac{\xi^2}{2\sigma(\rho)}} \\ &= \int \mathcal{D}[J, \rho] \delta(\partial_\tau \rho + \partial_x J) e^{L \int_0^T d\tau \int_0^1 dx \left[h(x, \tau) J(x, \tau) - \frac{(J + D(\rho)\partial_x \rho)^2}{2\sigma(\rho)} \right]}, \end{aligned} \quad (2.C.4)$$

where T is an arbitrary large time and \mathcal{D} is the expression of path integral. The path integral is over all density and current fields with a boundary condition

$$\rho(0, \tau) = \rho_a \quad \rho(1, \tau) = \rho_b. \quad (2.C.5)$$

The delta function can be written as an integral with another field $\hat{\rho}(x, \tau)$. $\hat{\rho}(x, \tau)$ have to vanish at the boundary as the particles are not conserved

$$\hat{\rho}(0, \tau) = 0 = \hat{\rho}(1, \tau). \quad (2.C.6)$$

Then, by using the classical action $S[\hat{\rho}, \rho]$, the generating function of the current $J(x, \tau)$ is calculated as

$$\left\langle e^{L \int_0^T d\tau \int_0^1 dx h(x, \tau) J(x, \tau)} \right\rangle = \int \mathcal{D}[\hat{\rho}, \rho] e^{-LS[\hat{\rho}, \rho]}. \quad (2.C.7)$$

In addition, the action $S[\hat{\rho}, \rho]$ has the relation with Hamiltonian $\mathcal{H}[\hat{\rho}, \rho]$. It is given by

$$S[\hat{\rho}, \rho] = \int_0^T d\tau \left(\int_0^1 dx \hat{\rho} \partial_\tau \rho - \mathcal{H}[\hat{\rho}, \rho] \right) \quad (2.C.8)$$

with a Hamiltonian

$$\mathcal{H}[\hat{\rho}, \rho] = \int_0^1 dx \left(\frac{\sigma[\rho]}{2} (\partial_x \hat{\rho} + h)^2 - D(\rho) (\partial_x \hat{\rho} + h) \partial_x \rho \right), \quad (2.C.9)$$

where we use the following computation.

$$\begin{aligned}
& \left\langle e^{L \int_0^T d\tau \int_0^1 dx h(x, \tau) J(x, \tau)} \right\rangle \\
&= \int d\xi \delta(\partial_\tau \rho + \partial_x J) e^{L \int_0^T d\tau \int_0^1 dx h(x, \tau) J(x, \tau)} e^{-\frac{\xi^2}{2\sigma(\rho)}} \\
&= \int \mathcal{D}[\rho, \hat{\rho}] \int d\xi e^{L \int_0^T d\tau \int_0^1 dx (-\hat{\rho}[\partial_\tau \rho + \partial_x (D(\rho) \partial_x \rho - \xi)]) + h[\xi - D(\rho) \partial_x \rho]} e^{-\frac{\xi^2}{2\sigma(\rho)}} \\
&= \int \mathcal{D}[\rho, \hat{\rho}] \int d\xi e^{L \int_0^T d\tau \int_0^1 dx [-\hat{\rho} \partial_\tau \rho - \partial_x \hat{\rho} D(\rho) \partial_x \rho - \frac{1}{2\sigma} (\xi + \sigma(h + \partial_x \hat{\rho}))^2 + \frac{1}{2\sigma} (\sigma^2 (h + \partial_x \hat{\rho})^2) - h D(\rho) \partial_x \rho]} \\
&= \int \mathcal{D}[\rho, \hat{\rho}] e^{L \int_0^T d\tau \int_0^1 dx [-\hat{\rho} \partial_\tau \rho + (\frac{\sigma}{2} (h + \partial_x \hat{\rho})^2 - D(\rho) \partial_x \rho (\partial_x \hat{\rho} + h))]}
\end{aligned} \tag{2.C.10}$$

Denoting the paths associated to the least Action by $(\hat{\rho}, \rho) \equiv (p, q)$ one gets the CGF of current

$$\phi(h) = \lim_{L \rightarrow \infty} \frac{1}{L} \log \left\langle e^{L \int_0^T d\tau \int_0^1 dx h(x, \tau) J(x, \tau)} \right\rangle = -S(p, q). \tag{2.C.11}$$

By optimizing the fields (p, q) , which is the variational principle of the action, we have Hamilton's equation

$$\partial_\tau p + \partial_x (\partial_x p + h) = -\frac{\sigma'[q]}{2} (\partial_x p + h)^2 \tag{2.C.12}$$

$$\partial_\tau q - \partial_{xx} q = -\partial_x (\sigma[q] (\partial_x p + h)). \tag{2.C.13}$$

The corresponding boundary conditions are given by

$$p(x, T) = 0 \quad q(x, 0) = \bar{\rho}(x) = \rho_a(1 - x) + \rho_b x. \tag{2.C.14}$$

Moreover,

$$p(0, \tau) = 0 = q(1, \tau) \quad q(0, \tau) = \rho_a \quad q(1, \tau) = \rho_b \tag{2.C.15}$$

at all time τ . By using (2.C.12) for the action, the CGF is calculated as

$$\phi(h) = - \int_0^T dt \int_0^1 dx \left[\frac{\sigma(q)}{2} (\partial_x p + h)^2 + h \partial_x q - h \sigma(q) (\partial_x p + h) \right]. \tag{2.C.16}$$

Using the SCGF for the action and the definition

$$\phi(h) = \int_0^T d\tau \int_0^1 dx \langle J(x, \tau) \rangle + \frac{1}{2} \int_0^T d\tau_1 d\tau_2 \int_0^1 dx_1 dx_2 \langle J(x_1, \tau_1) J(x_2, \tau_2) \rangle + \dots \tag{2.C.17}$$

one gets for large L ,

$$\langle J(x_1, \tau_1), \dots, J(x_k, \tau_k) \rangle_c \simeq \frac{1}{L^{k-1}} f(x_1, t_1, \dots, x_k, t_k), \tag{2.C.18}$$

where $f(x_1, t_1, \dots, x_k, t_k)$ is a scaling function. Therefore, we've clarified the relation between CGF and hydrodynamics equation (diffusion equation). In this context, the large deviation function is related to macroscopic equations. Thus, macroscopic fluctuation theory is one of the strong ways to analyze the large deviation function in dynamical systems.

Chapter 3

Analysis of Finite Time Large Deviation Theory with Heavy-tailed Distributions

In this chapter, we study the large time asymptotic of renewal-reward processes with a heavy-tailed waiting time distribution. It is known that the heavy tail of the distribution produces an extremely slow dynamics, resulting in a singular large deviation function. This amounts to a “flattened” bottom of the large deviation function, manifesting anomalous fluctuations of the renewal-reward processes. In the following sections, we aim to study how these singularities emerge as the time increases. Using a classical result on the sum of random variables with regularly varying tail, we develop an expansion approach to prove an upper bound of the finite-time MGF for the Pareto waiting time distribution (power law) with an integer exponent. We perform numerical simulations using Pareto (with a real value exponent), inverse Rayleigh and log-normal waiting time distributions, and demonstrate similar results are anticipated in these waiting time distributions. First of all, we introduce the previous research, which is the analysis of affine (flat) part of LDF, and clarify the conditions for the affine part.

3.1 Background

3.1.1 The Affine Part of LDF

In a previous work [23], it has been observed that the LDF of the average energy current carried by a particle between two thermal walls with different temperatures has a singular part within a specific range. In that model the energy current is written as a renewal-reward process with a heavy tailed distribution (inverse Rayleigh distribution). We want to understand the emergence of that singular part of the LDF, see Fig.3.1.

The SCGF of the current displays a similar singularity see Fig. 3.2. After a rescaling the arguments it is possible [23] to obtain an explicit form for both functions. Below, τ is the rescaled temperature gradient applied at the boundaries of the interval and T the arithmetic mean of the temperatures.

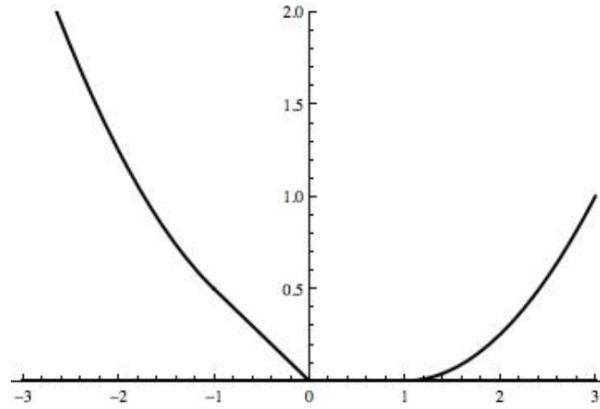


Fig. 3.1: The rate function of the current \mathcal{H} with an affine part in previous work [1].

1. If $\tau \neq 0$, then

$$\lim_{\epsilon \downarrow 0} \epsilon^{-2} \mathcal{F}(\epsilon\lambda, \epsilon\tau, T) = \mathcal{H}(\lambda, \tau, T) := \begin{cases} \lambda\kappa\tau + \kappa\lambda^2 T^2 & \text{if } \lambda\tau > 0, \\ 0 & \text{if } \lambda\tau \in [-\tau^2, 0], \\ -(\lambda + \tau)\kappa\tau + \kappa(\tau + \lambda)^2 T^2 & \text{if } \lambda\tau < -\tau^2 \end{cases} \quad (3.1.1)$$

and

$$\lim_{\epsilon \downarrow 0} \epsilon^{-2} \mathcal{I}(\epsilon j, \epsilon\tau, T) = \mathcal{G}(j, \tau, T) := \begin{cases} \frac{(j - \kappa\tau)^2}{4\kappa T^2} & \text{if } j\tau > \kappa\tau^2 \\ 0 & \text{if } j\tau \in [0, \kappa\tau^2] \\ \frac{-j\tau}{2T^2} & \text{if } j\tau \in [-\kappa\tau^2, 0] \\ \frac{j^2 + \kappa^2\tau^2}{4\kappa T^2} & \text{if } j\tau < -\kappa\tau^2. \end{cases} \quad (3.1.2)$$

2. If $\tau = 0$, $\lim_{\epsilon \downarrow 0} \epsilon^{-2} \mathcal{F}(\epsilon\lambda, \epsilon\tau, T) = \kappa\lambda^2 T^2$ and $\lim_{\epsilon \downarrow 0} \epsilon^{-2} \mathcal{I}(\epsilon j, \epsilon\tau, T) = \frac{j^2}{4\kappa T^2}$,

where $\mathcal{H}(\lambda, \tau, T)$ is the SCGF, $\mathcal{G}(j, \tau, T)$ is the scaling rate function and $\kappa = (T/2\pi)^{1/2}$. The following subsection, we will clarify the conditions of the affine part. The affine part of LDF implies the system has a phase transition even though the system is finite. We will also re-derive the SCGF by using variational principle in the following section (appendix).

3.1.2 Tsirelson's Work

In reference [16], Tsirelson considered a renewal-reward process under the condition $\mathbb{E}X = 0$, where he proved that the large deviation function does not have any affine part. On the other hand, an affine part of LDF has been observed in the counting process and some physical models [4] in the range of a negative biasing field. In the following discussion, we illustrate the difference between the conditions used in Tsirelson's theorems [16] and in these results [4].

In [16], Tsirelson considered the renewal process with the conditions:

$$\mathbb{E}X = 0, \quad \mathbb{E}X^2 = 1, \quad \mathbb{E}\tau = 1, \quad \mathbb{E}[e^{hX - \epsilon\tau}] < \infty \quad (3.1.3)$$

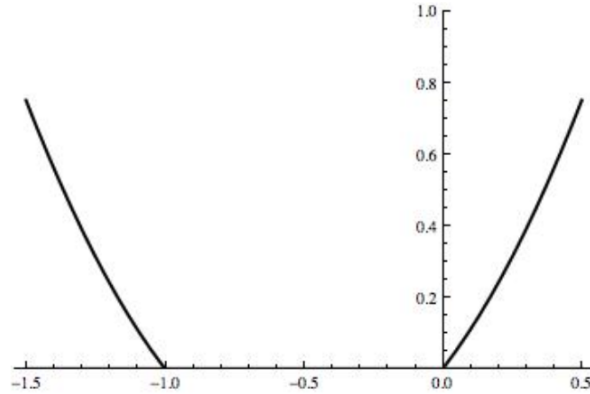


Fig. 3.2: The SCGF \mathcal{G} with an affine part in previous work [1].

for $\forall h \in \mathbb{R}$ and $\forall \epsilon > 0$. He then proved

$$\frac{1}{t} \ln \mathbb{E}[e^{hR(t)}] = \eta_h + O\left(\frac{1}{t}\right) \quad (3.1.4)$$

as $t \rightarrow \infty$, where $\eta_h \in [0, \infty)$ is uniquely determined by this relation:

$$\mathbb{E}[e^{hX - \eta_h \tau}] = 1. \quad (3.1.5)$$

This Tsirelson's theorem cannot be directly applied to our counting process because the counting process does not satisfy $\mathbb{E}X = 0$. When $\mathbb{E}X = 0$ is not satisfied, the proof of (3.1.5) needs an extra condition. Without loss of generality, we consider $\mathbb{E}X = 1$ and we can prove the following theorem:

Theorem 3.1.1. *If $\mathbb{E}X = 1$ and $\mathbb{E}[e^{hX - \epsilon \tau}] < \infty$ hold for $\forall h > 0$ and $\forall \epsilon > 0$, there exists a unique η_h that satisfies*

$$\mathbb{E}[e^{hX - \eta_h \tau}] = 1$$

for $\forall h > 0$.

Proof. Defining $\psi(h, \eta) = \mathbb{E}[e^{hX - \eta \tau}]$, we can prove (i) $\psi(h, \eta)$ is strictly decreasing as η increases with $\tau > 0$ and $\psi(h, \eta)$ is a continuous function, (ii) $\psi(h, 0) > \exp(h) > 1$ and (iii) $\psi(h, \infty) = 0$. From these properties, the theorem 3.1.1 is derived. To prove (i), we use $\tau > 0$. To prove (ii), we use the Jensen's inequality applied to $\psi(h, \eta)$, $\mathbb{E}X = 1$ and $\mathbb{E}\tau = 1$. \square

Remark 3.1.2. Following the same argument as in [16], (3.1.4) can be proven from this theorem 3.1.1. When $h < 0$, we cannot directly apply this method, as η that satisfies (3.1.5) does not exist. Because if we consider negative h for $\psi(-|h|, \cdot)$, the function $\psi(-|h|, \cdot)$ does not satisfy the condition (ii). The function $\psi(-|h|, \cdot)$ has the condition $\psi(-|h|, 0) > \exp(-|h|) < 1$. Thus, we cannot apply this method to the range of h negative. There is the possibility of taking the unique value of η_h within the range of η_h negative, however,

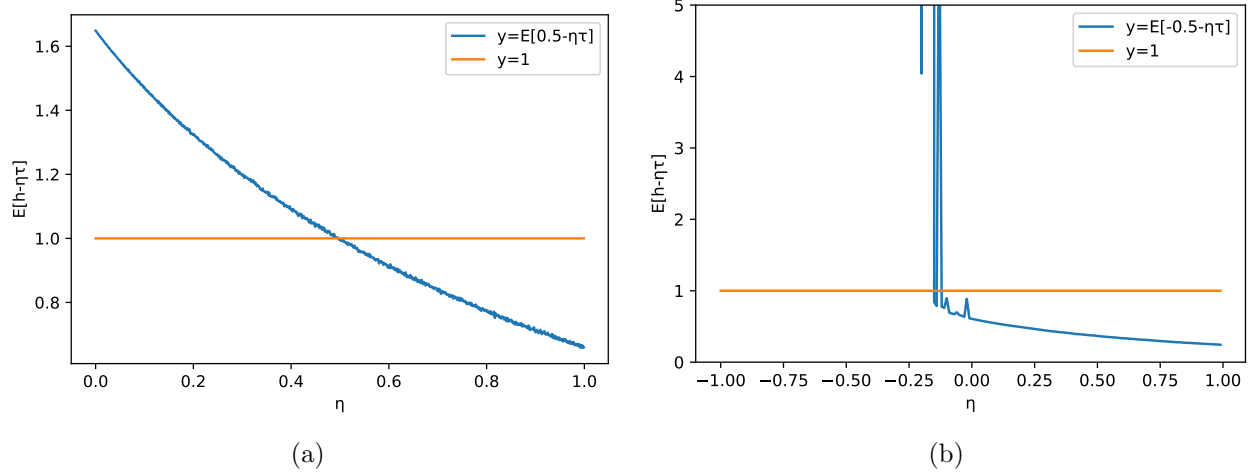


Fig. 3.3: **(a)** Numerical calculation of $\mathbb{E}[e^{0.5-\eta_h\tau}]$ within the range of h positive. $h = 0.5$ is an example of the range of h positive. From this result, there is a scaling parameter η_h that satisfies the condition of $\mathbb{E}[e^{0.5-\eta_h\tau}] = 1$, where $\eta_h = 0.495$ and we use Rayleigh distribution ($\beta = 1$) for this simulation. **(b)** Numerical calculation of $\mathbb{E}[e^{-0.5-\eta_h\tau}]$ within the range of h negative. $h = -0.5$ is an example of the range of h negative. In contrast to left panel, there is no scaling parameters η_h that satisfies the condition of $\mathbb{E}[e^{-0.5-\eta_h\tau}] = 1$. In the range of h negative, the behavior of $\mathbb{E}[e^{h-\eta_h\tau}]$ is broken in this simulation.

in equation (2.13) of [16], negative η_h is not satisfied the relation, which is derived by reformulating $\frac{1}{t}\ln\mathbb{E}[e^{hR(t)}] = \eta_h + O(\frac{1}{t})$. It is given by

$$\sup |-\eta_h t + \ln\mathbb{E}[e^{hR(t)}]| < \infty. \quad (3.1.6)$$

Thus, we cannot define uniqueness of η_h with the range of h negative.¹ We also show this in Fig. 3.3 using the numerical simulation. Finally, we can see the relation of (2.13) of [16] for h positive of our case.

$$\sup_{h \in [c, C]} |-\eta_h t + \ln\mathbb{E}[e^{hR(t)}]| < \infty, \quad (3.1.7)$$

where $0 < c < C < \infty$. Following the procedure of (2.13) of [16], we can get the relation

$$\frac{1}{t}\ln\mathbb{E}[e^{hN_t}] = \eta_h + O(\frac{1}{t}) \quad (h \geq 0, \eta_h \geq 0) \quad (3.1.8)$$

as $t \rightarrow \infty$. Here, we use $R(t) = N_t$, which is a counting process. In addition, we check these condition for the CGF by using numerical simulation. The following figures refer to the condition that the stochastic process satisfies (3.1.4).

¹The convergence of (2.13) of [16] is calculated as

$$e^{-\eta_h t} \mathbb{E}[e^{hR(t)}] \rightarrow A \quad \text{as } t \rightarrow \infty,$$

where A is constant. Therefore, when η_h is negative, left-handside diverges as $t \rightarrow \infty$

3.2 Set-up

Let us consider again a random walk with arbitrary distributions of jump lengths and waiting times. In this section, we use a simple example of the renewal-reward process, which is a counting process N_t .

The well-known fields that exploit the renewal-reward process (and the theory related to this process) are, among others, the actuarial science, where models describing an insurer's vulnerability to ruin are studied (known as ruin theory) [24], the queueing theory that studies the queue length and waiting time in telecommunication, traffic- and industrial engineering [25], and epidemiology using a renewal-reward process for estimating the basic quantity of virus spreading [26, 27]. A number of studies have also reported various physical and biological phenomena which are described by renewal-reward processes [17, 28–32].

In this thesis, we study the fluctuations of the renewal-reward process $R(t)$. Under mild assumptions [23], the family of random variables $(R(t)/t)_{t>0}$ satisfies a large deviation principle

$$\mathbb{P}\left(\frac{R(t)}{t} \simeq s\right) \sim e^{-tI(s)}, \quad \text{as } t \rightarrow \infty, \quad (3.2.1)$$

where the non zero function I is called the rate function. See [23] for more mathematical formulation of the large deviation principle. In good cases [23], the rate function I is equal to the Legendre transform of the sCGF

$$\varphi(h) = \lim_{t \rightarrow \infty} \frac{1}{t} \log \mathbb{E}[e^{hR(t)}], \quad (3.2.2)$$

i.e., $I(s) = \sup\{hs - \varphi(h)\}$. Here $h \in \mathbb{R}$ is called a biasing field.

An interesting point to keep in mind when studying renewal-reward processes is that the process is in general not Markov and a strong time correlation in the dynamics can be introduced by choosing a heavy-tailed probability density as the waiting time distribution. One can intuitively expect that a single waiting time could become dominant in the dynamics because of the heavy tail in the waiting time distribution, leading to an unusually high occurrence of certain rare events (see, for example, a single-big jump principle [13, 33–35]). Considering renewal-reward processes with heavy-tailed waiting-time distributions, the presence of a singular behaviour in the rate function and the CGF was established in [1, 23, 36] related to these rare events. For example, let us consider the counting process $R(t) = N_t$ with waiting times distributed according to a Pareto's law with a parameter $m > 2$:

$$p(t) : = \begin{cases} 0 & t \leq 0 \\ \frac{(m-1)}{(1+t)^m} & t > 0 \end{cases} \quad (3.2.3)$$

or equivalently by its cumulative distribution F

$$F(t) := \mathbb{P}[\tau \leq t] = \begin{cases} 0 & t \leq 0 \\ 1 - \frac{1}{(1+t)^{m-1}} & t > 0. \end{cases} \quad (3.2.4)$$

Then the result of [23] implies that

$$\begin{aligned} I(x) &= 0 & (0 \leq x \leq \mu) \\ \varphi(h) &= 0 & (h \leq 0), \end{aligned} \quad (3.2.5)$$

where $\mu = 1/\mathbb{E}[\tau]$. The fact that the rate function I takes the value zero below $\mu = 1/\mathbb{E}[\tau]$, indicates an unusually high occurrence of the rare events where N_t is below its average value $\mu = 1/\mathbb{E}[\tau]$. In this thesis, we call this singularity an *affine part* and we focus on this specific affine part obtained with $R(t) = N_t$.

Our goal in this thesis is to study the finite time asymptotic of CGF when the affine part emerges. The finite time asymptotics of the CGF and of the rate function in the context of renewal-reward processes have been studied by Tsirelson [16] under the assumption that the rewards are centred, namely $\mathbb{E}[X_i] = 0, i \in \mathbb{N}$. Tsirelson theorem however cannot be applied to the counting process N_t as it satisfies $X_i = 1, i \in \mathbb{N}$. The affine part is indeed not observed in the Tsirelson theorem [16]. To approach this problem, we rely on a classical result on the sum of random variables with regularly varying tails that can be found in Feller's book [37]. Applied to the special case of the distribution (3.2.3), the behaviour for $t \rightarrow \infty$ of $\mathbb{P}[N_t \leq k]$ is determined by

$$\lim_{t \rightarrow \infty} t^{m-1} \mathbb{P}[N_t \leq k-1] = k. \quad (3.2.6)$$

for any $k \geq 1$. Using this theorem, we study the asymptotics in time of the CGF. The strategy is that we first expand the MGF of N_t as the infinite sum of $P[N_t < k]$ ($k = 1, 2, \dots$) and then use this theorem in each term. Technically, the key in this step is to justify the fact that the infinite sum and the large t limit can be exchanged. This leads to the asymptotic form of the upper bound for the finite-time moments generating function (MGF) (Theorem 3.3.1 and Theorem 3.3.2) for Pareto waiting time distribution with an integer exponent. In numerical simulations we then test the validity of this theorem using Pareto distribution with a real value exponent, inverse Rayleigh distribution and log-normal distribution, demonstrating the extent of this theorem beyond what we study mathematically in this thesis.

The structure of this section is the following: In Section 3.3, we will state and prove our results on the speed of convergence of the moments generating function (MGF). In Section 3.4, we will show how to prove a result providing uniform bounds that are used in the proof of the main theorem. In Section 3.5.1, we will perform numerical simulations and study if the theorem in Section 3.3 can be extended to the problems with different heavy-tailed waiting-time distributions. In Section 3.5.2, we numerically study the rate function of N_t , observe a general asymptotic form, and discuss the relation with the results in Section 3.3. Finally in Section 3.6, we will conclude this section.

3.3 Results

Our goal is to study for $h < 0$:

$$M(t, h) := \mathbb{E}[e^{hN_t}] = \sum_{k=0}^{\infty} e^{hk} \mathbb{P}[N_t = k]. \quad (3.3.1)$$

We observe that, since obviously $0 \leq \mathbb{P}[N_t = k] \leq 1$, the series is normally convergent for any $h < 0$, as a function defined for $t \in [0, \infty[$. Let

$$S_k = \tau_1 + \dots + \tau_k$$

Since for any $t \geq 0$, any $k \in \mathbb{N} \setminus \{0\}$,

$$\mathbb{P}[N_t = k] = \mathbb{P}[N_t \leq k] - \mathbb{P}[N_t \leq k - 1]$$

and any $k \in \mathbb{N}$:

$$\mathbb{P}[N_t \leq k] = \mathbb{P}[S_{k+1} > t],$$

we obtain :

$$M(t, h) = \sum_{k=1}^{\infty} (e^{h(k-1)} - e^{hk}) \mathbb{P}[S_k > t].$$

Introducing $z = e^h$, this may be rewritten :

$$M(t, h) = \frac{1-z}{z} \sum_{k=1}^{\infty} z^k \mathbb{P}[S_k > t]$$

The behaviour for $t \rightarrow \infty$ of $\mathbb{P}[S_k \geq t]$ when S_k is the sum of independent variables distributed with a regularly varying distribution may be found in Feller's book [37] Chapter VIII.9 p. 278. The Pareto distribution with $m \geq 3$ enters this class and Feller's result implies that for any $k \geq 1$:

$$\lim_{t \rightarrow \infty} t^{m-1} \mathbb{P}[S_k > t] = k. \quad (3.3.2)$$

Thus, if one is allowed to take the limit inside the above series, one gets the following

Theorem 3.3.1. *Let $(N_t)_{t \geq 0}$ the counting process with waiting times distributed according to a Pareto's law with an integer parameter $m \geq 3$, then for any $h < 0$:*

$$\lim_{t \rightarrow \infty} t^{m-1} M(t, h) = \frac{1}{1 - e^h}.$$

The proof of the theorem boils down to proving that this exchange is justified and using $\sum_{k=1}^{\infty} k z^k = \frac{z}{(1-z)^2}$ for $0 \leq z < 1$. The justification of the exchange of the series and the limit is guaranteed by (3.3.3) in the next theorem.

Theorem 3.3.2. *Let $(N_t)_{t \geq 0}$ the counting process with waiting times distributed according to a Pareto's law with an integer parameter $m \geq 3$, then for any $h < 0$*

$$\sum_{k=1}^{\infty} e^{hk} \sup_{t \in [0, \infty[} t^{m-1} \mathbb{P}[S_k > t] < \infty. \quad (3.3.3)$$

Moreover, for any $m \geq 3$, there exist $C_m > 0$ and \bar{c} such that for any $h < 0$, and for any $d > \frac{\bar{c}}{e^{-h}-1}$:

$$M(t, h) \leq \frac{1}{1 - e^h} (1 - F(t)) + C_m \frac{d^m}{(d+t)^m} \frac{\alpha(d) e^h}{(1 - \alpha(d) e^h)^2} \quad (3.3.4)$$

where $\alpha(d) = 1 + \frac{\bar{c}}{d}$.

Remark Note that the first term in (3.3.4) is $O(\frac{1}{t^{m-1}})$ while the second term is $O(\frac{1}{t^m})$.

Proof. We introduce the notation $M_k(t) = \mathbb{P}[N_t = k]$ for $k \in \mathbb{N}$. We note the two straightforward relations : for any $k \geq 1$

$$\begin{aligned} M_0(t) &= 1 - F(t) \\ M_k(t) &= \int_0^t M_{k-1}(t-s)p(s)ds \end{aligned} \quad (3.3.5)$$

We use the telescopic identity that holds for any $n \geq 1$

$$M_n(t) = M_0(t) + \sum_{k=1}^n (M_k(t) - M_{k-1}(t)). \quad (3.3.6)$$

which, together with Proposition 3.4.1 below implies that for any integer $m \geq 3$ there exists $\bar{c} > 0$ such that for any $d > 1$, any $t \geq 0$ and for $n \geq 1$:

$$\mathbb{P}[N_t = n] = M_n(t) \leq M_0(t) + nC_m \frac{d^m}{(d+t)^m} \left[1 + \frac{\bar{c}}{d}\right]^{n-1} \quad (3.3.7)$$

and

$$\begin{aligned} \mathbb{P}[S_n \geq t] &= \mathbb{P}[N_t \leq n-1] \\ &= \sum_{k=0}^{n-1} \mathbb{P}[N_t = k] \\ &\leq nM_0(t) + n^2C_m \frac{d^m}{(d+t)^m} \left[1 + \frac{\bar{c}}{d}\right]^{n-1}. \end{aligned} \quad (3.3.8)$$

Thus for any $h < 0$, and any $d > \frac{\bar{c}}{e^{-h}-1}$ the series (3.3.3) converges and the bound (3.3.4) holds. \square

Remarks

If $m \geq 3$ is not an integer, it is easy to see that

$$\mathbb{P}[S_k \geq t] \leq \mathbb{P}[\tilde{S}_k \geq t]$$

where $\tilde{S}_k = \tilde{\tau}_1 + \dots + \tilde{\tau}_k$ and $(\tau_k)_k$ is an i.i.d sequence such that

$$\mathbb{P}[\tilde{\tau}_i > t] = \frac{1}{(1+t)^{\lfloor m \rfloor - 1}}$$

because we have that

$$\mathbb{P}[\tau_i > t] \leq \mathbb{P}[\tilde{\tau}_i > t].$$

Thus, using the same methods, we can conclude that

$$\lim_{t \rightarrow \infty} t^{\lfloor m \rfloor - 1} M(t, h) = 0$$

but not more than that. We expect however the theorem to be true also in the non-integer case. (See Section 3.5.1 for the study based on numerical simulations.)

3.4 Uniform Bounds

Proposition 3.4.1. *For any integer $m \geq 3$, there exists $\bar{c} > 0$ such that for any $n \geq 1$, $d \geq 1$, and any $t > 0$:*

$$M_n(t) - M_{n-1}(t) \leq C_m \frac{d^m}{(d+t)^m} \left[1 + \frac{\bar{c}}{d}\right]^{n-1}. \quad (3.4.1)$$

Proof. We first prove for the case $n = 1$ and then proceed by induction. First, $M_0(t)$ and $M_1(t)$ are given by

$$\begin{aligned} M_0(t) &= 1 - F(t) = \frac{1}{(1+t)^{m-1}} \\ M_1(t) &= \int_0^t M_0(s)p(t-s)ds \\ &= \int_0^t \frac{1}{(1+s)^{m-1}} \frac{(m-1)ds}{(1+t-s)^m}, \end{aligned} \quad (3.4.2)$$

In order to calculate this integral, we perform a partial-fraction decomposition by viewing the denominator in the integral of (3.4.2) as a polynomial in s :

$$\frac{1}{(1+s)^{m-1}(1+t-s)^m} = \sum_{k=1}^{m-1} \frac{a_k(t)}{(1+s)^k} + \sum_{k=1}^m \frac{b_k(t)}{(1+t-s)^k} \quad (3.4.3)$$

where

$$\begin{aligned} a_k(t) &= \frac{1}{(m-1-k)!} \lim_{s \rightarrow -1} \frac{d^{m-1-k}}{ds^{m-1-k}} \left(\frac{1}{(1+t-s)^m} \right), \quad 1 \leq k \leq m-1 \\ b_k(t) &= \frac{1}{(m-k)!} \lim_{s \rightarrow 1+t} \frac{d^{m-k}}{ds^{m-k}} \left(\frac{1}{(1+s)^{m-1}} \right), \quad 1 \leq k \leq m. \end{aligned} \quad (3.4.4)$$

And thus :

$$\begin{aligned} a_k(t) &= \frac{A_k(m)}{(2+t)^{2m-1-k}} \\ b_k(t) &= \frac{B_k(m)}{(2+t)^{2m-1-k}}. \end{aligned}$$

where the $A_k(m)$ and $B_k(m)$ are combinatorial factors. Now with $A'_k(m) = (m-1)A_k(m)$ and $B'_k(m) = (m-1)B_k(m)$ we have

$$M_1(t) = \sum_{k=1}^{m-1} \frac{A'_k(m) + B'_k(m)}{(2+t)^{2m-k-1}} \int_0^t \frac{ds}{(1+s)^k} + \frac{m-1}{(2+t)^{m-1}} \int_0^t \frac{ds}{(1+t-s)^m}, \quad (3.4.5)$$

since from (3.4.4) we see that $B_m(m) = 1$ and thus $B'_m(m) = (m-1)$. We bound the last term in the following way :

$$\begin{aligned} \frac{m-1}{(2+t)^{m-1}} \int_0^t \frac{ds}{(1+t-s)^m} &= \frac{1}{(2+t)^{m-1}} \left(1 - \frac{1}{(1+t)^{m-1}}\right) \\ &\leq \frac{1}{(1+t)^{m-1}} = M_0(t). \end{aligned} \quad (3.4.6)$$

It is easy to see that for $k > 1$, the remaining integrals are all bounded by 1. Thus we have :

$$M_1(t) \leq M_0(t) + \sum_{k=2}^{m-1} \frac{A'_k(m) + B'_k(m)}{(2+t)^{2m-k-1}} + \frac{A'_1(m) + B'_1(m)}{(2+t)^{2m-2}} \log(1+t) \quad (3.4.7)$$

and because $\log(1+t) \leq (2+t)$ and $m \geq 3$:

$$\begin{aligned} M_1(t) &\leq M_0(t) + \frac{C_m}{(2+t)^m} \\ &\leq M_0(t) + \frac{C_m}{(1+t)^m} \\ &\leq M_0(t) + C_m \frac{d^m}{(d+t)^m} \end{aligned} \quad (3.4.8)$$

for some constant C_m depending on m and for any $d \geq 1$.

Thus, we find the bound we were looking for :

$$M_1(t) - M_0(t) \leq C_m \frac{d^m}{(d+t)^m}. \quad (3.4.9)$$

We now proceed to prove the claim of the proposition for general $n > 1$ by induction : we see that

$$M_n(t) - M_{n-1}(t) = \int_0^t (M_{n-1}(s) - M_{n-2}(s))p(t-s) ds \quad (3.4.10)$$

and we assume that for some $\bar{c} > 0$:

$$M_{n-1}(t) - M_{n-2}(t) \leq C_m \frac{d^m}{(d+t)^m} \left[1 + \frac{\bar{c}}{d}\right]^{n-2}$$

for any $d \geq 1$ and any $t \geq 0$. Then we conclude the proof of the proposition with the use of the following Lemma.

Lemma 3.4.2. *There exists $\bar{c} > 0$, such that for any $d \geq 1$ and any $t \geq 0$:*

$$\int_0^t \frac{1}{(d+s)^m} \frac{(m-1)ds}{(1+t-s)^m} \leq \left[1 + \frac{\bar{c}}{d}\right] \frac{1}{(d+t)^m} \quad (3.4.11)$$

□

We give now the proof of Lemma 3.4.2.

Proof. For $d \geq 1$, $t \geq 0$, let

$$I_m(d, t) = \int_0^t \frac{1}{(d+s)^m} \frac{(m-1)ds}{(1+t-s)^m}. \quad (3.4.12)$$

We first perform partial fraction decomposition in the integrand of $I_m(d, t)$,

$$\begin{aligned} \frac{1}{(d+s)^m} \frac{m-1}{(1+t-s)^m} &= \frac{(m-1)}{(1+d+t)^m} \left[\left(\frac{1}{(d+s)^m} + \frac{1}{(1+t-s)^m} \right) \right. \\ &\quad + \frac{L_1}{(1+d+t)} \left(\frac{1}{(d+s)^{m-1}} + \frac{1}{(1+t-s)^{m-1}} \right) + \dots \\ &\quad \left. + \frac{L_{m-1}}{(1+d+t)^{m-1}} \left(\frac{1}{(d+s)} + \frac{1}{(1+t-s)} \right) \right], \end{aligned} \quad (3.4.13)$$

where L_i ($i = 1, 2, \dots, m-1$) are constants. Integrating these terms over the interval between $s = 0$ and $s = t$, we then get

$$\begin{aligned} I_m(d, t) &= \frac{(m-1)}{(1+d+t)^m} \left[\frac{1}{m-1} \left(\frac{1}{d^{m-1}} + 1 - \frac{1}{(d+t)^{m-1}} - \frac{1}{(1+t)^{m-1}} \right) \right. \\ &\quad + \frac{L_1}{(1+d+t)} \frac{1}{m-2} \left(\frac{1}{d^{m-2}} + 1 - \frac{1}{(d+t)^{m-2}} - \frac{1}{(1+t)^{m-1}} \right) + \dots \\ &\quad \left. + \frac{L_{m-1}}{(1+d+t)^{m-1}} \left(\log \left(\frac{(d+t)(1+t)}{d} \right) \right) \right] \\ &\leq \frac{1}{(d+t)^m} \left[1 + \frac{\bar{c}}{d} \right], \end{aligned} \quad (3.4.14)$$

for some $\bar{c} > 0$. We have used the relation $t > \log(t)$ to derive the inequality in the second line. □

3.5 Numerical Study

3.5.1 Generality of Theorem 3.3.1

In this section, we numerically study the validity of Theorem 3.3.1 beyond its hypotheses. We first test if our numerical simulations capture correctly Theorem 3.3.1 by using Pareto distribution with an integer value exponent (with which Theorem 3.3.1 was proven). We then numerically study the validity of this theorem for different waiting time distributions, such as Pareto distribution with a real value exponent, inverse Rayleigh distribution and lognormal distribution.

Using numerical simulations, we estimate $M(t, h)$ for the Pareto distribution (with $m = 3$) and divide it by $M_0(t) = 1/(1+t)^{m-1}$. We plot $M(t, h)/M_0(t)$ as a function of t in Fig.3.4 together with $1/(1-e^h)$ as horizontal dashed lines. This demonstrates the reliability of our numerical simulations.

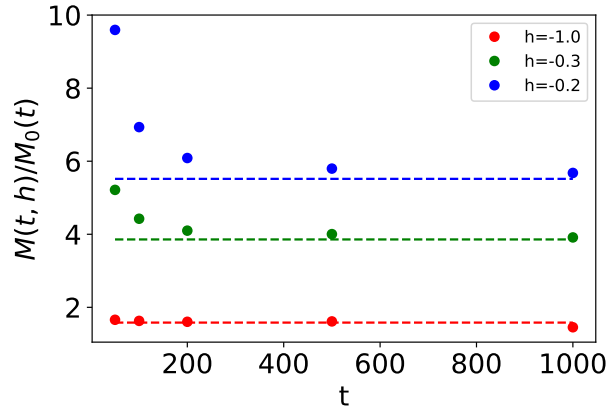


Fig. 3.4: The numerical results of $M(t, h)/M_0(t)$ with the Pareto distribution ($m = 3$). Dashed lines are $1/(1 - e^h)$.

Next we consider the Pareto distribution with a real value exponent ($m = 3.5$), inverse Rayleigh distribution

$$p_{Ray}(t) := \begin{cases} 0 & t \leq 0 \\ \frac{\beta}{t^3} e^{-\frac{\beta}{2t^2}} & t > 0 \end{cases} \quad (3.5.1)$$

with a parameter β and log-normal distribution

$$p_{log}(t) := \begin{cases} 0 & t \leq 0 \\ \frac{1}{\sqrt{2\pi}\sigma t} e^{-\frac{(\log(t)-\mu)^2}{2\sigma^2}} & t > 0 \end{cases} \quad (3.5.2)$$

with parameters μ and σ . The corresponding cumulative distributions for the latter two distributions are

$$F_{Ray}(t) := \mathbb{P}[\tau \leq t] = \begin{cases} 0 & t \leq 0 \\ e^{-\frac{\beta}{2t^2}} & t > 0. \end{cases} \quad (3.5.3)$$

and

$$F_{log}(t) := \mathbb{P}[\tau \leq t] = \begin{cases} 0 & t \leq 0 \\ \frac{1}{2} \operatorname{erfc} \left[-\frac{\log(t)-\mu}{\sqrt{2}\sigma} \right] & t > 0, \end{cases} \quad (3.5.4)$$

respectively.

We perform numerical simulations with these waiting time distributions and plot in Fig.3.5 the finite-time CGF of the counting process N_t , defined as

$$\varphi_t(h) := \frac{1}{t} \log M(t, h). \quad (3.5.5)$$

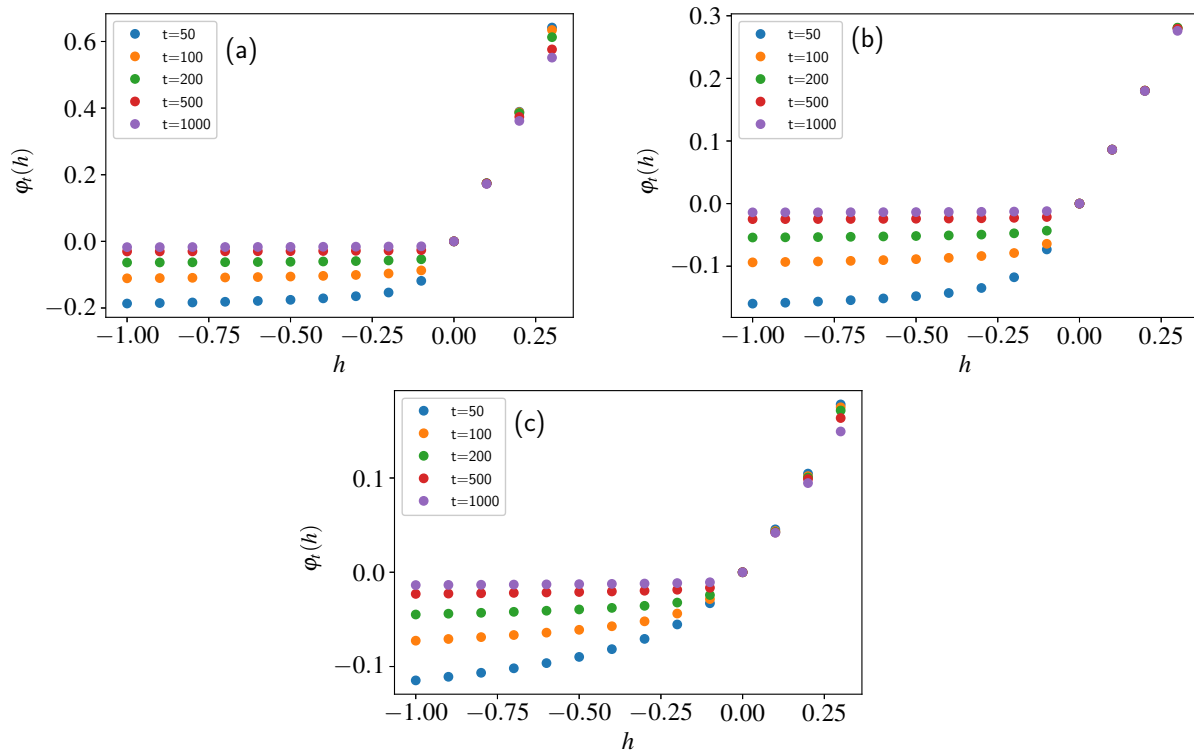


Fig. 3.5: Numerical results of the finite-time CGF $((1/t) \log \mathbb{E}[e^{hN_t}])$ of the counting process with Pareto distribution with $m = 3.5$ (a), inverse Rayleigh distribution with $\beta = 1$ (b) and log-normal waiting-time distribution with $\mu = 0$ and $\sigma = 1.5$ (c). We observe the emergence of the affine part when h is negative.

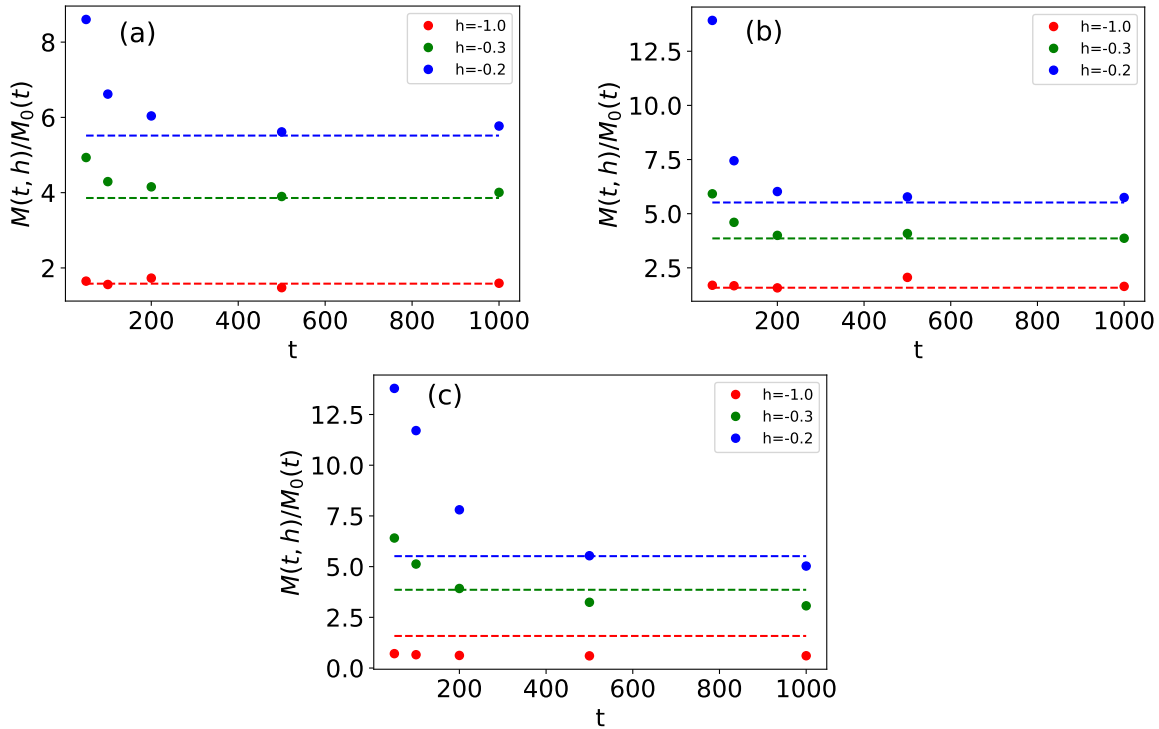


Fig. 3.6: $M(t, h)/M_0(t)$ (filled circles) together with $1/(1 - e^h)$ (dashed lines) for Pareto distribution with $m = 3.5$ (a), inverse Rayleigh distribution with $\beta = 1$ (b) and log-normal waiting-time distribution with $\mu = 0$ and $\sigma = 1.5$ (c).

The figure shows the emergence of the affine part for the negative h [1, 23, 36], indicating that $M(t, h)$ decreases sub-exponentially. Theorem 3.3.2 states that, when the waiting time distribution is the Pareto distribution with an integer exponent m , this sub-exponential decrease is proportional with $M_0(t)$ (where $M_0(t) = 1 - F(t)$) with a coefficient $1/(1 - e^h)$. To study if the same statement is satisfied with the various waiting-time distributions introduced above, we then plot $M(t, h)/M_0(t)$ (where $M_0(t) = 1 - F(t)$) in Fig.3.6 as a function of t . In the figure, $M(t, h)/M_0(t)$ seems to converge to $1/(1 - e^h)$ for Pareto distribution ($m = 3.5$) and inverse Rayleigh distribution, while it converges to a value close to $1/(1 - e^h)$ for lognormal distribution. We note that the Pareto and inverse Rayleigh distribution are both regularly varying at infinity while the log-normal is not. It is an interesting future perspective to quantitatively understand these convergences and prove the corresponding Theorem 3.3.1 for these waiting time distributions.

3.5.2 Study of the Rate Function

In this section, we numerically study the asymptotic behaviour of the finite-time rate function $i_t(x)$

$$i_t(x) := -\frac{1}{t} \log \mathbb{P} \left(\frac{N_t}{t} \simeq x \right). \quad (3.5.6)$$

We first plot $i_t(x) - \min_x i_t(x)$ for several t with different waiting-time distributions (introduced in the previous sub-section) in Fig. 3.7. The figure indicates the emergence of the affine part, which manifests anomalously large probability of rare fluctuations where N_t/t takes smaller values than the expectation. To study the finite-time asymptotic, we then plot $\log \mathbb{P}[N_t < xt]$ (for a fixed x) as a function of t in Fig. 3.8. We observe the asymptotic behaviour of $\log \mathbb{P}[N_t < xt]$ as

$$\log \mathbb{P}[N_t < xt] \sim a \log M_0(t) + \log(t) + b \quad (3.5.7)$$

with constants a, b (that can potentially depend on x). For Pareto and the inverse Rayleigh waiting time distributions, a seems to be 1, while a is different from 1 for the log-normal waiting-time distribution.

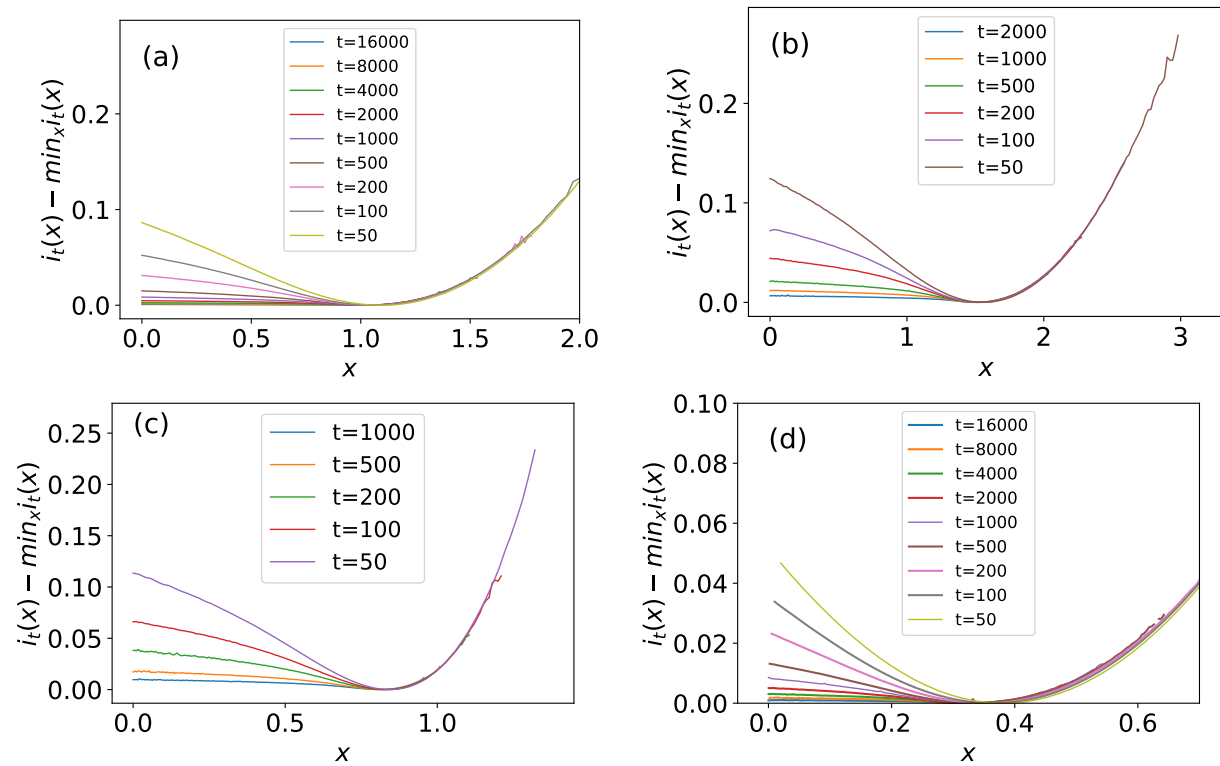


Fig. 3.7: The finite time rate function $i_t(x) - \min_x i_t(x)$ for several t with different waiting time distributions: (a) Pareto distribution with $m = 3$, (b) Pareto distribution with $m = 3.5$, (c), inverse Rayleigh distribution with $\beta = 1$ and (d) the log-normal waiting-time distribution with $\mu = 0$ and $\sigma = 1.5$. In all panels, the affine part emerges as t increases.

Mathematically justifying this asymptotic expression is an open problem. For example, we can immediately derive a lower bound for $\mathbb{P}[N_t < xt]$ for any $x > 0$ as

$$\mathbb{P}[N_t < xt] \geq \mathbb{P}[N_t = 0] = \mathbb{P}[\tau_1 > t] = M_0(t), \quad (3.5.8)$$

which is consistent with the observation. For the upper bound it is natural to use the relation

$$\mathbb{P}[N_t < xt] = \mathbb{P}[S_{[xt]} > t] \quad (3.5.9)$$

and the bound (3.3.8) with replacing n by $\lfloor xt \rfloor$. This leads to

$$\mathbb{P}[S_n \geq t] \leq nM_0(t) + n^2 C_m \frac{d^m}{(d+t)^m} \left[1 + \frac{\bar{c}}{d}\right]^{n-1} \quad (3.5.10)$$

valid for any $d \geq 1$. Unfortunately the bound provided by this inequality (and in particular its second term) is not strong enough to derive a meaningful asymptotic expression. Indeed, it is easy to see that when $t \rightarrow \infty$ the second term diverges even if one takes $d \rightarrow \infty$ first. Interestingly, the logarithm of the first term yields

$$\log(\lfloor xt \rfloor M_0(t)) \sim \log M_0(t) + \log(xt) \quad (3.5.11)$$

as $t \rightarrow \infty$, which is coincidentally the same as the observed expression (3.5.7) for Pareto and inverse Rayleigh waiting time distributions. This implies that refining the bound (3.3.8) could be the key to derive (3.5.7) at least for these waiting time distributions. Pursuing this direction is out of scope in the current manuscript but an interesting future perspective.

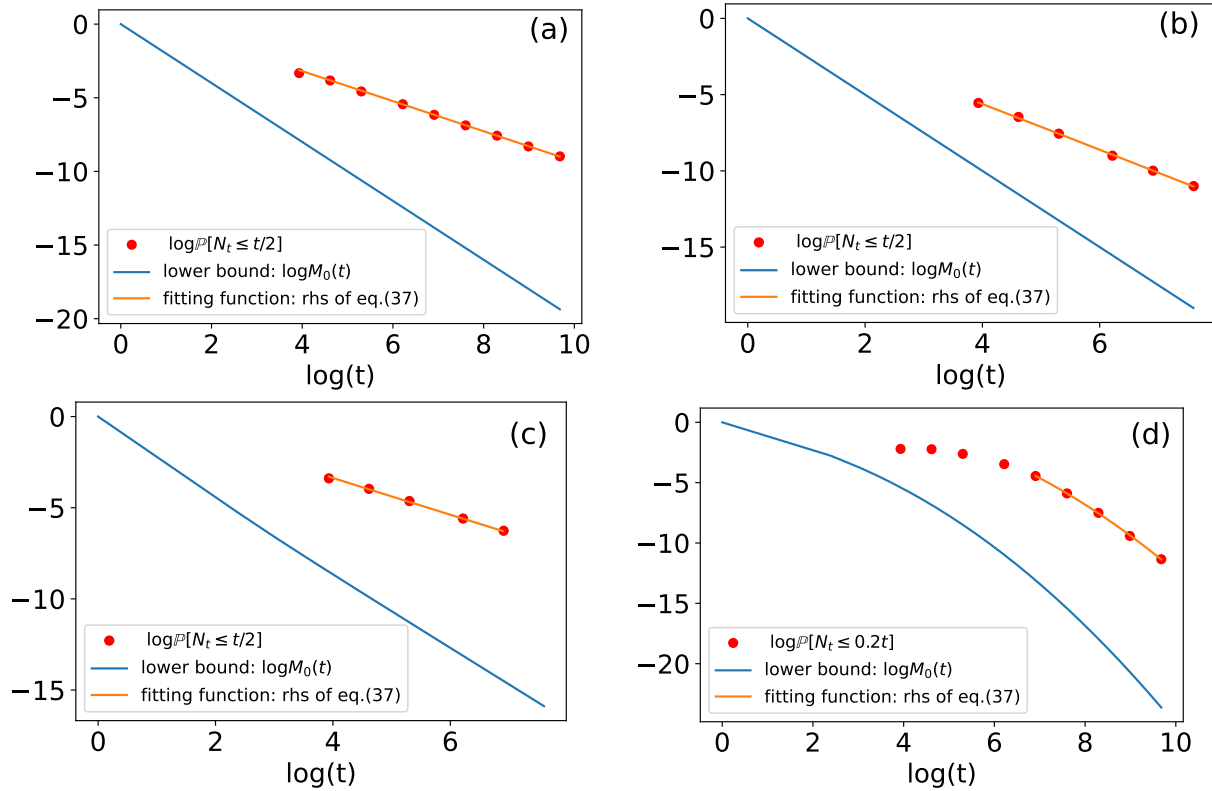


Fig. 3.8: $\log \mathbb{P}[N_t < xt]$ for several waiting time distributions: (a) Pareto distribution with $m = 3$, (b) Pareto distribution with $m = 3.5$, (c), inverse Rayleigh distribution with $\beta = 1$ and (d) the log-normal waiting-time distribution with $\mu = 0$ and $\sigma = 1.5$. The lower bound $\log M_0(t)$ and a fitting function $a \log M_0(t) + \log(t) + b$ (with fitting parameters a, b) are also plotted. These fitting parameters are determined as $a = 1.01, b = 0.92$ for (a), $a = 1.00, b = 0.43$ for (b), $a = 1.00, b = 2.00$ for (c) and $a = 0.89, b = 2.51$ for (d).

3.6 Conclusion

In this section, we studied the finite-time asymptotic of the MGF in a counting process N_t with Pareto distributions (3.2.3). To this end, we applied the result (3.3.2) and we proved an explicit expression of the bounds for the finite-time MGF (Theorem 3.3.2) using an expansion approach. The method to prove these expressions could be applied to more general cases, as the validity of the relation (3.3.2) is not restricted to Pareto distribution. Also we expect that the bound of Theorem 3.3.2 may be extended beyond the case where one can perform a partial fraction decomposition to estimate the integrals. The same affine part has been observed in heat currents with the inverse Rayleigh distribution [1] and in the counting process with lognormal distribution (Fig.3.5). Similar finite-time asymptotics for the MGF are anticipated as numerically demonstrated in Section 3.5.1. Studying how the methods of this section can be generalised in these cases would be an interesting future perspective.

In physics, there have been tremendous efforts to understand and characterise singularities appearing in large deviation functions (rate functions and CGFs). In equilibrium statistical physics, these singularities correspond to phase transitions because the large deviation functions are the thermodynamic functions ([21, 38–41] for instance). Studying large deviation functions of time-averaged quantities in non-equilibrium systems have attracted a strong attention of statistical physicists since the discovery of fluctuation theorem in 1993 [40, 42–45]. The singularities of the large deviation functions are related to dynamical phase transitions and are studied in lattice gas models [46–52], high-dimensional chaotic dynamics [53–55], glass formers [3, 56–61], diffusive hydrodynamic equations [62–64] and active matters [65–68]. In these studies, the dynamics are defined using Markov processes (or deterministic processes), where the CGF and the rate function are introduced in the large time limit. These functions are analytic, but taking another limit (usually the large system size limit), a singularity emerges. See [69] for an illustrative example. In our case, the CGF and the rate function (defined in the large time limit) already include a singularity without taking this second limit due to the heavy tailed waiting time distributions. Studying how this difference can alter the well-studied dynamical phase transitions in physics context would be an interesting perspective, in the similar way that heat conductions in aerogels were studied using renewal-reward processes [1].

3.A Perturbative Construction of MGF

In the main section, we've already derived the finite time asymptotic form of MGF with Pareto-distribution. Here, we show another perturbative method to derive the expression of finite time asymptotic form of MGF by using the renewal equation. Recalling (2.1.46), the

MGF can be written as

$$\begin{aligned}
M(t, h) &= \int_0^\infty \mathbb{E}[e^{hN_t} | X_1 = s]p(s) = \int_0^t \mathbb{E}[e^{hN_t} | X_1 = s]p(s) + \int_t^\infty \mathbb{E}[e^{hN_t} | X_1 = s]p(s) \\
&= e^h \int_0^t \mathbb{E}[e^{hN_{t-s}}]p(s) + \int_t^\infty p(s) \\
M(t, \epsilon) &= [1 - F(t)] + \epsilon \int_0^t M(t-s, \epsilon)p(s) \tag{3.A.1}
\end{aligned}$$

with $\epsilon = e^h$. Thus, we see that the MGF $M(t, h)$ satisfies a renewal equation. In order to find a solution to this renewal equation, we try to expand $M(t, \epsilon)$ as a formal power series in ϵ :

$$M(t, \epsilon) = \sum_{n=0}^{\infty} \epsilon^n M_n(t). \tag{3.A.2}$$

We will determine these coefficients $M_n(t)$, $n \in \mathbb{N}$ by substituting this formal power series for $M(t, \epsilon)$ in (3.A.1), leading to the following theorem.

Proposition 3.A.1. *Let F an arbitrary cumulative distribution function and let $(M_n)_{n \in \mathbb{N}}$ a sequence of functions defined inductively by*

$$M_0(t) = 1 - F(t), \quad t \geq 0$$

and for $n \geq 1$

$$M_n(t) = \int_0^t M_{n-1}(t-s)p(s), \tag{3.A.3}$$

If $0 \leq \epsilon < 1$, then the formal power series (3.A.2) is normally convergent, namely :

$$\sum_{n=0}^{\infty} \epsilon^n \sup_{t \in [0, \infty)} |M_n(t)| < \infty. \tag{3.A.4}$$

Moreover the power series solves the equation (3.A.1).

Proof. We are going to prove inductively that for any $n \geq 0$,

$$\sup_{t \in [0, \infty)} |M_n(t)| \leq 1.$$

This implies that (3.A.4) holds. First, we note that by definition : $\sup_{t \in [0, \infty)} |M_0(t)| \leq 1$. Assume next that the claim is true for a given $n \geq 1$, then by (3.A.3) we see that for any $t \geq 0$,

$$M_{n+1}(t) = \int_0^t M_n(t-s)p(s) \leq \int_0^t p(s) = F(t) \leq 1 \tag{3.A.5}$$

The proof of the fact that the power series (3.A.2) solves the renewal equation follows by inserting it in (3.A.1) and identifying coefficients of equal power in ϵ and using (3.A.3). \square

This approach gives the same result, which is Proposition 3.4.1. By considering the case of the negative biasing field for the renewal equation, we can expand the MGF within the specific range.

Chapter 4

Application of The Variational Principle for SCGF with Affine Parts

In this chapter, we re-visit the affine part in the CGF [1] by using a variational principle and a numerical simulation technique (population dynamics algorithm [3]) developed in large deviation theory. These techniques have been applied to study a singularity appearing in the LDF in, among others, kinetically constrained models (KCM) [2] and active matters [3]. These models are defined using Markov processes, because of which the LDF of time-averaged quantities does not have any singularity whenever the system size (not the averaging time) is finite. Our focus is on how the same methodology can be extended to our non-Markovian problem to derive the affine part.

4.1 Background

4.1.1 Model

We first illustrate our model. We confine a tracer particle in a one-dimensional box that has two different temperatures at both ends. The confined tracer has a random speed v distributed according to the following distribution:

$$q_{\beta_{-1,1}}(v) = \beta_{-1,1} v e^{-\beta_{-1,1} \frac{v^2}{2}} \mathbb{1}_{(v)>0} \quad (4.1.1)$$

where $\beta_{-1,1} = 1/T_{-1,1}$ is the inverse temperature of the left- or right-wall where the collision takes place. We introduce a sign variable σ_k that takes a value either 1 or -1 depending on the direction to which the particle moves between k -th and $(k+1)$ -th collisions. We denote the state space of this variable by $E \equiv \{-1, +1\}$. The initial position and velocity of the particle are denoted by (x_0, v_0) , from which we can derive $\sigma_0 = v_0/|v_0|$, $\sigma_k = (-1)^k \sigma_0$. We also define the velocity v_k of the particle between k -th and $(k+1)$ -th collisions. These are drawn randomly from one of the Rayleigh distributions (4.1.1) depending on the previous hot wall with which the particle collides. Note that v_k and σ_k have the same sign each events. We denote by S_k the time at which $(k+1)$ -th collision occurs. Introducing $\hat{\sigma}_k = \frac{1}{2}(\sigma_k + 1)$, the time of the first collision with a wall is written as

$$S_0 = S_0(x_0, v_0) := \frac{\hat{\sigma}_0 - x_0}{v_0} > 0. \quad (4.1.2)$$

Note that k -th inter-arrival time is given as

$$\tau_k := \frac{\sigma_k}{v_k}, \quad (4.1.3)$$

which is distributed according to the inverse Rayleigh waiting time density:

$$p(\tau_k | \sigma_{k-1}) = \frac{\beta_{\sigma_{k-1}}}{\tau^3} \exp\left(-\frac{\beta_{\sigma_{k-1}}}{2\tau^2}\right) \mathbb{1}_{(\tau) > 0}. \quad (4.1.4)$$

The arrival time S_k is then written as

$$S_k := S_0 + \tau_1 + \tau_2 + \cdots + \tau_k, \quad k \geq 1. \quad (4.1.5)$$

The energy exchanged between the two walls during a time interval $[0, t]$ is given by

$$J[0, t] := \frac{1}{2} \sum_{k \geq 1: S_k \leq t} v_k^2 \sigma_k. \quad (4.1.6)$$

We call J the energy current. Then, we can calculate the expected value of J in the large time limit. It is given by

$$\lim_{t \rightarrow \infty} \frac{\mathbb{E}[J(t)]}{t} = \kappa \left(\frac{1}{\beta_+} - \frac{1}{\beta_-} \right), \quad (4.1.7)$$

where κ is the conductivity

$$\kappa^{-1} = \left(\frac{\pi\beta_-}{2} \right)^{\frac{1}{2}} + \left(\frac{\pi\beta_+}{2} \right)^{\frac{1}{2}}. \quad (4.1.8)$$

We will show more details of the calculation around (5.3.17) in chapter 5. We also calculate the convergence of the number of hitting times N_t . It is given by

$$\lim_{t \rightarrow \infty} \frac{\mathbb{E}[N_t]}{t} = 2\kappa \quad (4.1.9)$$

as with the similar derivation of the first moment of J .

4.1.2 Properties of a Path Probability

We next introduce a path probability of this model [1]. We consider a dynamics (or a path) that ends at time t . This path is specified by the number of collisions N (between the particle and the walls) and a sequence of inter-arrival times $(\tau_i)_{i=1}^N$. The probability density of this path (thus the path probability) is then given as

$$\mathbb{P}(N_t = N, (\tau_i)_{i=1}^N) \propto \left(\prod_{i=1}^N p(\tau_i | \sigma_{i-1}) \right) \Theta(S_N - t) \Theta(t - S_{N-1}), \quad (4.1.10)$$

where $\Theta(x)$ is a Heaviside step function.

Below we numerically demonstrate an interesting property related to this path probability. When t is large, one can expect an approximated form of (4.1.10) as

$$\mathbb{P}(N_t = N, (\tau_i)_{i=1}^N) \simeq \left(\prod_{i=1}^N p(\tau_i | \sigma_{i-1}) \right) \delta(S_N - t) \quad (4.1.11)$$

with the Dirac delta function $\delta(x)$. The probability of observing N jumps for a fixed target time t is then derived as

$$\mathbb{P}(N|t) \propto \int (d\tau)_{i=1}^N \mathbb{P}(N, (\tau_i)_{i=1}^N). \quad (4.1.12)$$

Meanwhile, the probability of the final time t for a fixed number of jumps N is derived as

$$\mathbb{P}(t|N) \propto \int (d\tau)_{i=1}^N \left(\prod_{i=1}^N p(\tau_i | \sigma_{i-1}) \right) \delta(S_N - t) \quad (4.1.13)$$

by definition. From (4.1.11), (4.1.12) and (4.1.13), we thus find

$$\mathbb{P}(N|t) \simeq \mathbb{P}(t|N). \quad (4.1.14)$$

In Fig.4.1, we numerically demonstrate this relation.

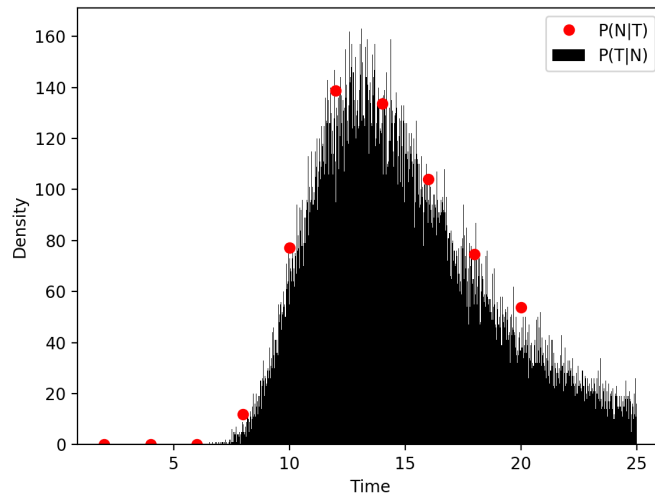


Fig. 4.1: A numerical comparison between $\mathbb{P}(N|T)$ and $\mathbb{P}(T|N)$ from the numerical simulations.

4.1.3 A Bound Function of CGF

Let us denote a path of a system by \mathcal{C} and its path probability by $\mathbb{P}[\mathcal{C}]$. We denote a time cumulative quantity of this system by $A[\mathcal{C}]$ (e.g., J in the heat-conduction model introduced

in the previous sub-section). We introduce the analogue for the canonical ensemble in this dynamical problem as

$$\mathbb{P}_h[\mathcal{C}] \propto \mathbb{P}[\mathcal{C}]e^{-hA[\mathcal{C}]}, \quad (4.1.15)$$

where h is a field playing a role of an “inverse temperature”. The CGF of $A[\mathcal{C}]$ is given as the “free energy” of this canonical ensemble:

$$\phi(h, t) = \log \mathbb{E}[e^{-hA[\mathcal{C}]}] \quad (4.1.16)$$

Note that it is not clear *a priori*, if this canonical ensemble can be generated in a numerical simulation, where only “physical” rules (e.g., the temperatures of the walls in the heat-conduction model) of the dynamics are modified [70]

To further understand this problem, let us consider a control model that can be defined by modifying only “physical” rules. The path probability of this control model is denoted by \mathbb{P}^{con} . We then have [71, 72]

$$\begin{aligned} \phi(h, t) &= \log \int e^{-hA[\mathcal{C}]} \mathbb{P}[\mathcal{C}] d\mathcal{C} \\ &= \log \int e^{-hA[\mathcal{C}]} \mathbb{P}^{\text{con}}[\mathcal{C}] \frac{\mathbb{P}[\mathcal{C}]}{\mathbb{P}^{\text{con}}[\mathcal{C}]} d\mathcal{C} \\ \phi(h, t) &\geq -h\mathbb{E}_{\text{con}}[A] - D(\mathbb{P}^{\text{con}}||\mathbb{P}) \end{aligned} \quad (4.1.17)$$

with

$$D(\mathbb{P}^{\text{con}}||\mathbb{P}) = \mathbb{E}_{\text{con}} \left[\log \frac{\mathbb{P}^{\text{con}}(t, \mathcal{C})}{\mathbb{P}(t, \mathcal{C})} d\mathcal{C} \right], \quad (4.1.18)$$

where $\mathbb{E}_{\text{con}}[\cdot]$ denotes the expected value in the controlled system. Here, we used Jensen’s inequality. Note that $D(\mathbb{P}^{\text{con}}||\mathbb{P})$ is a Kullback-Leibler (KL) divergence, which is non-negative and becomes 0 only when $\mathbb{P}^{\text{con}} = \mathbb{P}$. The “physical” control system produces the ensemble of the canonical distribution (4.1.15) if and only if this inequality becomes an equality. Indeed, the right-hand side of (4.1.17) can be rewritten as [73]

$$-h\mathbb{E}_{\text{con}}[A] - D(\mathbb{P}^{\text{con}}||\mathbb{P}) = \phi(h, t) - D(\mathbb{P}^{\text{con}}||\mathbb{P}_h) \quad (4.1.19)$$

using (4.1.15). Therefore, the equality is possible only when $\mathbb{P}^{\text{con}} = \mathbb{P}_h$. It is straightforward to construct such a control process in the large time limit for a stochastic differential equation (See Appendix 4.A).

It is not always true that a control model for a given constraint of “physical” rules is equivalent to a canonical ensemble: This inequality provides us a tool to investigate how far the control model is to the canonical ensemble. In Section 4.2, by using this method, we study approximations of the canonical ensemble for the heat-conduction system. We will derive, as a result, the affine part in the CGF [1].

4.1.4 Population Dynamics Algorithm to Compute $\lim_{t \rightarrow \infty} \phi(h, t)/t$

To check how close the right-hand side of the inequality (4.1.17) is to the left-hand side, we use a population dynamics algorithm to numerically evaluate $\lim_{t \rightarrow \infty} \phi(h, t)/t$ [3]. We introduce the details of the method below.

1. Generate the N_c initial conditions, for example, drawn from the stationary state of the unbiased ($h = 0$) dynamics.
2. Simulate the N_c dynamics for the time interval t . During these simulations, repeat the following procedure every small time step Δt :

(2-a) (Let us assume that we are at time t' .) For each copy of the system, calculate

$$s_a = \exp \{h[A(t') - A(t' - \Delta t)]\}, \quad (4.1.20)$$

where the time cumulative quantity of interest is denoted $A(t)$ (equivalent to $A[\mathcal{C}]$ in the previous subsection).

(2-b) For each copy, we calculate an integer n_a defined as

$$n_a = \left\lfloor \frac{s_a}{\sum_b s_b} N_c + \xi \right\rfloor, \quad (4.1.21)$$

where ξ is a random number uniformly distributed on $[0, 1]$. We calculate and store the quantity $S_m = \sum_b s_b$, where m represents the number of the repetition (of this step 2) that has been performed.

(2-c) Multiply or eliminate each trajectory a so that it appears n_a times in the new population. (For example, if $n_a = 0$ then trajectory a is deleted. If $n_a = 6$ then we retain trajectory a and we introduce 5 new copies of that trajectory.) This strategy extracts the rare events in this simulation.

(2-d) Eliminate or multiply trajectories within the population, chosen randomly and uniformly, so that the total number of surviving trajectories is N_c .

For this population dynamics algorithm, we can calculate CGF as

$$\lim_{\tilde{t} \rightarrow \infty} \frac{\phi(h, \tilde{t})}{\tilde{t}} \sim \frac{1}{t} \sum_m \log \frac{S_m}{N_c}. \quad (4.1.22)$$

This method has been applied to several physical systems, for instance, dynamical phase transitions in kinetically constrained models [2, 74] and current fluctuations of a simple lattice gas model between the two reservoirs [75].

4.2 Bound Functions for the Heat-conduction System

4.2.1 A Control System with Modifying Wall Temperatures

We consider the one-particle heat-conduction system (as defined in the previous section), but with different wall temperatures $\beta_{-1}^{\text{con}}, \beta_1^{\text{con}}$, as our control system. The waiting time density $p^{\text{con}}(\tau_k | \sigma_{k-1})$ in this system is written as (4.1.4) with β_σ replaced by $\beta_\sigma^{\text{con}}$. The path probability \mathbb{P}^{con} is then

$$\mathbb{P}^{\text{con}}(N_t = N, (\tau_i)_{i=1}^N) \propto \left(\prod_{i=1}^N p^{\text{con}}(\tau_i | \sigma_{i-1}) \right) \Theta(S_N - t) \Theta(t - S_{N-1}). \quad (4.2.1)$$

From (4.1.17), the lower bound for the CGF of the heat current J is given by

$$\phi(h, t) \geq -h\mathbb{E}_{\text{con}}[J] - D(\mathbb{P}^{\text{con}} \|\mathbb{P}). \quad (4.2.2)$$

Using (4.1.6), (4.1.10) and (4.2.1), the right-hand side of this inequality is evaluated as

$$\begin{aligned} & \text{RHS of (4.2.2)} \\ &= -\mathbb{E}_{\text{con}} \left[\frac{h}{2} \sum_{i=1}^N \frac{\sigma_i}{\tau_i^2} + \sum_{i=1}^N \log \frac{p^{\text{con}}(\tau_i | \sigma_{i-1})}{p(\tau_i | \sigma_{i-1})} \right] \\ &= -\mathbb{E}_{\text{con}} \left[\sum_{i=1}^N \left(\frac{h}{2} \frac{\sigma_i}{\tau_i^2} + \log \frac{\frac{\beta_{\sigma_{i-1}}^{\text{con}}}{\tau_i^3} \exp\left(-\frac{\beta_{\sigma_{i-1}}^{\text{con}}}{2\tau_i^2}\right)}{\frac{\beta_{\sigma_{i-1}}}{\tau_i^3} \exp\left(-\frac{\beta_{\sigma_{i-1}}}{2\tau_i^2}\right)} \right) \right] \\ &= -\mathbb{E}_{\text{con}} \left[\sum_{i=1}^N \left[\frac{h\sigma_i - \beta_{\sigma_{i-1}}^{\text{con}} + \beta_{\sigma_{i-1}}}{2\tau_i^2} + \log \frac{\beta_{\sigma_{i-1}}^{\text{con}}}{\beta_{\sigma_{i-1}}} \right] \right] \\ &\geq -\mathbb{E}_{\text{con}} \left[\frac{N}{2} \left[\left(\frac{-h - \beta_1^{\text{con}} + \beta_1}{\beta_1^{\text{con}}} + \frac{h - \beta_{-1}^{\text{con}} + \beta_{-1}}{\beta_{-1}^{\text{con}}} \right) + \left(\log \frac{\beta_1^{\text{con}}}{\beta_1} + \log \frac{\beta_{-1}^{\text{con}}}{\beta_{-1}} \right) \right] \right], \end{aligned} \quad (4.2.3)$$

where we use Wald's identity (lemma 2.1.3) to derive the last line. Finally, dividing both sides by t , taking the large t limit and using (4.1.9), we obtain

$$\lim_{t \rightarrow \infty} \frac{\phi(h, t)}{t} \geq -\kappa^{\text{con}} L(\beta_1^{\text{con}}, \beta_{-1}^{\text{con}}), \quad (4.2.4)$$

where

$$L(\beta_1^{\text{con}}, \beta_{-1}^{\text{con}}) = \left[\frac{-h - \beta_1^{\text{con}} + \beta_1}{\beta_1^{\text{con}}} + \frac{h - \beta_{-1}^{\text{con}} + \beta_{-1}}{\beta_{-1}^{\text{con}}} + \log \frac{\beta_1^{\text{con}} \beta_{-1}^{\text{con}}}{\beta_1 \beta_{-1}} \right] \quad (4.2.5)$$

and κ^{con} is the conductivity with the inverse controlled temperatures. Namely, it is given by

$$(\kappa^{\text{con}})^{-1} = \left(\frac{\pi \beta_{-1}^{\text{con}}}{2} \right)^{\frac{1}{2}} + \left(\frac{\pi \beta_1^{\text{con}}}{2} \right)^{\frac{1}{2}}. \quad (4.2.6)$$

Note that, as shown in [4], the fluctuation relation holds for the CGF $\phi(h)$: $\phi(h) = \phi(\beta_1 - \beta_{-1} - h)$. A similar property is satisfied in the right-hand side of (4.2.4). Indeed, denoting the right-hand side of (4.2.4) by $f(h, \beta_1^{\text{con}}, \beta_{-1}^{\text{con}})$, we obtain $f(h, \beta_1^{\text{con}}, \beta_{-1}^{\text{con}}) = f(\beta_1 - \beta_{-1} - h, \beta_{-1}^{\text{con}}, \beta_1^{\text{con}})$.

We numerically maximise the right-hand side of this inequality over β_1^{con} and β_{-1}^{con} and plot it in Fig.4.2(a) as an orange line. We can clearly see that the affine part does not take place in this bound.

4.2.2 A Control System with $N_t = 0$

In order to get the affine part, we take into the account an extremely slow jump event in our system. The probability of this slow jump is calculated as

$$\mathbb{P}(\tau_1 > t) = 1 - e^{-\frac{\beta}{2t^2}}, \quad (4.2.7)$$

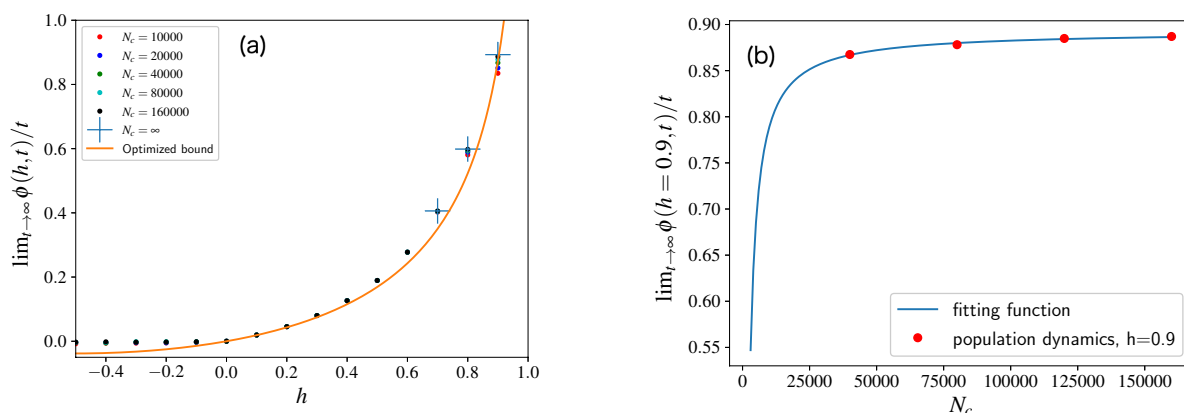


Fig. 4.2: **(a)** Numerical demonstration of the bound (4.2.4). We numerically optimize the control inverse temperatures β_{\pm}^{con} and plot the corresponding bound as an orange line. We compare this bound with the results obtained from the population dynamics algorithm. N_c is the number of copies used in the algorithm (the algorithm produces the correct $\phi(h)$ in the large N_c limit.) We can see that the bound is close to the correct value for $h > 0$. The inverse temperatures are set to $\beta_1 = 1, \beta_{-1} = 2$. See Fig.4.4(a) as a comparison. **(b)** The estimator of $\lim_{t \rightarrow \infty} \phi(h, t)/t$ in the population dynamics algorithm as a function of N_c . In the population dynamics algorithm, the estimator of $\lim_{t \rightarrow \infty} \phi(h, t)/t$ converges to the correct result as N_c increases following the asymptotic form $A/N_c + B$. We used this scaling to infer $\lim_{t \rightarrow \infty} \phi(h, t)/t$ for $h = 0.7, 0.8, 0.9$ where large values of N_c are required for the convergence. For example $\phi(h = 0.9)$ has an asymptotic form $A/N_c + B$ with $A = -1037.587$, $B = 0.893$ (blue line in the panel (b)), from which we estimate $\phi(h = 0.9) = 0.893$.

which means that the confined particle does not reach to the wall. The corresponding path probability is

$$\mathbb{P}^{\text{con}} = \delta_{N_t, 0}, \quad (4.2.8)$$

as the counting process is always $N_t = 0$. According to the relation (4.2.2), we get

$$\begin{aligned} \lim_{t \rightarrow \infty} \frac{\phi(h, t)}{t} &\geq \lim_{t \rightarrow \infty} \left\{ -h \frac{\mathbb{E}_{\text{con}}[J]}{t} - \frac{1}{t} D(P^{\text{con}} \| P) \right\} \\ &\geq - \lim_{t \rightarrow \infty} \frac{1}{t} \mathbb{E}_{\text{con}} \left[\log \frac{1}{\left(1 - e^{-\frac{\beta}{2t^2}}\right)} \right] = 0, \end{aligned} \quad (4.2.9)$$

where $\mathbb{E}_{\text{con}}[J] = 0$ because of no energy exchange. This bound proves the presence of the affine part.

4.2.3 Taking Hydrodynamic Limit

In [4], the CGF was studied in the hydrodynamic limit. Taking the same limit, we study the bound (4.2.4) in this subsection. We first express the inverse temperatures β_1, β_{-1} as $1/\beta_1(\tau, T) = (T + \tau/2)$, $1/\beta_{-1}(\tau, T) = (T - \tau/2)$. In the similar manner, we define the controlled inverse temperatures $\beta_1^{\text{con}}, \beta_{-1}^{\text{con}}$ as

$$\begin{aligned} \frac{1}{\beta_1^{\text{con}}} &= T + \Delta T_1 \\ \frac{1}{\beta_{-1}^{\text{con}}} &= T + \Delta T_{-1}. \end{aligned} \quad (4.2.10)$$

We next introduce a scaling parameter ϵ , by which we scale $\tau \rightarrow \epsilon\tau$ and $h \rightarrow \epsilon h$, $\Delta T_{\pm 1} \rightarrow \epsilon \Delta T_{\pm 1}$. We then expand the right-hand side of (4.2.4) up to the second-order by ϵ .

$$\begin{aligned} \lim_{t \rightarrow \infty} \frac{\phi(\epsilon h, t)}{t} &\geq -\kappa_{\text{con}}(\epsilon) L(\epsilon) \\ &= - \left(\kappa_{\text{con}}(0) + \epsilon \frac{\partial \kappa_{\text{con}}(\epsilon)}{\partial \epsilon} \Big|_{\epsilon \rightarrow 0} + \frac{\epsilon^2}{2} \frac{\partial^2 \kappa_{\text{con}}(\epsilon)}{\partial \epsilon^2} \Big|_{\epsilon \rightarrow 0} + O(\epsilon^3) \right) \\ &\quad \times \left(L(0) + \epsilon \frac{\partial L(\epsilon)}{\partial \epsilon} \Big|_{\epsilon \rightarrow 0} + \frac{\epsilon^2}{2} \frac{\partial^2 L(\epsilon)}{\partial \epsilon^2} \Big|_{\epsilon \rightarrow 0} + O(\epsilon^3) \right) \\ &\simeq -\frac{\epsilon^2}{2} \kappa_{\text{con}}(0) \frac{\partial^2 L(\epsilon)}{\partial \epsilon^2} \Big|_{\epsilon \rightarrow 0}, \end{aligned} \quad (4.2.11)$$

where we use $\frac{\partial \kappa_{\text{con}}(0)}{\partial \epsilon}, L(0), \frac{\partial L(0)}{\partial \epsilon}$ are 0, and

$$\frac{\partial^2 L(\epsilon)}{\partial \epsilon^2} \Big|_{\epsilon \rightarrow 0} = 2h[\Delta T_{-1} - \Delta T_1] - \frac{\tau \Delta T_1}{T^2} + \frac{\tau \Delta T_{-1}}{T^2} + \frac{\tau^2}{2T^2} + \frac{\Delta T_1^2 + \Delta T_{-1}^2}{T^2}. \quad (4.2.12)$$

To identify the optimal bound, we look for $\Delta T_{\pm 1}$ that maximise this right-hand side:

$$\begin{aligned} \frac{\partial}{\partial \Delta T_1} \frac{\partial^2 L(\epsilon)}{\partial \epsilon^2} \Big|_{\epsilon \rightarrow 0} &= -2h - \frac{\tau}{T^2} + \frac{2\Delta T_1}{T^2} = 0 \\ &\rightarrow \Delta T_1 = \frac{\tau}{2} + hT^2 \end{aligned} \quad (4.2.13)$$

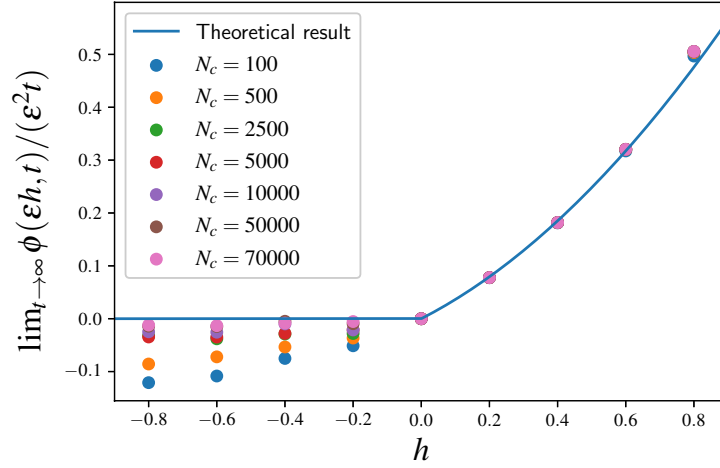


Fig. 4.3: The estimator of $\lim_{t \rightarrow \infty} \phi(\epsilon h, t)/(\epsilon^2 t)$ obtained from the population dynamics method is plotted as a function of h for several values of N_c . In the same figure, we also plot the right-hand side of (4.2.17) as a blue line. We observe a convergence of the estimator to the blue line as N_c increases. We set $\tau = 1$, $T = 1$, and $\epsilon = 1$.

$$\begin{aligned} \left. \frac{\partial}{\partial \Delta T_{-1}} \frac{\partial^2 L(\epsilon)}{\partial \epsilon^2} \right|_{\epsilon \rightarrow 0} &= 2h + \frac{\tau}{T^2} + \frac{2\Delta T_{-1}}{T^2} = 0 \\ &\rightarrow \Delta T_{-1} = -\frac{\tau}{2} - hT^2 \end{aligned} \quad (4.2.14)$$

The optimized temperatures $1/\beta_{\pm 1}^{*,\text{con}}$ are then obtained as

$$\frac{1}{\beta_{\pm 1}^{*,\text{con}}} = \frac{1}{\beta_{\pm 1}} \pm hT^2. \quad (4.2.15)$$

Finally, dividing $\phi(\epsilon h, t)/t$ by ϵ^2 , we arrive at

$$\lim_{\epsilon \rightarrow 0} \lim_{t \rightarrow \infty} \frac{\phi(\epsilon h, t)}{\epsilon^2 t} \geq \kappa h \tau + \kappa h^2 T^2. \quad (4.2.16)$$

Summarising the two bounds obtained in this and the previous subsections, we have

$$\lim_{\epsilon \rightarrow 0} \lim_{t \rightarrow \infty} \frac{\phi(\epsilon h, t)}{\epsilon^2 t} \geq \begin{cases} \kappa h \tau + \kappa h^2 T^2 & (h > 0, h < -\frac{\tau}{T^2}) \\ 0 & (-\frac{\tau}{T^2} \leq h \leq 0) \end{cases} \quad (4.2.17)$$

when the hydrodynamic limit is taken. The equality in this equation corresponds to the previously obtained result in [4], indicating that this inequality is saturated. In Fig.4.3, we plot this right-hand side as a blue line. In Appendix 4.B, we derive another bound functions without taking hydrodynamic limit and compare numerically them with (4.2.17).

4.3 Numerical Study

In this section, we numerically compute the left-hand side of the bound, *i.e.*, $\lim_{t \rightarrow \infty} \phi(h, t)/t$, by using the population dynamics algorithm, and compare it with the bounds we have

obtained in the previous section. In the population dynamics algorithm, the systematic errors of the algorithm exist due to the finite-size effect of the number of copies N_c . To mitigate these errors, we perform a finite-size scaling following this article [3], where the systematic errors are shown to be proportional with $1/N_c$. Using this scaling, we extrapolate the result in $N_c \rightarrow \infty$ from the finite N_c simulations.

In Fig.4.2(b), we plot the results of the population dynamics as a function of N_c for $h = 0.9$, and fit a function $A/N_c + B$ to these results. The obtained coefficient B is our estimator of $\lim_{t \rightarrow \infty} \phi(0.9, t)/t$ in the large N_c limit. In Fig.4.2(a), the results obtained in this way and the results with several finite N_c are plotted as a function of h . First of all, we observe that the population dynamics algorithm can perfectly capture the affine part. Next, the optimized bound (4.2.4) are almost saturated for $h > 0$ as it is close to the results of the population dynamics with $N_c \rightarrow \infty$. Note that this optimized bound cannot capture the affine part.

Finally, we study the formula (4.2.17) obtained in the hydrodynamic limit using the population dynamics method. In Fig.4.3, we plot the estimator of $\lim_{t \rightarrow \infty} \phi(\epsilon h, t)/(\epsilon^2 t)$ as a function of h for several values of the number of copies N_c . In the same figure, we also plot the right-hand side of (4.2.17) as a blue line. Even though ϵ is set to a relatively large value ($\epsilon = 1$), we can see that the results of the population dynamics method converge to the blue line as N_c increases, demonstrating that the inequality (4.2.17) is indeed saturated. Our two control systems (4.2.1) and (4.2.8) fully capture the CGF containing the affine part in the hydrodynamic limit.

4.A Optimal Control System in a Stochastic Differential Equation

In this Appendix, we show an example of an optimal control system in a stochastic differential equation. Let us consider

$$dx_t = v(x_t)dt + \sqrt{2}dW_t, \quad (4.A.1)$$

where x_t is a d -dimensional vector, W_t is a d -dimensional standard Brownian motion and $v(x)$ is a vector field representing deterministic law of evolution. We are interested in a quantity $a = a(x)$, and its time cumulative value

$$A = \int_0^t dt a(x_t) \quad (4.A.2)$$

and its CGF $\phi(h, t)$. Using the operator method, the SCGF, defined as $\lim_{t \rightarrow \infty} \phi(h, t)/t$, is obtained as the largest eigenvalue of the following eigenproblem

$$\mathbb{W}_h \mathbb{P} = \psi(h) \mathbb{P}, \quad (4.A.3)$$

where $\psi(h)$ and \mathbb{P} are the eigenvalue and the eigenvector, and the operator \mathbb{W}_h is defined as

$$\mathbb{W}_h \mathbb{P} = \nabla^2 \mathbb{P} - \nabla \cdot (v \mathbb{P}) - h a \mathbb{P}. \quad (4.A.4)$$

By replacing v with $(v - \nabla \mathcal{V})$ for (4.A.1) where \mathcal{V} is a control-potential, we obtain

$$dx_t = [v(x_t) - \nabla \mathcal{V}(x_t)]dt + \sqrt{2}dW_t. \quad (4.A.5)$$

Recalling the inequality for CGF (4.1.17), a bound function for $\lim_{t \rightarrow \infty} \phi(h, t)/t$ is given by

$$\lim_{t \rightarrow \infty} \frac{1}{t} \phi(h, t) \geq \lim_{t \rightarrow \infty} \left[-\frac{h}{t} \mathbb{E}_{\text{con}}[A] - \frac{1}{t} D(\mathbb{P}^{\text{con}} \|\mathbb{P}) \right]. \quad (4.A.6)$$

Finding an optimal control potential that maximises the right-hand side of this bound is equivalent to solving the eigenproblem (4.A.3), because the optimal control potential can be expressed as $\mathcal{V} = -2 \log \mathcal{F}$ where \mathcal{F} is the eigenvector associated with the largest eigenvalue of the Hermitian conjugate of \mathbb{W}_h . The derivation of this claim can be found, for example, in Appendix A of [73].

4.B Analytical Expressions for the Lower Bound of $\phi(h, t)$

In this appendix, we derive two analytical expressions of the lower bound of $\phi(h, t)$ by using two different control temperatures in the right-hand side of (4.2.4).

First, we substitute the optimal temperatures $\beta^{*, \text{con}}(T, \tau)$ given as (4.2.15) (obtained in the hydrodynamic limit) into (4.2.4). We obtain

$$\lim_{t \rightarrow \infty} \frac{\phi(h, t)}{t} \geq \Sigma_1(h, \tau), \quad (4.B.1)$$

where $\Sigma_1(h, \tau)$ is defined as

$$\begin{aligned} \Sigma_1(h, \tau) &= - \left(\sqrt{\frac{\pi}{2(T + \frac{\tau}{2} + hT^2)}} + \sqrt{\frac{\pi}{2(T - \frac{\tau}{2} - hT^2)}} \right)^{-1} \\ &\times \left(-2h[hT^2 + \tau] + \frac{hT^2}{T + \frac{\tau}{2}} - \frac{hT^2}{T - \frac{\tau}{2}} + \log \frac{(T + \frac{\tau}{2})(T - \frac{\tau}{2})}{(T + \frac{\tau}{2} + hT^2)(T - \frac{\tau}{2} - hT^2)} \right). \end{aligned} \quad (4.B.2)$$

Note that this bound is not optimal as the hydrodynamic limit is not taken.

Next, we consider the following temperatures

$$\begin{aligned} \frac{1}{\beta_1^{**, \text{con}}} &= \frac{1}{\beta_1} + \frac{h}{\beta_1 \beta_{-1}} \\ \frac{1}{\beta_{-1}^{**, \text{con}}} &= \frac{1}{\beta_{-1}} - \frac{h}{\beta_1 \beta_{-1}}, \end{aligned} \quad (4.B.3)$$

that keep even symmetry. Substituting these temperatures into (4.2.4), we obtain

$$\lim_{t \rightarrow \infty} \frac{\phi(h, t)}{t} \geq \Sigma_2(h, \tau), \quad (4.B.4)$$

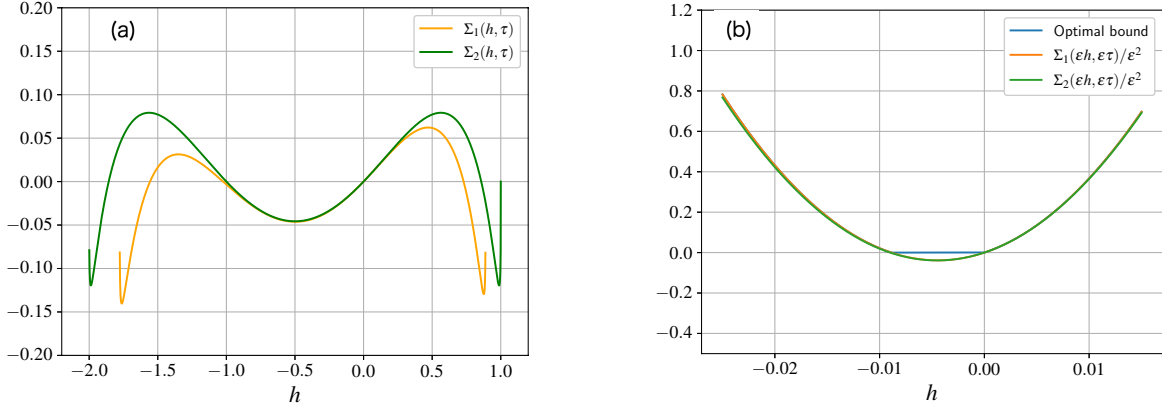


Fig. 4.4: **(a)** $\Sigma_1(h, \tau)$ in (4.B.1) and $\Sigma_2(h, \tau)$ in (4.B.5) with $T = 0.75$ and $\tau = 0.5$. **(b)** $\Sigma_1(\epsilon h, \epsilon \tau)/\epsilon^2$, $\Sigma_2(\epsilon h, \epsilon \tau)/\epsilon^2$ and the optimal bound (4.2.17) under the hydrodynamic limit. We set $\epsilon = 0.01$, $T = 0.75$ and $\tau = 0.5$.

where $\Sigma_2(h, \tau)$ is defined as

$$\begin{aligned} \Sigma_2(h, \tau) = & - \left(\sqrt{\frac{\pi}{2(T + \frac{\tau}{2} + \frac{h}{(T + \frac{\tau}{2})(T - \frac{\tau}{2})})}} + \sqrt{\frac{\pi}{2(T - \frac{\tau}{2} - \frac{h}{(T + \frac{\tau}{2})(T - \frac{\tau}{2})})}} \right)^{-1} \\ & \times \left(-2h \left[\frac{h}{(T + \frac{\tau}{2})(T - \frac{\tau}{2})} + \tau \right] + \frac{\frac{h}{(T + \frac{\tau}{2})(T - \frac{\tau}{2})}}{T + \frac{\tau}{2}} - \frac{\frac{h}{(T + \frac{\tau}{2})(T - \frac{\tau}{2})}}{T - \frac{\tau}{2}} \right. \\ & \left. + \log \frac{(T + \frac{\tau}{2})(T - \frac{\tau}{2})}{\left(T + \frac{\tau}{2} + \frac{h}{(T + \frac{\tau}{2})(T - \frac{\tau}{2})}\right) \left(T - \frac{\tau}{2} - \frac{h}{(T + \frac{\tau}{2})(T - \frac{\tau}{2})}\right)} \right). \end{aligned} \quad (4.B.5)$$

We plot these two functions $\Sigma_1(h, \tau)$ and $\Sigma_2(h, \tau)$ as a function of h in Fig.4.4(a). We also compare these two functions under the the hydrodynamic limit: We plot in Fig.4.4(b) $\Sigma_1(\epsilon h, \epsilon \tau)/\epsilon^2$ and $\Sigma_2(\epsilon h, \epsilon \tau)/\epsilon^2$ as a function of h together with the right-hand side of (4.2.17) (which is the optimal bound in the hydrodynamic limit). We observe that these two bounds are almost optimal in this regime except the affine part.

Chapter 5

Analysis of Anomalous Fluctuations of Renewal-Reward Processes with Heavy-tailed Distributions

In this chapter, we discuss anomalous fluctuations with memory effects in a renewal-reward process instead of focusing on the probability of rare events. A renewal-reward process, a generalisation of continuous time Markov processes, is one of the simplest stochastic processes that can describe random sequences with memory effects [5, 76, 77]. In contrast to its the Markov counterpart, in renewal-reward processes, the waiting time to move from one state to the next one can be distributed by a non-exponential function. The process can thus describe a broad spectrum of phenomena in physics [78] and other fields, including a melt up of the stock market [9, 10] and a super spreader in epidemics [11, 12], where memory effects are known to be important.

When the waiting time distribution has a power law, the dynamics show a slow convergence to its stationary states due to its heavy tail. For example, the probability that the state of the system always stays in the initial state during the dynamics remains non-negligible in the large time limit [79]. This anomalous behaviour can be characterised using a LDP [18, 80]. LDP states that the logarithmic probability of a time-averaged quantity is proportional with the averaging time (with a negative proportional constant), except for the trivial probability where the time averaged quantity takes its expectation. In renewal reward processes with power-law waiting time distributions, this proportional constant, known as a rate function or LDF, can take the value 0 not only for the expectation but also for a certain range of the values [1, 4, 79]. This indicates that these events are *more* likely to occur than in standard systems. We call this range of LDF taking the value 0 *the affine part*.

The affine part tells us that these rare events occur more likely than usual, but does not tell us how likely they do. To solve this problem, finite-time analyses of the LDP are necessary. One such attempt could be a so-called strong LDP, where the next order corrections of the logarithmic probability from the LDP are computed [15]. However, at present, it is not clear how this general theory can be extended to the case with the affine part. In [16], Tsirelson studied a renewal-reward process with general waiting time distributions and derived the next order correction to the LDP. But he used a condition in which an affine part can not be present. In chapter 3, we have studied finite-time corrections of the MGF under the

condition that the affine part appears (Theorem 2.1) but we do not succeed to translate it to the correction term of the LDP.

The variance can tell us directly how much the averaged quantities fluctuate. If one considers an exponential function for the waiting time distribution, the variance of the time-averaged quantity decreases proportionally to the inverse of the averaging time because this corresponds to the case of a process having a short memory. This indicates that the averaged value mostly falls in the range around the expectation with an error that is proportional with the inverse square root of the averaging time. In the presence of the affine part when heavy-tailed distributions are used for the waiting times, we identify, in this chapter, a condition under which this scaling of the variance changes. This is consistent with the fact that heavy-tailed distributions introduce memory effects. Interestingly, not every power-law decaying distribution will result in this scaling modification of the variance: We show that for distributions whose density decay faster than $1/t^3$, the variance keeps its normal scaling. In that case, we expect that the scaling of higher order cumulants are affected, as discussed at the end of this chapter.

5.1 Background

5.1.1 Model

A renewal-reward process is a model to describe events that occur sequentially. For a given event, the next event occurs after a random waiting time (also called a renewal time or arrival time). The waiting times are independent-and-identically distributed random positive variables $(\tau_k)_{k \in \mathbb{N}}$ with a probability density p . For this density, we consider the inverse Rayleigh distribution

$$p_\beta(\tau) = \frac{\beta}{\tau^3} \exp\left(-\frac{\beta}{2\tau^2}\right) \mathbb{1}(\tau > 0), \quad (5.1.1)$$

and the Pareto distribution

$$p_\alpha(\tau) = \frac{\alpha - 1}{(1 + \tau)^\alpha} \mathbb{1}(\tau > 0) \quad (5.1.2)$$

with $\alpha = 3$, both of which do not have a finite second moment, *i.e.*, $\mathbb{E}[\tau^2] = \infty$. The main quantity of interest in this section is the number of events that have occurred up to time $t > 0$. This is the counting process N_t

$$N_t = \sup\{k : S_k \leq t\}, \quad (5.1.3)$$

where $S_k = \tau_1 + \dots + \tau_k$. We denote its q -th order moment by $m_q(t)$:

$$m_q(t) := \mathbb{E}[N_t^q]. \quad (5.1.4)$$

Note that with respect to [81], we consider the case where the expectation of the waiting time is finite and the renewal theorem implies that the counting process N_t behaves as $N_t \sim t/\mathbb{E}[\tau]$ for $t \rightarrow \infty$. We study the fluctuations around that behaviour.

5.1.2 Renewal Equations for q th-moments

To analyse the asymptotics of $m_q(t)$, we rely on renewal equations: a powerful tool to analyse renewal-reward processes. Recalling a renewal equation for a renewal function $m_1(t)$, we have

$$m_1(t) = F(t) + \int_0^t ds m_1(t-s)p(s), \quad (5.1.5)$$

where F is the cumulative waiting time distribution function. From this equation, a simple expression for the Laplace transform of $m_1(t)$ is derived. The Laplace transform of a function f is

$$\tilde{f}(s) := \int_0^\infty e^{-st} f(t) dt, \quad (5.1.6)$$

we then derive, from the equation (5.1.5),

$$\tilde{m}_1(s) = \frac{\tilde{F}(s)}{1 - s\tilde{F}(s)}, \quad (5.1.7)$$

where we have used $\tilde{p}(s) = s\tilde{F}(s)$. We have derived this formulation in Section 2.1.3.

Similarly, one can also derive a renewal equation for $m_2(t)$,

$$\begin{aligned} m_2(t) &= \int_0^t \mathbb{E}[N_{t-s}^2] p(s) ds \\ &\quad + 2 \int_0^t m_1(t-s)p(s) ds + F(t), \end{aligned} \quad (5.1.8)$$

from which the Laplace transform of $m_2(t)$ is obtained as

$$\tilde{m}_2(s) = \tilde{m}_1(s)(1 + 2s\tilde{m}_1(s)). \quad (5.1.9)$$

Moreover, a renewal equation for the moment-generating function can be derived. (See Appendix 5.A). From the equation, we derive the Laplace transform of $m_q(t)$ as

$$\tilde{m}_q(s) = \sum_{k=1}^q \left[\sum_{i=1}^k \binom{k}{i} i^q (-1)^{k-i} \right] s^{k-1} [\tilde{m}_1(s)]^k. \quad (5.1.10)$$

5.2 Convergence Law of a Counting Process

5.2.1 Convergence of the First Moment

When a waiting-time density p has a finite mean $\mathbb{E}[\tau] = \mu$ and a finite variance σ^2 , Feller has proven (Chapter 11, section3, theorem 1) [77] that

$$\frac{m_1(t)}{t} - \frac{1}{\mu} \sim \frac{\sigma^2 - \mu^2}{2\mu^2 t}. \quad (5.2.1)$$

This result can be easily derived by using the following expansion:

$$s\tilde{F}(s) = 1 - \mu s + (\sigma^2 + \mu^2)\frac{s^2}{2} + o(s^2). \quad (5.2.2)$$

Indeed, by inserting it into (5.1.7), we get

$$\tilde{m}_1(s) = \frac{1}{\mu s^2} + \frac{\sigma^2 - \mu^2}{2\mu^2 s} + o\left(\frac{1}{s}\right), \quad (5.2.3)$$

which leads to

$$m_1(t) = \frac{1}{\mu}t + \frac{\sigma^2 - \mu^2}{2\mu^2} + o(1). \quad (5.2.4)$$

A rigorous justification to derive (5.2.4) from (5.2.3) is based on the Tauberian theorem [77]. See Appendix 5.B for more details. From this argument, we can see that the condition $\mathbb{E}[\tau^2] = \infty$ is necessary for $m_1(t)$ to have an anomalous scaling. For this reason, we study in this section the two waiting-time distributions behaving at infinity like $1/t^3$.

Let us first consider the case of the inverse Rayleigh distribution. Let

$$\phi(s) = \int_0^\infty e^{-st} e^{-\frac{1}{2t^2}} dt. \quad (5.2.5)$$

We then have for its cumulative distribution function,

$$\tilde{F}_\beta(s) = \beta^{\frac{1}{2}}\phi(\beta^{\frac{1}{2}}s), \quad (5.2.6)$$

and

$$\tilde{m}_1(s) = \frac{\beta^{\frac{1}{2}}\phi(\beta^{\frac{1}{2}}s)}{1 - s\beta^{\frac{1}{2}}\phi(\beta^{\frac{1}{2}}s)}, \quad (5.2.7)$$

from (5.1.7). We then expand $\phi(s)$ in s :

$$\phi(s) = \frac{1}{s} - \sqrt{\frac{\pi}{2}} - \frac{1}{2}s \ln(s) + O(s), \quad (5.2.8)$$

leading to

$$\tilde{m}_1(s) = \sqrt{\frac{2}{\beta\pi}} \frac{1}{s^2} - \frac{1}{\pi s} \ln(s) + o\left(\frac{\ln(s)}{s}\right). \quad (5.2.9)$$

By using the Tauberian theorem (Appendix 5.B), we obtain

$$\frac{m_1(t)}{t} - \sqrt{\frac{2}{\beta\pi}} = \frac{\ln(t)}{t\pi} + o\left(\frac{\ln(t)}{t}\right), \quad (5.2.10)$$

for large t . This is to be compared to (5.2.1): we see that the convergence is slower in our case.

We can repeat the same analysis in the case of the Pareto distribution. The cumulative distribution is derived as

$$F_3(t) := \mathbb{P}[\tau \leq t] = \begin{cases} 0 & t \leq 0 \\ 1 - \frac{1}{(1+t)^2} & t > 0. \end{cases} \quad (5.2.11)$$

when $m = 3$. We insert the Laplace transform of F_3 in (5.1.7) and again look at the expansion around s of \tilde{m} and get

$$\tilde{m}_1(s) = \frac{1}{s^2} - \frac{\ln(s)}{s} + o\left(\frac{\ln(s)}{s}\right). \quad (5.2.12)$$

We thus obtain the following behaviour for $m(t)$ for large t :

$$\frac{m_1(t)}{t} - 1 = \frac{\ln(t)}{t} + o\left(\frac{\ln(t)}{t}\right). \quad (5.2.13)$$

5.2.2 Convergence of the Variance

We then study the large time behaviour of the variance

$$c_2(t) = \frac{m_2(t) - m_1(t)^2}{t^2}. \quad (5.2.14)$$

In the case that a waiting time density p has a finite mean $\mathbb{E}[\tau] = \mu$ and a finite variance σ^2 , we obtain from (5.1.9) and (5.2.3)

$$\tilde{m}_2(s) = \frac{2}{\mu^2 s^3} + \frac{1}{s^2} \frac{1}{\mu} \left(\frac{2\sigma^2 - \mu^2}{\mu^2} \right) + o\left(\frac{1}{s^2}\right), \quad (5.2.15)$$

which yields

$$m_2(t) = \frac{1}{\mu^2} t^2 + \frac{1}{\mu} \left(\frac{2\sigma^2 - \mu^2}{\mu^2} \right) t + o(t) \quad (5.2.16)$$

with the aid of the Tauberian theorem (5.B.1). $c_2(t)$ is finally obtained as

$$c_2(t) = \frac{\sigma^2}{\mu^3 t} + o\left(\frac{1}{t}\right). \quad (5.2.17)$$

Let us now consider the case of the inverse Rayleigh distribution. Inserting the expression (5.2.9) for $\tilde{m}_1(s)$ in (5.1.9), we obtain,

$$\tilde{m}_2(s) = \frac{4}{\beta\pi} \frac{1}{s^3} - \frac{4\sqrt{2}}{\sqrt{\beta\pi^{3/2}}} \frac{\ln s}{s^2} + o\left(\frac{\ln(s)}{s^2}\right), \quad (5.2.18)$$

and then

$$m_2(t) = \frac{2}{\beta\pi} t^2 + \frac{4\sqrt{2}}{\sqrt{\beta\pi^{3/2}}} t \ln(t) + o(t \ln(t)). \quad (5.2.19)$$

Therefore

$$c_2(t) = \frac{2\sqrt{2}}{\sqrt{\beta\pi^{3/2}}} \frac{\ln(t)}{t} + o\left(\frac{\ln(t)}{t}\right). \quad (5.2.20)$$

Proceeding in the same way for the Pareto distribution, we obtain in that case

$$c_2(t) = 2 \frac{\ln t}{t} + o\left(\frac{\ln(t)}{t}\right). \quad (5.2.21)$$

5.2.3 Numerical Study

We perform numerical simulations of the counting process N_t to illustrate the accuracy of (5.2.10), (5.2.13), (5.2.20) and (5.2.21). First, $m_1(t) - t\sqrt{2/(\beta\pi)}$ (resp. $m_1(t) - t$) computed from the numerical simulations is plotted as an orange line in Fig.5.1(a) (resp. Fig.5.1(b)) for the inverse Rayleigh (resp. Pareto) waiting time distribution. According to (5.2.10) and (5.2.13), these lines are equivalent to $\ln(t)/\pi + o(\ln(t))$ and $\ln(t) + o(\ln(t))$. Assuming that these $o(\ln(t))$ terms are constant over time when t is large, we next plot $\ln(t)/\pi + \text{const.}$ (Fig.5.1(a)) and $\ln(t) + \text{const.}$ (Fig.5.1(b)) in the same figures.

We then plot $(m_2(t) - m_1(t)^2)/t$ computed from the same numerical simulations in Fig.5.1 (c,d) for the inverse Rayleigh (Fig.5.1(c)) and the Pareto (Fig.5.1(d)) waiting time distributions. Reference lines $\frac{2\sqrt{2}}{\sqrt{\beta\pi^{3/2}}}\ln(t) + \text{const.}$ (Fig.5.1(c)) and $2\ln(t) + \text{const.}$ (Fig.5.1(d)) are also plotted in the same figures. In these four figures, we observe good agreements between the slopes of the reference lines and the results of numerical simulations in semi-log scale. This demonstrates the validity of (5.2.10), (5.2.13), (5.2.20) and (5.2.21).

5.3 A Particle Confined between Two Hot Walls

Our aim in this section is to show that the slow convergence of the renewal function of processes having density $\sim 1/t^3$ as $t \rightarrow \infty$ also holds for physical observables in a Knudsen gas [75]. For this, let us consider the model of a single particle bouncing back between two thermal walls.

5.3.1 Knudsen Gas Model

We consider a particle in a one-dimensional box that has two different temperatures at both ends. The confined tracer moves freely in the box of size 1 and is reflected at the end of the box with a random speed v distributed according to the following Rayleigh distribution:

$$q_{\beta_{\pm}}(v) = \beta_{\pm} v e^{-\beta_{\pm} \frac{v^2}{2}} \mathbb{1}(v > 0), \quad (5.3.1)$$

where $\beta_+ = 1/T_+$ (resp. $\beta_- = 1/T_-$) is the inverse temperature of the right (resp. left) wall. This model has been introduced in Chapter 4 but we re-define this model for generalization of length of the model.

Let $x_0 \in [0, 1]$ and v_0 the initial position and velocity of the particle and $\sigma_0 = v_0/|v_0|$. We denote the initial condition by θ , *i.e.*, $\theta = (x_0, v_0)$. The first time that the particle hits a wall is given by $S_{\theta,0} = (\frac{1}{2}(\sigma_0 + 1) - x_0)/v_0$, and the subsequent hitting times are given by

$$S_{\theta,k} = S_{\theta,0} + 1/v_1 + \dots + 1/v_k, \quad k \geq 1, \quad (5.3.2)$$

where v_k is a random variable distributed according to a law $q_{\beta_{\sigma_k}}$ and $\sigma_k = (-1)^k \sigma_0$. This may be rewritten as

$$S_{\theta,k} = S_{\theta,0} + \tau_1 + \dots + \tau_k, \quad k \geq 1 \quad (5.3.3)$$

with the sequence of independent waiting times $(\tau_k)_{k \in \mathbb{N}}$ distributed with the inverse Rayleigh distribution $p_{\beta_k}(\tau)$ defined as (5.1.1). The energy exchanged between the two walls during

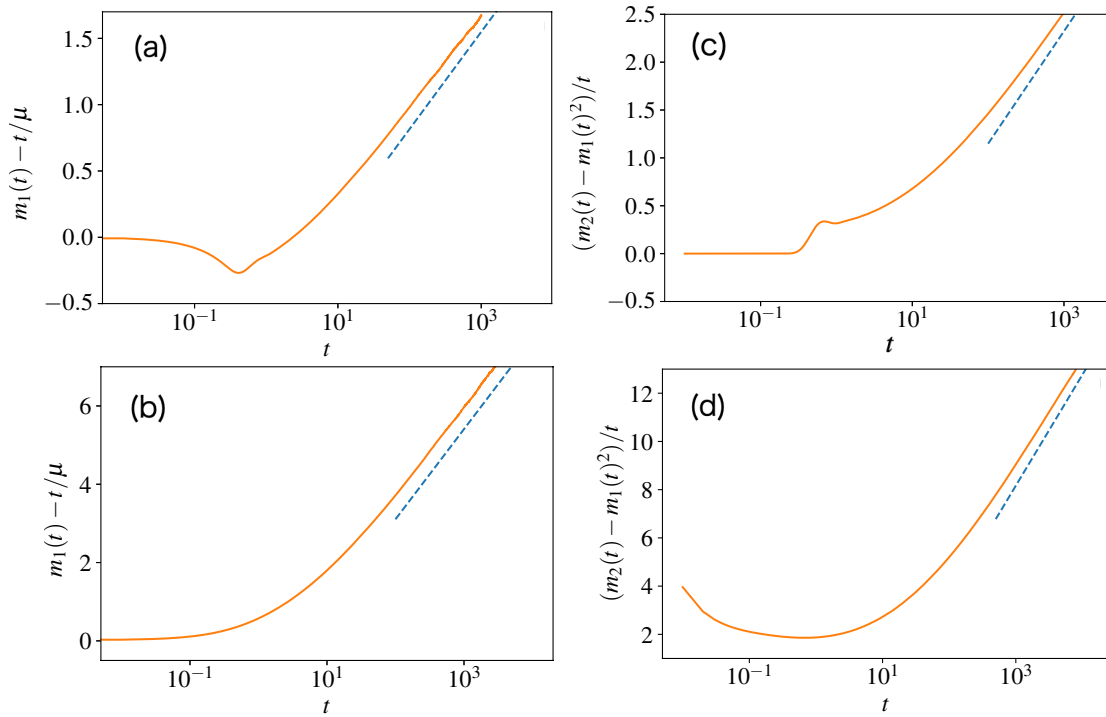


Fig. 5.1: **(a,b)** $m_1(t) - t/\mu$ obtained from numerical simulations of the counting process N_t (with 10^8 samples) are plotted as a function of time in log-scale as orange lines. For the inverse Rayleigh waiting time distribution (a), $\beta = 1$ and $\mu = 1/\sqrt{2/(\beta\pi)}$, while for the Pareto waiting time distribution (b), $m = 3$ and $\mu = 1$. $\ln(t)/\pi + \text{const.}$ and $\ln(t) + \text{const.}$ are also plotted as blue dashed lines for (a) and (b). **(c,d)** $(m_2(t) - m_1(t)^2)/t$ obtained from the same numerical simulations are plotted as a function of time as orange lines for the inverse Rayleigh waiting time distribution (c) and for the Pareto waiting time distribution (d). $\frac{2\sqrt{2}}{\sqrt{\beta\pi^{3/2}}}\ln(t) + \text{const.}$ for (c) and $2\ln(t) + \text{const.}$ for (d) are also plotted as blue dashed lines in the same figures. The agreements between the slopes of orange lines and those of blue lines in these semi-log graphs demonstrate the validity of (5.2.10), (5.2.13), (5.2.20) and (5.2.21), as detailed in the main text.

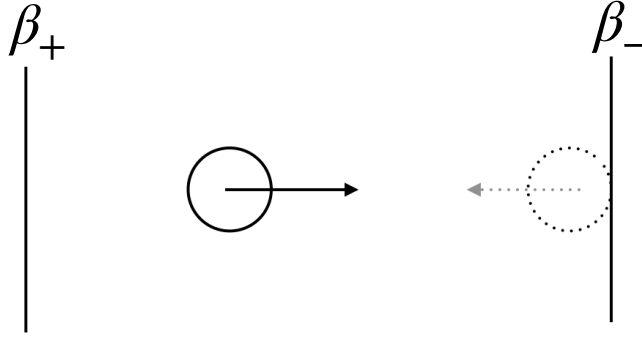


Fig. 5.2: Schematic figure to explain the setup of the 1 particle model. When the particle moves to the right (resp. left) wall, $\sigma_k = 1$ (resp. -1)

a time interval $[0, t]$ is defined as

$$J_\theta(t) := \frac{1}{2} \sum_{k=1}^{N_t} v_k^2 \sigma_k, \quad (5.3.4)$$

if $t \geq S_0^\theta$ and $J_\theta(t) = 0$ otherwise, where N_t is the counting process (5.1.3). We denote by $m_{\theta,q}(t)$ the q -th moment of $J_\theta(t)$:

$$m_{\theta,q}(t) = \mathbb{E}[J_\theta^q(t)]. \quad (5.3.5)$$

A generalisation to the system with an arbitrary box size L is straightforward. Indeed, denoting by $S_{\theta,k}^L$ the corresponding hitting times with the boundaries, it is easy to see that $S_{\theta,k}^L = L S_{\theta,k}^1$. This indicates that $N_t^L = N_{t/L}^1$ where N_t^L denotes the counting process corresponding to the hitting times $S_{\theta,k}^L$. For the energy current in a box of size L , we also have that

$$J_\theta^L(t) = J_\theta^1\left(\frac{t}{L}\right). \quad (5.3.6)$$

In the following we perform all computations with the case $L = 1$ and then obtain the result for an arbitrary $L > 0$ by using this scaling relation.

5.3.2 Convergence of the Current: First Moment

For simplicity, we consider only the following two types of initial conditions:

$$\theta_+ = (0, v_0) \quad (5.3.7)$$

with $v_0 < 0$ and

$$\theta_- = (1, v_0) \quad (5.3.8)$$

with $v_0 > 0$, *i.e.*, the cases of a particle just before hitting the left wall (temperature β_+) and of a particle just before hitting the right wall (inverse temperature β_-). As the particle

immediately hits each wall when the process starts, the value of the initial velocity v_0 is unimportant. We thus denote by $+$ the initial condition θ_+ and by $-$ the initial condition θ_- .

Dynamics with these two initial conditions are related via the renewal property:

$$\mathbb{E}[J_{\pm}(t) \mid \tau_1 = u] = \frac{\pm 1}{2u^2} + \mathbb{E}[J_{\mp}(t - u)], \quad (5.3.9)$$

if $0 \leq u \leq t$ and $\mathbb{E}[J_{\pm}(t) \mid \tau_1 = u] = 0$ if $u > t$. This means that the process conditioned by the first-waiting time (the left-hand side) is equal to the other process with some increments (the right-hand side). By integrating (5.3.9) with respect to the inverse Rayleigh waiting time density (5.1.1), we obtain the following coupled renewal-reward equations for the currents

$$m_{-,1}(t) = - \left(\frac{1}{2t^2} + \frac{1}{\beta_-} \right) e^{-\frac{\beta_-}{2t^2}} + \int_0^t du m_{+,1}(t - u) p_{\beta_-}(u), \quad (5.3.10)$$

$$m_{+,1}(t) = + \left(\frac{1}{2t^2} + \frac{1}{\beta_+} \right) e^{-\frac{\beta_+}{2t^2}} + \int_0^t du m_{-,1}(t - u) p_{\beta_+}(u). \quad (5.3.11)$$

In order to derive the speed of convergence of the current, we perform a Laplace transform of (5.3.10) and (5.3.11):

$$\tilde{m}_{-,1}(s) = -\tilde{H}_-(s) - \frac{1}{\beta_-} \tilde{F}_{\beta_-}(s) + s \tilde{m}_{+,1}(s) \tilde{F}_{\beta_-}(s), \quad (5.3.12)$$

$$\tilde{m}_{+,1}(s) = \tilde{H}_+(s) + \frac{1}{\beta_+} \tilde{F}_{\beta_+}(s) + s \tilde{m}_{-,1}(s) \tilde{F}_{\beta_+}(s), \quad (5.3.13)$$

where $\tilde{H}_{\pm}(s)$ is the Laplace transform of $H_{\pm}(t) = \frac{1}{2t^2} e^{-\frac{\beta_{\pm}}{2t^2}}$ and $\tilde{F}_{\beta_{\pm}}(s)$ is the Laplace transform of the cumulative inverse Rayleigh distribution. By substituting (5.3.12) into (5.3.13), we then obtain an equation for $\tilde{m}_{+,1}(s)$ as

$$\begin{aligned} \tilde{m}_{+,1}(s) &= \frac{\tilde{H}_+(s) + \frac{1}{\beta_+} \tilde{F}_{\beta_+}(s)}{1 - s^2 \tilde{F}_{\beta_+}(s) \tilde{F}_{\beta_-}(s)} \\ &\quad - s \tilde{F}_{\beta_+}(s) \frac{\tilde{H}_-(s) + \frac{1}{\beta_-} \tilde{F}_{\beta_-}(s)}{1 - s^2 \tilde{F}_{\beta_+}(s) \tilde{F}_{\beta_-}(s)}, \end{aligned} \quad (5.3.14)$$

which leads to

$$\tilde{m}_{\pm,1}(s) = \kappa \left(\frac{1}{\beta_+} - \frac{1}{\beta_-} \right) \frac{1}{s^2} - \kappa^2 \frac{(\beta_+ + \beta_-)}{2} \left(\frac{1}{\beta_+} - \frac{1}{\beta_-} \right) \frac{\ln(s)}{s} + o\left(\frac{\ln(s)}{s}\right), \quad (5.3.15)$$

where κ is the conductivity given by

$$\kappa^{-1} = \left(\frac{\pi \beta_-}{2} \right)^{\frac{1}{2}} + \left(\frac{\pi \beta_+}{2} \right)^{\frac{1}{2}}. \quad (5.3.16)$$

Using again the Tauberian theorem for Laplace transform (Appendix 5.B), we finally get,

$$\frac{m_{\pm,1}(t)}{t} = \kappa \left(\frac{1}{\beta_+} - \frac{1}{\beta_-} \right) + \kappa^2 \frac{(\beta_+ + \beta_-)}{2} \left(\frac{1}{\beta_+} - \frac{1}{\beta_-} \right) \frac{\ln t}{t} + o\left(\frac{\ln(t)}{t}\right). \quad (5.3.17)$$

Note that the asymptotic form of the average current $m_{+,1}(t)$ and $m_{-,1}(t)$ have opposite signs, but this is because the definition of the current includes $(-1)^{\pm 1}$ term: these two expressions are physical equivalent. For the average current in a box of size L , we get

$$\begin{aligned} \frac{m_{\pm,1}^L(t)}{t} &= \frac{1}{L} \frac{m_{\pm,1}^1(\frac{t}{L})}{\frac{t}{L}} \\ &= \frac{\kappa}{L} \left(\frac{1}{\beta_+} - \frac{1}{\beta_-} \right) + \kappa^2 \frac{(\beta_+ + \beta_-)}{2} \left(\frac{1}{\beta_+} - \frac{1}{\beta_-} \right) \frac{\ln(t)}{t} + o\left(\frac{\ln(t)}{t}\right). \end{aligned} \quad (5.3.18)$$

5.3.3 Variance of the Current of Energy between Heat Baths

We next discuss the large time asymptotics of the variance of the current. The renewal property for the second moment of the current is expressed by

$$\mathbb{E}[J_{\pm}^2(t) \mid \tau_1 = u] = \left[\frac{1}{2u^2} \right]^2 + \frac{\sigma}{u^2} \mathbb{E}[J_{\mp}(t-u)] + \mathbb{E}[J_{\mp}^2(t-u)] \quad (5.3.19)$$

if $0 \leq u \leq t$ and $\mathbb{E}[J_{\pm}(t) \mid \tau_1 = u] = 0$ if $u > t$. Let us introduce for $t > 0$,

$$\begin{aligned} L_{\pm}(t) &= \left(\frac{1}{4t^4} + \frac{1}{\beta_{\pm}t^2} + \frac{2}{\beta_{\pm}^2} \right) e^{-\frac{\beta_{\pm}}{2t^2}}, \\ g_{\pm}(t) &= \frac{\beta_{\pm}}{t^5} e^{-\frac{\beta_{\pm}}{2t^2}}. \end{aligned}$$

Then, integrating (5.3.19) with respect to the inverse Rayleigh waiting time density (5.1.1) and using the relation

$$\int_0^t du \frac{1}{4u^4} p_{\beta_{\pm}}(u) = \left(\frac{1}{4t^4} + \frac{1}{\beta_{\pm}t^2} + \frac{2}{\beta_{\pm}^2} \right) e^{-\frac{\beta_{\pm}}{2t^2}} \quad (5.3.20)$$

for $t > 0$, the renewal equations for the second moment of the current are derived as

$$\begin{aligned} m_{+,2}(t) &= L_+(t) + \int_0^t du m_{-,1}(t-u)g_+(u) \\ &\quad + \int_0^t du m_{-,2}(t-u)p_{\beta_+}(u), \end{aligned} \quad (5.3.21)$$

$$\begin{aligned} m_{-,2}(t) &= L_-(t) - \int_0^t du m_{+,1}(t-u)g_-(u) \\ &\quad + \int_0^t du m_{+,2}(t-u)p_{\beta_-}(u), \end{aligned} \quad (5.3.22)$$

In order to derive the large time asymptotic of the second moment of the current, we perform Laplace transform of (5.3.21) and (5.3.22),

$$\tilde{m}_{+,2}(s) = \tilde{L}_+(s) + \tilde{m}_{-,1}(s)\tilde{g}_+(s) + s\tilde{m}_{-,2}(s)\tilde{F}_{\beta_+}(s), \quad (5.3.23)$$

$$\tilde{m}_{-,2}(s) = \tilde{L}_-(s) - \tilde{m}_{+,1}(s)\tilde{g}_-(s) + s\tilde{m}_{+,2}(s)\tilde{F}_{\beta_-}(s). \quad (5.3.24)$$

We solve these linear equations for $\tilde{m}_{-,2}(s)$ and $\tilde{m}_{+,2}(s)$ by using $\tilde{m}_{\pm,1}(s)$ obtained in section 5.3.2 and the following expansions of $\tilde{L}_{\pm}(s)$ and $\tilde{g}_{\pm}(s)$

$$\tilde{L}_{\pm}(s) = \frac{2}{\beta_{\pm}^2 s} - \frac{3}{4\beta_{\pm}^{3/2}}\sqrt{\frac{\pi}{2}} + \frac{s}{4\beta_{\pm}} + O(s^2), \quad (5.3.25)$$

$$\tilde{g}_{\pm}(s) = \frac{2}{\beta_{\pm}} - \frac{1}{\sqrt{\beta_{\pm}}}\sqrt{\frac{\pi}{2}}s + O(s^2). \quad (5.3.26)$$

Recalling $\tilde{F}_{\beta_{\pm}}(s) = \beta_{\pm}^{\frac{1}{2}}\phi(\beta_{\pm}^{\frac{1}{2}}s)$ with

$$\phi(s) = \frac{1}{s} - \sqrt{\frac{\pi}{2}} - \frac{1}{2}s\ln(s) + O(s), \quad (5.3.27)$$

the Laplace transform of the second moment of the current is derived as

$$\tilde{m}_{\pm,2}(s) = 2\kappa^2 \left(\frac{1}{\beta_+} - \frac{1}{\beta_-} \right)^2 \frac{1}{s^3} - \frac{2\kappa^3 \ln(s)}{s^2} (\beta_+ + \beta_-) \left(\frac{1}{\beta_+} - \frac{1}{\beta_-} \right)^2 + o\left(\frac{\ln(s)}{s^2}\right). \quad (5.3.28)$$

From the Tauberian theorem (Appendix 5.B), we finally arrive at the asymptotic form of the variance

$$\begin{aligned} \text{Var} \left(\frac{J_{\pm}(t)}{t} \right) &= \frac{m_{\pm,2}(t)}{t^2} - \frac{(m_{\pm,1}(t))^2}{t^2} \\ &= \kappa^3 (\beta_+ + \beta_-) \left(\frac{1}{\beta_+} - \frac{1}{\beta_-} \right)^2 \frac{\ln(t)}{t} \\ &\quad + o\left(\frac{\ln(t)}{t}\right). \end{aligned} \quad (5.3.29)$$

This result agree with our previous work [1]. As for the variance of the current in a box of size L , we get:

$$\begin{aligned} \text{Var} \left(\frac{J_{\pm}^L(t)}{t} \right) &= \frac{1}{L^2} \text{Var} \left(\frac{J_{\pm}^1(\frac{t}{L})}{t/L} \right) \\ &= \frac{1}{L} \kappa^3 (\beta_+ + \beta_-) \left(\frac{1}{\beta_+} - \frac{1}{\beta_-} \right)^2 \frac{\ln(t)}{t} \\ &\quad + o\left(\frac{\ln(t)}{t}\right). \end{aligned} \quad (5.3.30)$$

5.3.4 Convergence of the Thermal Energy

A similar formulation can be applied to study the convergence of the time-averaged kinetic energy defined as

$$E_{\pm}(t) = \frac{1}{2} \sum_{k=1}^{N_t} \frac{1}{\tau_k}. \quad (5.3.31)$$

The expected values of the energy are denoted by

$$m_E^{\pm}(t) = \mathbb{E}[E_{\pm}(t)]. \quad (5.3.32)$$

As in the section 5.3.2, we construct two equations in Laplace space

$$\tilde{m}_E^+(s) = \tilde{h}_+(s) + \tilde{g}_+(s) + s\tilde{m}_E^-(s)\tilde{F}_{\beta_+}(s), \quad (5.3.33)$$

$$\tilde{m}_E^-(s) = \tilde{h}_-(s) + \tilde{g}_-(s) + s\tilde{m}_E^+(s)\tilde{F}_{\beta_-}(s), \quad (5.3.34)$$

Here, $h(t)$ and $g(t)$ are given by

$$h_{\pm}(t) = \frac{e^{-\frac{\beta_{\pm}}{2t^2}}}{2t}, \quad (5.3.35)$$

$$g_{\pm}(t) = \frac{1}{2} \sqrt{\frac{\pi}{2\beta_{\pm}}} \operatorname{Erfc} \left[\sqrt{\frac{\beta_{\pm}}{2}} \frac{1}{t} \right]. \quad (5.3.36)$$

Thus, $\tilde{m}_E^+(s)$ is calculated as

$$\begin{aligned} \tilde{m}_E^+(s) &= \frac{\tilde{h}_+(s) + \tilde{g}_+(s)}{1 - s^2 \tilde{F}_{\beta_+}(s) \tilde{F}_{\beta_-}(s)} \\ &\quad + s \tilde{F}_{\beta_+}(s) \frac{\tilde{h}_-(s) + \tilde{g}_-(s)}{1 - s^2 \tilde{F}_{\beta_+}(s) \tilde{F}_{\beta_-}(s)}. \end{aligned} \quad (5.3.37)$$

Proceeding in the same way as for the current, we can expand the functions involved for small s and obtain

$$\tilde{m}_E^+(s) = \sqrt{\frac{\pi}{8}} \kappa \left(\sqrt{\frac{1}{\beta_+}} + \sqrt{\frac{1}{\beta_-}} \right) \frac{1}{s^2} - \frac{1}{4} \sqrt{\frac{\pi}{2}} \kappa^2 (\beta_+ + \beta_-) \left(\sqrt{\frac{1}{\beta_+}} + \sqrt{\frac{1}{\beta_-}} \right) \frac{\ln(s)}{s} + o\left(\frac{\ln(s)}{s}\right). \quad (5.3.38)$$

As with the derivation of (5.3.17), the large time asymptotics of $m_E^{\pm}(t)$ are derived as

$$m_E(t) = \sqrt{\frac{\pi}{8}} \kappa \left(\sqrt{\frac{1}{\beta_+}} + \sqrt{\frac{1}{\beta_-}} \right) t + \frac{1}{4} \sqrt{\frac{\pi}{2}} \kappa^2 (\beta_+ + \beta_-) \left(\sqrt{\frac{1}{\beta_+}} + \sqrt{\frac{1}{\beta_-}} \right) \ln(t) + o(\ln(t)). \quad (5.3.39)$$

5.3.5 Numerical Simulations

We numerically simulate the one-particle model to check the validity of (5.3.17) and (5.3.29). We estimate $m_{+,1}(t)$ and $m_{+,2}(t)$ from the numerical simulations, and plot $m_{+,1}(t) - \kappa(1/\beta_+ - 1/\beta_-)$ and $m_{\pm,2}(t)/t^2 - (m_{\pm,1}(t))^2/t^2$ in Fig. 5.3 (a,b). In the same figures, we also plot $(\kappa^2/2)(\beta_+ + \beta_-)(1/\beta_+ - 1/\beta_-)(\ln t)/t + \text{const.}$ and $\kappa^3(\beta_+ + \beta_-)(1/\beta_+ - 1/\beta_-)^2 + \text{const.}$ as blue dashed lines. We observe that the slopes of the orange lines in semi-log scale asymptotically converge to those of blue dashed lines. This demonstrates (5.3.17) and (5.3.29).

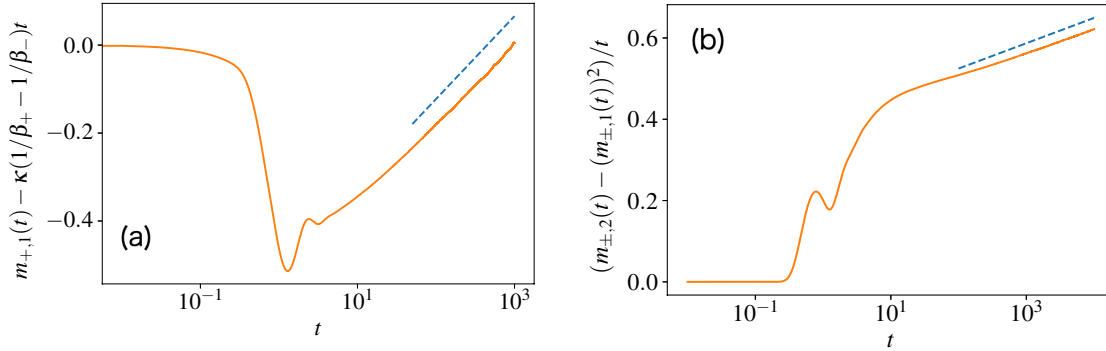


Fig. 5.3: $m_{+,1}(t) - \kappa(1/\beta_+ - 1/\beta_-)$ (a) and $m_{\pm,2}(t)/t^2 - (m_{\pm,1}(t))^2/t^2$ (b) obtained from numerical simulations (with 10^8 samples) are plotted as orange lines. $\beta_+ = 1$, $\beta_- = 2$. Blue dashed lines are $(\kappa^2/2)(\beta_+ + \beta_-)(1/\beta_+ - 1/\beta_-)(\ln t)/t + \text{const.}$ and $\kappa^3(\beta_+ + \beta_-)(1/\beta_+ - 1/\beta_-)^2 + \text{const.}$ The slopes of the numerical-simulation results in semi-log scale converge to those of the dashed reference lines, showing the validity of (5.3.17) and (5.3.29).

5.4 Discussion

5.4.1 A Counting Process with Smaller Power-law Exponents

In the first part of this chapter, we studied a counting process N_t with two heavy-tail waiting time distributions: the Pareto distribution with $\alpha = 3$ and the inverse Rayleigh distribution. These two waiting time distributions have an asymptotic form $1/\tau^3$ when the waiting time τ is large, implying that the variance of the waiting time $\mathbb{E}[\tau^2]$ diverges. Because of this divergence, we discussed that the scaled variance $c_2(t)t$ of the counting process N_t also diverges in the large t limit. We indeed derived that it is asymptotically proportional with $\ln(t)$, diverging as $t \rightarrow \infty$.

A natural question would be, can we get a similar result with a waiting time distribution that has an asymptotic form $1/\tau^\alpha$ with $\alpha > 3$? As demonstrated in Appendix 5.A, one can formulate a general framework, for the Pareto distribution, to derive analytical expressions of the Laplace transform of $\mathbb{E}[N_t^k]$ ($k = 1, 2, 3, \dots$) for any α . As an example, we computed the first, second and third moments for $\alpha = 4$, from which we show the third cumulant of N_t/t has an asymptotic form $\ln(t)/t^2$ when t is large. This indicates that the third-order

cumulant multiplied by t^2 is asymptotically proportional with $\ln(t)$, which is also diverging in the large t limit.

For the counting process with a general fat tail waiting time distribution (that has a power law decay as $t \rightarrow \infty$), an existence of the affine part in the sCGF $G(h) = \lim_{t \rightarrow \infty} (1/t) \ln \mathbb{E}[e^{hN_t}]$ has been proven in chapter 3. When the sCGF is analytic, it can be expanded using scaled cumulants \bar{c}_i ($i = 1, 2, \dots$) as $G(h) = \sum_{i=1}^{\infty} (\bar{c}_i/i!) h^i$ by definition, where \bar{c}_i is defined as $\lim_{t \rightarrow \infty} c_i t^{i-1}$ with the i -th order cumulant c_i of N_t/t . In the presence of the affine part, sCGF is not analytic, implying that some scaled cumulants $\lim_{t \rightarrow \infty} c_i t^{i-1}$ diverge. Based on the observation above, we conjecture that the k -th order scaled cumulant converges when $k < \alpha - 2$. When $k = \alpha - 2$, the k -th order cumulant c_i increases proportionally with $\ln(t)/t^{i-1}$, resulting in $\ln(t)$ divergence of $\lim_{t \rightarrow \infty} c_i t^{i-1}$. It is an interesting future work to study this conjecture.

5.4.2 Many Particles Confined in the Two Hot Walls

In the second part of this chapter, we studied a particle confined in the two walls in different temperatures, and observed that the scaled variance diverges proportionally with $\ln(t)$. Here we discuss if we can observe the same divergence in many-body particles confined in the walls.

One-dimensional hard-core interacting particles exchange their velocities when they collide. The dynamics of these particles can thus be exactly mapped to the dynamics of non-interacting many-body particles. Let $J_{\infty}^{\mathcal{N},L,D}(t)$ and $J_0^{\mathcal{N},L,D}(t)$ be the energy currents of \mathcal{N} hard-core interacting and non-interacting particles of diameter D confined in a one-dimensional box of size L , respectively. Then, we get

$$\mathbb{E} \left[\frac{J_{\infty}^{\mathcal{N},L+\mathcal{N}D,D}(t)}{t} \right] = \mathbb{E} \left[\frac{J_0^{\mathcal{N},L+D,D}(t)}{t} \right] \quad (5.4.1)$$

$$= \mathcal{N} \frac{m_{\pm,1}^L(t)}{t}, \quad (5.4.2)$$

$$\text{Var} \left(\frac{J_{\infty}^{\mathcal{N},L+\mathcal{N}D,D}(t)}{t} \right) = \text{Var} \left(\frac{J_0^{\mathcal{N},L+D,D}(t)}{t} \right) \quad (5.4.3)$$

$$= \mathcal{N} \text{Var} \left(\frac{J_{\pm}^L(t)}{t} \right), \quad (5.4.4)$$

where $m_{\pm,1}^L(t)$ and $\text{Var}(J_{\pm}^L(t)/t)$ are given in Eqs. (5.3.18) and (5.3.30), respectively. This implies that the logarithmic divergence of the scaled variance should be observed in hard-core interacting systems. In soft-core interacting systems, on the other hand, the same mapping cannot be used. This is because of the collisions involving more than two particles, where the exchange rule of velocities no longer holds. To demonstrate this insight, we have performed simulations of hard-core and soft-core interacting particles. The details of the simulations are explained in Appendix 5.C, and the results are shown in Fig. 5.4, where $J_{\text{MD}}(t)$ is the total energy transferred to the colder wall from time 0 to t , and k is a parameter corresponding to the softness of particles. Note that $k = \infty$ corresponds to the case of the hard-core interacting system. We observed that the $\ln(t)$ divergence disappears as soon as particles start to interact via soft-core interactions. It is an interesting future problem to develop

a framework to quantitatively understand the disappearance of the divergence in soft-core particles.

5.4.3 Related Studies

Finally, we list related studies. Studying a variance in a process that is defined with power-law decaying distribution is not something new. In [81], several anomalous diffusion models were studied using continuous-time random walk, and revealed anomalous scaling in their diffusion coefficients. These anomalous scalings were argued to be universally observed in transports in random media [78]. One of the authors also studied a single big jump principle, which states that the sum of random variables can be approximated by their maximum when the probability distribution of the variables has a power-law [82].

Singularities of large deviation functions of time-cumulative quantities are also known as dynamical phase transitions, and have been studied in many physical models, such as glass formers [3, 56–61], lattice gas models [46–52], diffusive hydrodynamic equations [62–64], and high-dimensional chaotic dynamics [53–55] and active matters [65–68]. Finite-size scalings of the large deviation functions have been performed in several works (see an interesting recent work [83] for example), but variance scalings have not been intensively studied in this field yet.

5.A k -th Moment of a Counting Process with Heavy-tailed Distributions

Here, we derive the k -th moment of a counting process N_t (with a waiting time density p) by using a renewal equation. Recalling the derivation for the renewal equation of the MGF (subsection 2.1.4), $M_h(t)$ is defined by

$$M_h(t) \equiv \mathbb{E} [e^{hN_t}]. \quad (5.A.1)$$

Using

$$\begin{aligned} \mathbb{E} [e^{hN_t}] &= \int_0^\infty du \mathbb{E} [e^{hN_t} | \tau_1 = u] p(u) \\ &= \int_0^t du \mathbb{E} [e^{h(N_t - u + 1)}] p(u) \\ &\quad + \int_t^\infty du p(u), \end{aligned} \quad (5.A.2)$$

we obtain the following renewal equation

$$M_h(t) = e^h \int_0^t du M_h(t - u) p(u) + \int_t^\infty du p(u). \quad (5.A.3)$$

The Laplace transform of this equation gives

$$\tilde{M}_h(s) = e^h \tilde{M}_h(s) \tilde{p}(s) + \frac{1 - \tilde{p}(s)}{s}, \quad (5.A.4)$$

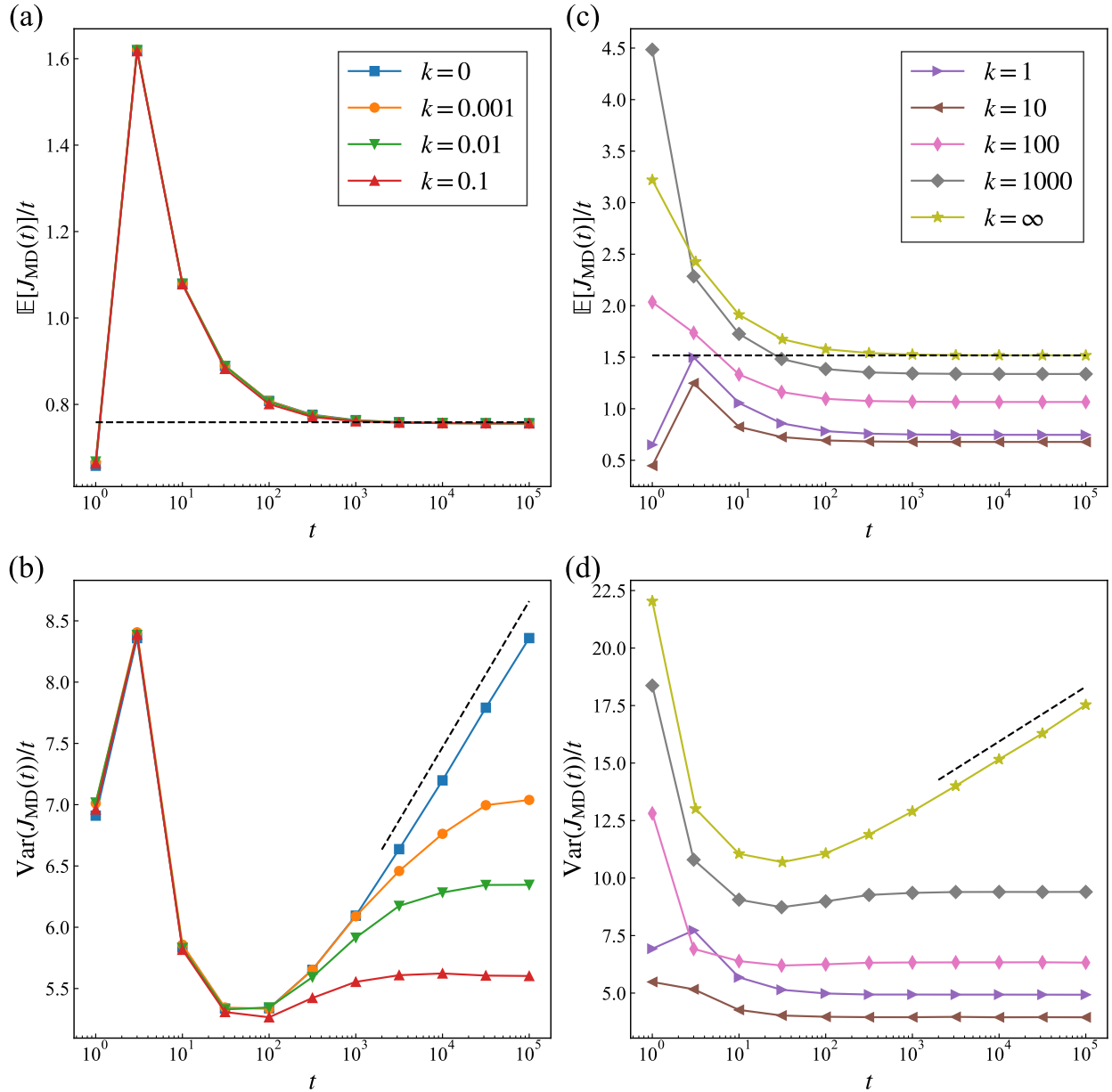


Fig. 5.4: Statistical properties of $J_{\text{MD}}(t)$ over time for different particle softnesses averaged over 10^6 samples when $\mathcal{N} = 3$, $D = 1$, $L = 5$, $\beta_+ = 1/3$, and $\beta_- = 1$. (a) $\mathbb{E}[J_{\text{MD}}(t)]/t$ versus t for $k = 0, 0.001, 0.01$, and 0.1 . The dashed line is $\mathbb{E}[J_{\text{MD}}(t)]/t = \mathcal{N}\kappa(\beta_+^{-1} - \beta_-^{-1})/(L - D)$. (b) $\text{Var}(J_{\text{MD}}(t))/t$ versus t for $k = 0, 0.001, 0.01$, and 0.1 . The dashed line is $\text{Var}(J_{\text{MD}}(t))/t = \mathcal{N}\kappa^3(\beta_+ + \beta_-)(\beta_+^{-1} - \beta_-^{-1})^2 \ln(t)/(L - D) + \text{const.}$ (c) $\mathbb{E}[J_{\text{MD}}(t)]/t$ versus t for $k = 1, 10, 100, 1000$, and ∞ . The dashed line is $\mathbb{E}[J_{\text{MD}}(t)]/t = \mathcal{N}\kappa(\beta_+^{-1} - \beta_-^{-1})/(L - \mathcal{N}D)$. (d) $\text{Var}(J_{\text{MD}}(t))/t$ versus t for $k = 1, 10, 100, 1000$, and ∞ . The dashed line is $\text{Var}(J_{\text{MD}}(t))/t = \mathcal{N}\kappa^3(\beta_+ + \beta_-)(\beta_+^{-1} - \beta_-^{-1})^2 \ln(t)/(L - \mathcal{N}D) + \text{const.}$

which leads to

$$\tilde{M}_h(s) = \frac{1}{s} \frac{1 - \tilde{p}(s)}{1 - \tilde{p}(s)e^h}. \quad (5.A.5)$$

Using

$$\tilde{m}_1(s) = \frac{\tilde{p}(s)}{s(1 - \tilde{p}(s))}, \quad (5.A.6)$$

we can rewrite (5.A.5) as

$$\begin{aligned} \tilde{M}_h(s) &= \frac{1}{s} \frac{1}{1 - s\tilde{m}_1(s)(e^h - 1)} \\ &= \sum_{q=0}^{\infty} (e^h - 1)^q s^{q-1} [\tilde{m}_1(s)]^q. \end{aligned} \quad (5.A.7)$$

Because

$$\lim_{h \rightarrow 0} \frac{d^k}{dh^k} (e^h - 1)^q = \sum_{i=0}^q \binom{q}{i} i^k (-1)^{q-i}, \quad (5.A.8)$$

$$\lim_{h \rightarrow 0} \frac{d^k}{dh^k} (e^h - 1)^q = 0, \quad \text{for } k < q, \quad (5.A.9)$$

and

$$\lim_{h \rightarrow 0} \frac{d^k}{dh^k} \tilde{M}_h(s) = \tilde{m}_k(s), \quad (5.A.10)$$

we have

$$\tilde{m}_k(s) = \sum_{q=1}^k \left[\sum_{i=1}^q \binom{q}{i} i^k (-1)^{q-i} \right] s^{q-1} [\tilde{m}_1(s)]^q. \quad (5.A.11)$$

Let us now consider the Pareto distribution (5.1.2) with $\alpha = 4$ as the waiting time density. In this case, we have

$$\tilde{m}_1(s) = \frac{2}{s^2} + \frac{1}{s} + o\left(\frac{1}{s}\right), \quad (5.A.12)$$

$$\tilde{m}_2(s) = \frac{8}{s^3} + \frac{10}{s^2} + \frac{16 \ln(s)}{s} + o\left(\frac{\ln(s)}{s}\right), \quad (5.A.13)$$

$$\begin{aligned} \tilde{m}_3(s) &= \tilde{m}_1(s) + 6s\tilde{m}_1^2(s) + 6s^2\tilde{m}_1^3(s) \\ &= \frac{48}{s^4} + \frac{96}{s^3} + \frac{144 \ln(s)}{s^2} + o\left(\frac{\ln(s)}{s^2}\right) \end{aligned} \quad (5.A.14)$$

from (5.A.11) for large s . Using the following inverse Laplace transform

$$\int_0^{\infty} e^{-st} \ln(t) dt = \left(-\frac{\ln(s) + \gamma}{s} \right), \quad (5.A.15)$$

we calculate the inverse Laplace transform of $\tilde{m}_k(s)$ as

$$m_1(t) \sim 2t + 1, \quad (5.A.16)$$

$$m_2(t) \sim 4t^2 + 10t - 16 \ln(t), \quad (5.A.17)$$

$$m_3(t) \sim 8t^3 + 48t^2 + 206t - 144t \ln(t) \quad (5.A.18)$$

as $t \rightarrow \infty$. The second cumulants c_2 defined as (5.2.14) and the third cumulant c_3 (defined as the third cumulant of N_t/t^3) are then given by

$$c_2(t) = \frac{6}{t} + o\left(\frac{1}{t}\right), \quad (5.A.19)$$

$$\begin{aligned} c_3(t) &= \frac{m_3(t) - 3m_1(t)m_2(t) + 2m_1^3(t)}{t^3} \\ &= -\frac{48 \ln(t)}{t^2} + o\left(\frac{\ln(t)}{t^2}\right). \end{aligned} \quad (5.A.20)$$

Another Proof

Here, we introduce the method to derive the k -th moment of a counting process by using a renewal equation. For considering the k -th moment of a counting process, we introduce an expected value of N_t^k , which is N_t to the power of k ($k \in \mathbb{N}$). It is given by

$$m_k(t) = \mathbb{E}[N_t^k]. \quad (5.A.21)$$

Then, the renewal equation of N_t^k is

$$\begin{aligned} m_k(t) &= \int_0^\infty \mathbb{E}[N_t^k \mid \tau_1 = s] p(s) \\ &= \int_0^t \mathbb{E}[N_t^k \mid \tau_1 = s] p(s) \\ &\quad + \int_t^\infty \mathbb{E}[N_t^k \mid \tau_1 = s] p(s). \end{aligned} \quad (5.A.22)$$

If $s > t$ then $\mathbb{E}[N_t^k \mid \tau_1 = s] = 0$. If $0 \leq s \leq t$, the renewal property says that $\mathbb{E}[N_t^k \mid \tau_1 = s] = \mathbb{E}[(1 + N_{t-s})^k]$. Thus we have

$$\begin{aligned} m_k(t) &= \int_0^t \mathbb{E}[(1 + N_{t-s})^k] p(s) \\ &= F(t) + \sum_{i=1}^k \binom{k}{i} m_i * p(t) \end{aligned} \quad (5.A.23)$$

To describe the large time asymptotic form of $m_k(t)$, we perform Laplace transform. Thereby, it is calculated as

$$\begin{aligned} \tilde{m}_k(s) &= \frac{\tilde{F}(s) + s\tilde{F}(s) \sum_{i=1}^{k-1} \binom{k}{i} \tilde{m}_i(s)}{1 - s\tilde{F}(s)} \\ &= \tilde{m}_1(s) + s\tilde{m}_1(s) \sum_{i=1}^{k-1} \binom{k}{i} \tilde{m}_i(s). \end{aligned} \quad (5.A.24)$$

This equation implies that $\tilde{m}_n(s)$ ($n \in \mathbb{N}$) is described by $\tilde{m}_1(s), \dots, \tilde{m}_{n-1}(s)$. For this fact, we can expect $\tilde{m}_n(s)$ is denoted by the combinations of $\tilde{m}_1(s)$.

Remark 5.A.1. Let us suppose that $\tilde{m}_k(s)$ is denoted as

$$\tilde{m}_k(s) = \sum_{i=1}^k A_i s^{i-1} \tilde{m}_1^i(s). \quad (5.A.25)$$

When we consider $k = 2$, by using the relation (5.A.24) the $\tilde{m}_2(s)$ is given by

$$\tilde{m}_2(s) = \tilde{m}_1(s) + 2s\tilde{m}_1^2(s). \quad (5.A.26)$$

Thus, $\tilde{m}_2(s)$ satisfies the assumption of $\tilde{m}_k(s)$ (5.A.25). Let us suppose that $\tilde{m}_k, k \leq n$ satisfies (5.A.25). For induction proof, we need to check the case of $k = n + 1$. From (5.A.24), $\tilde{m}_{n+1}(s)$ is given by

$$\tilde{m}_{n+1}(s) = \tilde{m}_1(s) + s\tilde{m}_1(s) \sum_{i=1}^n \binom{n+1}{i} \tilde{m}_i(s). \quad (5.A.27)$$

Moreover, by using the assumption, $\tilde{m}_{n+1}(s)$ is:

$$\begin{aligned} \tilde{m}_{n+1}(s) &= \tilde{m}_1(s) + s\tilde{m}_1(s) \sum_{i=1}^n \binom{n+1}{i} \sum_{r=1}^i A_r s^r \tilde{m}_1^{r+1} \\ &= \tilde{m}_1(s) + s\tilde{m}_1(s) \sum_{i=1}^n \sum_{r=1}^i \binom{n+1}{i} A_r s^r \tilde{m}_1^{r+1} \\ &= \tilde{m}_1(s) + s\tilde{m}_1(s) \sum_{r=1}^n \sum_{i=r}^n \binom{n+1}{i} A_r s^r \tilde{m}_1^{r+1} \\ &= \tilde{m}_1(s) + s\tilde{m}_1(s) \sum_{r=1}^n C_r s^r \tilde{m}_1^{r+1} \\ &= \sum_{i=1}^{n+1} D_r s^{i-1} \tilde{m}_1^i. \end{aligned} \quad (5.A.28)$$

Here, we use the constants C_r, D_r . Thus, we can describe $\tilde{m}_k(s)$ as the combination of $\tilde{m}_1(s)$

5.B Tauberian Theorem

The Tauberian theorem is stated in [77] Ch.XIII.5, theorem 4. In our context it can be stated as follows. If the Laplace transform \tilde{m} of the renewal function m satisfies

$$\tilde{m}(s) \sim \frac{1}{s^\rho} L\left(\frac{1}{s}\right), \quad s \rightarrow 0$$

for some $\rho > 0$ and some slowly varying (*i.e.*, a function L is slowly varying if for any $x > 0$, $\lim_{t \rightarrow \infty} \frac{L(xt)}{L(t)} = 1$) function L then

$$m(t) \sim \frac{1}{\Gamma(\rho)} t^{\rho-1} L(t). \quad (5.B.1)$$

5.C Simulation Detail

\mathcal{N} particles of mass m and diameter D are lined up on a line $[0, L]$. Let (r_i, p_i) be the position and momentum of the i th particle. The total energy transferred to the right wall from time 0 to t is defined by

$$J_{\text{MD}}(t) = \sum_i \sum_{k_i} \left\{ \frac{|p_i(t_{k_i} - 0)|^2}{2m} - \frac{|p_i(t_{k_i} + 0)|^2}{2m} \right\} \quad (5.C.1)$$

with $0 \leq t_{k_i} \leq t$, where $t_{k_i} \pm 0$ is the time just before/after the i th particle collides with the right wall for the k_i th time.

For the case of the soft-core interacting system, a short-range interaction potential Φ between two particles is given by

$$\Phi(|r_i - r_j|) = \frac{k}{2} (D - |r_i - r_j|)^2 \Theta(D - |r_i - r_j|), \quad (5.C.2)$$

where Θ is the Heaviside step function, and k is a parameter corresponding to the softness of particles. The boundary condition is the same as explained in Sec. 5.3.1. Using the second-order symplectic integrator, we numerically solved the equations of motion for the particles, and calculated $\mathbb{E}[J_{\text{MD}}(t)]$ and $\text{Var}(J_{\text{MD}}(t))$ for various values of k . In the simulation, we set the parameter values as $\mathcal{N} = 3$, $L = 5$, $m = D = 1$, $\beta_+ = 1/3$, and $\beta_- = 1$. The time-discretization step-size was set to 0.01.

For the case of the hard-core interacting system (denoted by $k = \infty$), we performed event-driven simulations in which two particles instantaneously exchange velocities when they come into contact. The boundary condition and the parameter values were the same as for the soft-core particle system.

Bibliography

- [1] Raphael Lefevre, Mauro Mariani, and Lorenzo Zambotti. Large deviations of the current in stochastic collisional dynamics. *Journal of Mathematical Physics* **52**, 033302 (2011).
- [2] Juan P Garrahan, Robert L Jack, Vivien Lecomte, Estelle Pitard, Kristina van Duijvendijk, and Frédéric van Wijland. Dynamical first-order phase transition in kinetically constrained models of glasses. *Physical review letters* **98**, 195702 (2007).
- [3] Takahiro Nemoto, Robert L Jack, and Vivien Lecomte. Finite-size scaling of a first-order dynamical phase transition: Adaptive population dynamics and an effective model. *Physical review letters* **118**, 115702 (2017).
- [4] Raphaël Lefevre, Mauro Mariani, and Lorenzo Zambotti. Macroscopic fluctuation theory of aerogel dynamics. *Journal of Statistical Mechanics: Theory and Experiment* **2010**, L12004 (2010).
- [5] Geoffrey Grimmett and David Stirzaker. *Probability and random processes*. Oxford university press 2020.
- [6] Pierre-Simon Laplace. *Théorie analytique des probabilités*. Courcier 1812.
- [7] Lokenath Debnath and Kanadpriya Basu. A short history of probability theory and its applications. *International Journal of Mathematical Education in Science and Technology* **46**, 13 (2015).
- [8] Penelope L Peterson, Eva Baker, and Barry McGaw. *International encyclopedia of education*. Elsevier Ltd. 2010.
- [9] Brendan O Bradley and Murad S Taquq. Financial risk and heavy tails. In *Handbook of heavy tailed distributions in finance* pages 35. Elsevier 2003.
- [10] Paul Glasserman, Philip Heidelberger, and Perwez Shahabuddin. Portfolio value-at-risk with heavy-tailed risk factors. *Mathematical Finance* **12**, 239 (2002).
- [11] Felix Wong and James J Collins. Evidence that coronavirus superspreading is fat-tailed. *Proceedings of the National Academy of Sciences* **117**, 29416 (2020).

- [12] Anne Schneeberger, Catherine H Mercer, Simon AJ Gregson, Neil M Ferguson, Constance A Nyamukapa, Roy M Anderson, Anne M Johnson, and Geoff P Garnett. Scale-free networks and sexually transmitted diseases: a description of observed patterns of sexual contacts in Britain and Zimbabwe. *Sexually transmitted diseases* **31**, 380 (2004).
- [13] Alessandro Vezzani, Eli Barkai, and Raffaella Burioni. Single-big-jump principle in physical modeling. *Physical Review E* **100**, 012108 (2019).
- [14] Denis J Evans, Ezechiel Godert David Cohen, and Gary P Morriss. Probability of second law violations in shearing steady states. *Physical review letters* **71**, 2401 (1993).
- [15] Cyrille Joutard. A strong large deviation theorem. *Mathematical Methods of Statistics* **22**, 155 (2013).
- [16] Boris Tsirelson. From uniform renewal theorem to uniform large and moderate deviations for renewal-reward processes. *Electronic Communications in Probability* **18**, 1 (2013).
- [17] Eli Barkai and Stanislav Burov. Packets of diffusing particles exhibit universal exponential tails. *Physical review letters* **124**, 060603 (2020).
- [18] Frank Den Hollander. *Large deviations* volume 14. American Mathematical Soc. 2008.
- [19] Raghu Raj Bahadur and R Ranga Rao. On deviations of the sample mean. *The Annals of Mathematical Statistics* **31**, 1015 (1960).
- [20] Lorenzo Bertini, Alberto De Sole, Davide Gabrielli, Giovanni Jona-Lasinio, and Claudio Landim. Non equilibrium current fluctuations in stochastic lattice gases. *Journal of statistical physics* **123**, 237 (2006).
- [21] Lorenzo Bertini, Alberto De Sole, Davide Gabrielli, Giovanni Jona-Lasinio, and Claudio Landim. Macroscopic fluctuation theory. *Reviews of Modern Physics* **87**, 593 (2015).
- [22] Bernard Derrida. Non-equilibrium steady states: fluctuations and large deviations of the density and of the current. *Journal of Statistical Mechanics: Theory and Experiment* **2007**, P07023 (2007).
- [23] Raphaël Lefevre, Mauro Mariani, and Lorenzo Zambotti. Large deviations for renewal processes. *Stochastic Processes and their Applications* **121**, 2243 (2011).
- [24] Hansjörg Albrecher and Onno J Boxma. A ruin model with dependence between claim sizes and claim intervals. *Insurance: Mathematics and Economics* **35**, 245 (2004).
- [25] John F Shortle, James M Thompson, Donald Gross, and Carl M Harris. *Fundamentals of queueing theory* volume 399. John Wiley & Sons 2018.
- [26] Christophe Fraser. Estimating individual and household reproduction numbers in an emerging epidemic. *PloS one* **2**, e758 (2007).

- [27] Michael George Roberts and Hiroshi Nishiura. Early estimation of the reproduction number in the presence of imported cases: pandemic influenza H1N1-2009 in New Zealand. *PloS one* **6**, e17835 (2011).
- [28] J Klafter and R Silbey. Derivation of the continuous-time random-walk equation. *Physical Review Letters* **44**, 55 (1980).
- [29] Miroslav S Tanushev and Richard Arratia. Central limit theorem for renewal theory for several patterns. *Journal of Computational Biology* **4**, 35 (1997).
- [30] Brian Berkowitz, Andrea Cortis, Marco Dentz, and Harvey Scher. Modeling non-Fickian transport in geological formations as a continuous time random walk. *Reviews of Geophysics* **44** (2006).
- [31] Marco Zamparo. Large deviations in renewal models of statistical mechanics. *J. Phys. A: Math. Theor.* **52**, 495004 (2019).
- [32] Marco Zamparo. Critical Fluctuations in Renewal Models of Statistical Mechanics. <https://arxiv.org/abs/2006.09298> (2020).
- [33] Jean-Philippe Bouchaud and Antoine Georges. Anomalous diffusion in disordered media: statistical mechanisms, models and physical applications. *Physics reports* **195**, 127 (1990).
- [34] Ryszard Kutner. Extreme events as foundation of Lévy walks with varying velocity. *Chemical physics* **284**, 481 (2002).
- [35] Clélia De Mulatier, Alberto Rosso, and Grégory Schehr. Asymmetric Lévy flights in the presence of absorbing boundaries. *Journal of Statistical Mechanics: Theory and Experiment* **2013**, P10006 (2013).
- [36] Raphaël Lefevre and Lorenzo Zambotti. Hot scatterers and tracers for the transfer of heat in collisional dynamics. *Journal of Statistical Physics* **139**, 686 (2010).
- [37] William Feller. An Introduction to Probability Theory and its Applications, vol 2. (2010).
- [38] Herbert B Callen. Thermodynamics and an Introduction to Thermostatistics 1998.
- [39] Richard S Ellis. *Entropy, large deviations, and statistical mechanics* volume 1431. Taylor & Francis 2006.
- [40] Hugo Touchette. The large deviation approach to statistical mechanics. *Physics Reports* **478**, 1 (2009).
- [41] Giovanni Jona-Lasinio et al. Large deviations and the Boltzmann entropy formula. *Brazilian Journal of Probability and Statistics* **29**, 494 (2015).
- [42] Denis J Evans, Ezechiel Godert David Cohen, and Gary P Morriss. Probability of second law violations in shearing steady states. *Physical review letters* **71**, 2401 (1993).

- [43] Jorge Kurchan. Fluctuation theorem for stochastic dynamics. *Journal of Physics A: Mathematical and General* **31**, 3719 (1998).
- [44] Joel L Lebowitz and Herbert Spohn. A Gallavotti–Cohen-type symmetry in the large deviation functional for stochastic dynamics. *Journal of Statistical Physics* **95**, 333 (1999).
- [45] Bernard Derrida. Non-equilibrium steady states: fluctuations and large deviations of the density and of the current. *Journal of Statistical Mechanics: Theory and Experiment* **2007**, P07023 (2007).
- [46] Thierry Bodineau and Bernard Derrida. Distribution of current in nonequilibrium diffusive systems and phase transitions. *Physical Review E* **72**, 066110 (2005).
- [47] Cécile Appert-Rolland, Bernard Derrida, Vivien Lecomte, and Frédéric Van Wijland. Universal cumulants of the current in diffusive systems on a ring. *Physical Review E* **78**, 021122 (2008).
- [48] T Bodineau, B Derrida, V Lecomte, and F Van Wijland. Long range correlations and phase transitions in non-equilibrium diffusive systems. *Journal of Statistical Physics* **133**, 1013 (2008).
- [49] Thierry Bodineau, Vivien Lecomte, and Cristina Toninelli. Finite size scaling of the dynamical free-energy in a kinetically constrained model. *Journal of Statistical Physics* **147**, 1 (2012).
- [50] Yongjoo Baek, Yariv Kafri, and Vivien Lecomte. Dynamical symmetry breaking and phase transitions in driven diffusive systems. *Physical review letters* **118**, 030604 (2017).
- [51] Ohad Shpielberg. Geometrical interpretation of dynamical phase transitions in boundary-driven systems. *Physical Review E* **96**, 062108 (2017).
- [52] Ohad Shpielberg, Takahiro Nemoto, and João Caetano. Universality in dynamical phase transitions of diffusive systems. *Physical Review E* **98**, 052116 (2018).
- [53] Julien Tailleur and Jorge Kurchan. Probing rare physical trajectories with Lyapunov weighted dynamics. *Nature Physics* **3**, 203 (2007).
- [54] Tanguy Laffargue, Khanh-Dang Nguyen Thu Lam, Jorge Kurchan, and Julien Tailleur. Large deviations of Lyapunov exponents. *Journal of Physics A: Mathematical and Theoretical* **46**, 254002 (2013).
- [55] F Bouchet, C Nardini, and T Tangarife. Stochastic averaging, large deviations and random transitions for the dynamics of 2D and geostrophic turbulent vortices. *Fluid Dynamics Research* **46**, 061416 (2014).
- [56] Lester O Hedges, Robert L Jack, Juan P Garrahan, and David Chandler. Dynamic order-disorder in atomistic models of structural glass formers. *Science* **323**, 1309 (2009).

- [57] Juan P Garrahan, Robert L Jack, Vivien Lecomte, Estelle Pitard, Kristina van Duijvendijk, and Frédéric van Wijland. First-order dynamical phase transition in models of glasses: an approach based on ensembles of histories. *Journal of Physics A: Mathematical and Theoretical* **42**, 075007 (2009).
- [58] Robert L Jack and Peter Sollich. Large deviations and ensembles of trajectories in stochastic models. *Progress of Theoretical Physics Supplement* **184**, 304 (2010).
- [59] Estelle Pitard, Vivien Lecomte, and Frédéric Van Wijland. Dynamic transition in an atomic glass former: A molecular-dynamics evidence. *EPL (Europhysics Letters)* **96**, 56002 (2011).
- [60] David T Limmer and David Chandler. Theory of amorphous ices. *Proceedings of the National Academy of Sciences* **111**, 9413 (2014).
- [61] Thomas Speck, Alex Malins, and C Patrick Royall. First-order phase transition in a model glass former: Coupling of local structure and dynamics. *Physical review letters* **109**, 195703 (2012).
- [62] Lorenzo Bertini, Alberto De Sole, Davide Gabrielli, Gianni Jona-Lasinio, and Claudio Landim. Current fluctuations in stochastic lattice gases. *Physical review letters* **94**, 030601 (2005).
- [63] Pablo I Hurtado and Pedro L Garrido. Spontaneous symmetry breaking at the fluctuating level. *Physical review letters* **107**, 180601 (2011).
- [64] N Tizón-Escamilla, PI Hurtado, and PL Garrido. Structure of the optimal path to a fluctuation. *Physical Review E* **95**, 032119 (2017).
- [65] Suriyanarayanan Vaikuntanathan, Todd R Gingrich, and Phillip L Geissler. Dynamic phase transitions in simple driven kinetic networks. *Physical Review E* **89**, 062108 (2014).
- [66] Francesco Cagnetta, Federico Corberi, Giuseppe Gonnella, and Antonio Suma. Large fluctuations and dynamic phase transition in a system of self-propelled particles. *Physical review letters* **119**, 158002 (2017).
- [67] Stephen Whitelam, Katherine Klymko, and Dibyendu Mandal. Phase separation and large deviations of lattice active matter. *The Journal of chemical physics* **148**, 154902 (2018).
- [68] Takahiro Nemoto, Étienne Fodor, Michael E Cates, Robert L Jack, and Julien Tailleur. Optimizing active work: Dynamical phase transitions, collective motion, and jamming. *Physical Review E* **99**, 022605 (2019).
- [69] Robert L Jack, Takahiro Nemoto, and Vivien Lecomte. Dynamical phase coexistence in the Fredrickson–Andersen model. *Journal of Statistical Mechanics: Theory and Experiment* **2020**, 053204 (2020).

- [70] Takahiro Nemoto. *Phenomenological Structure for the Large Deviation Principle in Time-Series Statistics: A method to control the rare events in non-equilibrium systems*. Springer 2015.
- [71] Wendell Helms Fleming, Tullio Zolezzi, and Italo Capuzzo Dolcetta. *Recent Mathematical Methods in Dynamic Programming: Proceedings of the Conference Held in Rome, Italy, March 26-28, 1984*. Springer-Verlag 1985.
- [72] Paul Dupuis and Richard S Ellis. *A weak convergence approach to the theory of large deviations*. John Wiley & Sons 2011.
- [73] Robert L Jack. Ergodicity and large deviations in physical systems with stochastic dynamics. *The European Physical Journal B* **93**, 1 (2020).
- [74] Yael S Elmatad, Robert L Jack, David Chandler, and Juan P Garrahan. Finite-temperature critical point of a glass transition. *Proceedings of the National Academy of Sciences* **107**, 12793 (2010).
- [75] Joel L Lebowitz and Harry L Frisch. Model of nonequilibrium ensemble: Knudsen gas. *Physical Review* **107**, 917 (1957).
- [76] Søren Asmussen. *Applied probability and queues* volume 51. Springer Science & Business Media 2008.
- [77] William Feller. *An introduction to probability theory and its applications, vol 2*. John Wiley & Sons 2008.
- [78] Eli Barkai and Stanislav Burov. Packets of diffusing particles exhibit universal exponential tails. *Physical review letters* **124**, 060603 (2020).
- [79] Raphaël Lefevre and Lorenzo Zambotti. Hot scatterers and tracers for the transfer of heat in collisional dynamics. *Journal of Statistical Physics* **139**, 686 (2010).
- [80] Hugo Touchette. The large deviation approach to statistical mechanics. *Physics Reports* **478**, 1 (2009).
- [81] Ralf Metzler, Jae-Hyung Jeon, Andrey G Cherstvy, and Eli Barkai. Anomalous diffusion models and their properties: non-stationarity, non-ergodicity, and ageing at the centenary of single particle tracking. *Physical Chemistry Chemical Physics* **16**, 24128 (2014).
- [82] Alessandro Vezzani, Eli Barkai, and Raffaella Burioni. Single-big-jump principle in physical modeling. *Physical Review E* **100**, 012108 (2019).
- [83] Luke Causer, Mari Carmen Bañuls, and Juan P Garrahan. Finite time large deviations via matrix product states. *Physical Review Letters* **128**, 090605 (2022).